PB81-201600

BuMines OFR 46(2)-81

RISK ANALYSIS FOR ROCK SLOPES IN OPEN PIT MINES

PART II

LIMIT EQUILIBRIUM ANALYSIS FOR ROCK WEDGE STABILITY

Prepared for

UNITED STATES DEPARTMENT OF THE INTERIOR BUREAU OF MINES

By

DEPARTMENT OF CIVIL ENGINEERING
MASSACHUSETTS INSTITUTE OF TECHNOLOGY
CAMBRIDGE, MASSACHUSETTS 02134

Bureau of Mines Open File Report
46(2)-81

FINAL TECHNICAL REPORT

Contract J 027 5015
RISK ANALYSIS FOR
ROCK SLOPES IN OPEN PIT MINES

November 1979

PRODUCED BY:
NATIONAL TECHNICAL
INFORMATION SERVICE
US DEPARTMENT OF COMMERCE
SPRINGFIELD, VA. 22161

50772-101

REPORT DOCUMENTATION PAGE	1. REPORT NO. BuMines OFR 46(2)-81	2.	3. Recipient's Accession No. PB81 201600

4. Title and Subtitle
Risk Analysis for Rock Slopes in Open Pit Mines. Part II. Limit Equilibrium Analysis for Rock Wedge Stability

5. Report Date
November 1979

6.

7. Author(s)
Herbert H. Einstein and others[1]

8. Performing Organization Rept. No.

9. Performing Organization Name and Address
Massachusetts Institute of Technology
Department of Civil Engineering
Cambridge, MA 02139

10. Project/Task/Work Unit No.

11. Contract(C) or Grant(G) No.
(C) J0275015
(G)

12. Sponsoring Organization Name and Address
Office of the Director--Mineral Resources Technology
Bureau of Mines
U.S. Department of the Interior
Washington, D.C. 20241

13. Type of Report & Period Covered
Contract research, 3/1/77--10/31/79

14.

15. Supplementary Notes

Approved by the Director, Bureau of Mines, for placement on open file, March 12, 1981.

16. Abstract (Limit: 200 words)

Instability of rock slopes often occurs in the form of excessive movement of bodies that are bounded by discontinuities. The well-known limit equilibrium analysis for wedges and blocks suffer from procedural simplifications and from the basic deficiency of limit equilibrium analysis--the rigid body assumption. Thus, stability analysis for two-and three-plane wedges with a wide range of additional features regarding failure mode and external forces have been developed. The deficiency, due to the rigid body assumption, was corrected by an approach that includes the effects of the in situ stress field and of the stiffness of discontinuities. The final step in making limit equilibrium approaches more valid was achieved with artificial supports which makes it possible to identify the most critical failure mode and to determine the corresponding factor to safety. The analytical development includes the creation of appropriate computer codes and routines for programmable pocket calculators.

17. Document Analysis a. Descriptors
Open pit mining
Rock slopes
Stability analysis

b. Identifiers/Open-Ended Terms
Analysis methods for rock wedge stability

[1]Gregory B. Baecher, Daniele Veneziano, Hing C. Chan, William S. Dershowitz, Edward F. Glynn, Jean Luc Galzi, Nicholas A. Lanney, Kevin O'Reilly, William S. Scull, and Peter Yip

c. COSATI Field/Group 08I

18. Availability Statement
Unlimited release by NTIS.

19. Security Class (This Report)
Unclassified

20. Security Class (This Page)
Unclassified

22. Price

The views and conclusions contained in this document are those of the authors and should not be interpreted as necessarily representing the official policies or recommendations of the Interior Department's Bureau of Mines or of the United States Government.

FOREWORD

This report was prepared by the Massachusetts Institute of Technology, Department of Civil Engineering, under USBM Contract number J0275051. The contract was initiated under the Advancing Metal and Nonmetal Mining Technology Program. It was administered under the technical direction of the Denver Research Center with Louis A. Panek acting as Technical Project Officer. Larry Rock was the contract administrator for the Bureau of Mines. This report is a summary of the work recently completed as a part of this contract during the period March 1, 1977 to October 31, 1979. This report was submitted by the authors on November 30, 1979.

The research leading to this report was only possible with the progressive and encouraging attitude of the responsible persons at the Bureau of Mines. J.W. Corwine and D.D. Bolstad were instrumental in preparing for and initiating the research. The Technical Monitor, L. Panek, contributed significantly, not only by providing supervision but by many valuable comments and questions. The mining and engineering industry provided support whose value cannot be overemphasized, mostly in the form of data on rock mass parameters but also through critical comments and through information on their design procedures. For reasons of not identifying data with particular projects we can only mention two of the many firms: Pincock, Allen and Holt (Tucson, Arizona) and Duvall Mines. Finally, we would like to point out that some of the students working on the research were only partially supported by research funds, the remainder came from Domestic Mining Mineral and Mineral Fuel Conservation Fellowships, U.S. Department of Education and from the Undergraduate Research Opportunities Program at M.I.T. The help and support of all the individuals, government agencies, and private firms is gratefully acknowledged.

Part II - Limit Equilibrium Analysis For Rock Wedge Stability

TABLE OF CONTENTS

CHAPTER I

INTRODUCTION TO LIMIT EQUILIBRIUM ANALYSES FOR ROCK WEDGE STABILITY

It was indicated at several occasions that the discontinuous character of rock masses predominates their behavior. As a consequence instability of rock slopes does ususally occur in form of excessive movement of rocks that are bounded by discontinuities or a combination of discontinuities and failure surfaces through intact rock: the well known wedge or block failures where movements can be in form of translational sliding and rotational sliding on one or several planes or, in form of toppling or in form of combined modes. Limit equilibrium analysis seems thus to be well suited for the treatment of these stability problems and has been extensively employed for that purpose. In addition to a few closed form approaches mainly charts and computer programs have been developed as analysis tools.

In spite of the wide use of limit equilibrium wedge analyses, they are still very restricted and to a large extent incorrect. The deficiencies occur in two main areas: 1) procedural simplifications and 2) basic deficiency of the limit equilibrium approach.

The procedural simplifications include geometric limitations (e.g., 2-joint wedges only), restriction to only one of a few failure modes (translational sliding failure), consideration of driving and resisting forces (simplified water pressure or seismic forces, external forces acting through the center of gravity). Such simplications may have been justified in hand calculations but most of them can be eliminated if machine computation is used.

More problematic is the second area, the basic deficiency of limit equilibrium approaches. Since these approaches are based on rigid body assumptions, deformations and as a consequence stresses are not known--the problem is fundamentally indeterminate. Usually limit equilibrium analysis methods work thus with forces (rather than stresses) and include implicit or explicit assumptions to make the problem determinate. These assumptions often introduce substantial inaccuracies and can lead to, unknown to most users, potentially unsafe conclusions.

Since basic correctness and also largely unlimited applicability of wedge stability analysis is essential in reliability analyses, it was necessary to first make a strong effort to reduce the aforementioned restrictions and to create less limited and more correct analysis methods. This has the additional advantage that these developments can be used independently of the reliability analysis.

Specifically, this led to the following results that will be described in this part of the report:

1. Stability Analysis for wedges formed by two or three planes (with a wide range of additional features regarding modes of failure and force application) (Chapter 2).

2. Simplified analysis for 2-plane wedges, to be used with programmable pocket calculators (Chapter 3).

3. Wedge stability analysis considering stress and stiffness effects (Chapter 4).

4. Method of artifical supports, an approach to complete limit equilibrium analysis

CHAPTER 2

STABILITY ANALYSIS FOR WEDGES FORMED BY TWO OR THREE JOINT PLANES—SWARS (SLIDING WEDGE ANALYSIS FOR ROCK SLOPES)

Summary and Practical Application

SWARS is a computerized analysis method for rock wedges formed from two or three joints and the slope. The designer simply has to list the attitude of up to eight (or more) joint sets in the rock mass under consideration, the attitude, length and height of the slope and the inclination of the surface above the slope. The analysis procedure combines all the joints the slope to determine all possible geometrically and kinematically feasible 2-and 3-joint wedges. The analysis is set up such that only wedges that fulfill the geometric and kinematic conditions are created, thus greatly reducing the following computations. The only separate kinematic test is that for size. The maximum extent of the wedge on the slope face has to be within the slope dimensions or within a specified smaller size, the latter being an important feature of the method that will be discussed later. The determination of geometrically and kinematically feasible wedges does actually not have to concern the user, since the analysis method proceeds directly from the geometric input to the kinetic analysis for which the user has to specify initially (simultaneously with the joint and slope geometry):

- unit weight of rock
- external driving forces in form of point loads or uniform loads
- internal driving forces in form of water pressure distributions and seismic forces
- internal resisting forces in form of the joint shear characteristics i.e., friction angle Φ, cohesion c, asperity angle, and joint persistence (continuity)
- external resisting forces e.g., bolt forces and their points of application and direction.

The kinetic analysis which is performed as limit equilibrium analysis on a rigid body includes large number of practically important and often innovative features. Point loads can act in any direction and can be applied at any point; in particular they do not have to act through the center of gravity. This is much more realistic than the usual center of gravity assumption of similar analysis methods. Particularly bolt (anchor) design can now be based on the actual physical features rather than on an idealized pressure. This is particularly advantageous together with the aforementioned possibility to limit and thus specify the size of examined wedges. Bolts (anchors) can be specified differently for different wedges both excluding over-design as well as the danger of missing a smaller wedge within a large one. Water pressure can be uniform or hydrostatic. The stability analysis for each wedge is conducted for both peak and residual joint resistance parameters and results in a peak and residual factor of safety. Very important is the capability of SWARS to analyze

a variety of modes of failure translational sliding on one or two planes, lifting off from all planes, and (for 2 joint wedges only) toppling about the edges and the lower apex.

The output can be a listing of all kinetically analyzed wedges or simply those that have a factor of safety below a specified value. In addition the geometry, resultant force vector and mode of failure are presented.

SWARS is a very effective and efficient design tool. The designer can simply describe the characteristics of the rock mass and can then concentrate on the engineering: varying slope geometry and stabilizing measures (reduction of external loads, application of bolts) to optimize slope stability i.e., prevent instability of wedges and reduce the number of marginally stable ones. Naturally, parameteric studies on the effect of variable natural characteristics can be conducted also.

Limitations of SWARS are the water pressure and seismic force assumptions that, although realistic, require some judgement by the user. Although the possibility to consider 2 and 3 joint wedges covers or approximates most geometries, a separate consideration of blocks would be desirable. Finally, toppling for 3 joint wedges and rotational sliding in all cases cannot be directly handled by SWARS nor can stress and stiffness effects; the user has to employ the specific approaches discussed in Chapter 4 and 5.

At the present time SWARS probably represents the most advanced and practically efficient method for analyzing rock wedge stability, one of the prime problems in rock slope design. In addition, the analysis methods considering stress and stiffness effects (Chapter 4) and additional modes of failure (Chapter 5) supplement SWARS to provide a complete set of rock wedge analyses.

2.1 Introduction

A standard approach to rock slope stability analysis is through limit equilibrium analyses of wedges formed by joints and the slope surface(s). Combining two joint planes and the slope surfaces typically leads to wedges like the one in Figure 2.1; three joint planes and the slope surface can form a wedge like that in Figure 2.2. Many other shapes, particularly in the case of 3 joint wedges, can occur depending on the relative orientation of joint planes and slope surfaces. It is also possible that three joint planes form both two-joint and three-joint wedges as shown in Figure 2.3. The wedges are assumed to be rigid bodies and the 'joint planes' each actually represent a joint set, i.e., other parallel joint planes exist and the wedges can thus have a variety of sizes but identical shapes (Figure 2.4.).

By assuming rigid body behavior wedge stability can be treated through limit equilibrium analysis. Most present approaches based upon Wittke's (1965a,b) are using vector analysis. Amongst others, further developments were those by Hendron et al (1971) simplifying and computerizing Wittke's approach, by Hoek et al. (1974) providing charts and by Londe et al. (1969) who expanded Wittke's method. Further contributions were made by Kovary et al. (1975) in form of pocket calculator versions for simplified wedge analysis and particularly by the M.I.T. group (Campbell, 1974) in form of the expanded computerized version SWARS-2P. The analysis method SWARS presented here uses the basic ideas of SWARS-2P but substantially extends that analysis. The capabilities of SWARS can best be illustrated by first discussing the requirements that an ideal wedge stability analysis should fulfill.

The factors influencing the behavior of a wedge, that should be considered, are

- slope geometry: single plane or multiple plane, orientation of planes, size of planes i.e., height and width.
- discontinuity* (joint)* geometry: joint orientation, number of joint sets (A joint may be a single

*Joint and discontinuity will be used interchangeably.

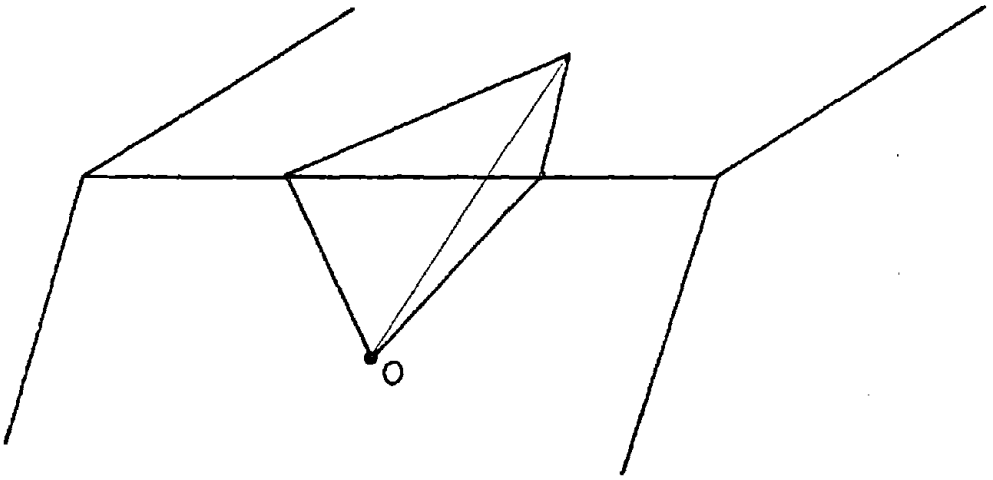

FIGURE 2.1 2-JOINT WEDGE

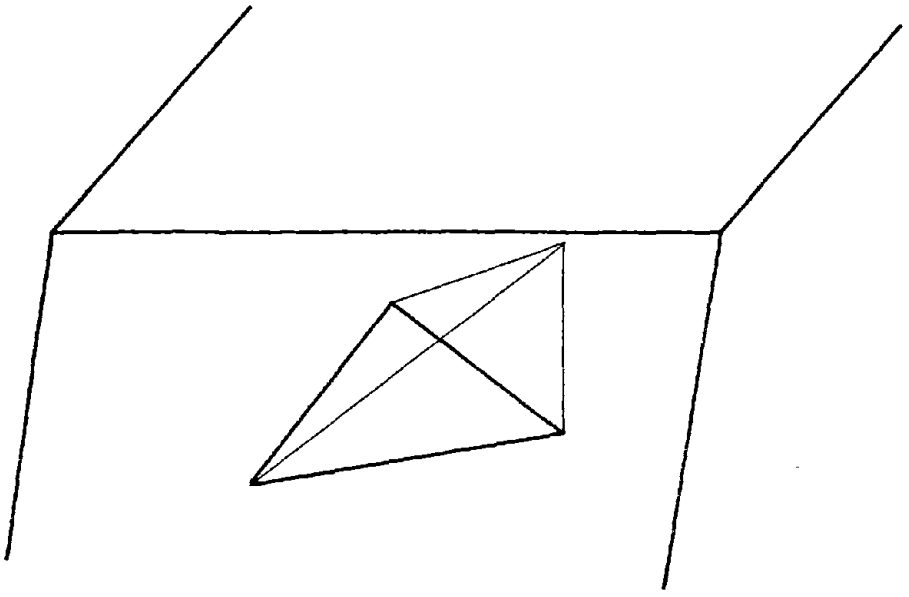

FIGURE 2.2 3-JOINT WEDGE

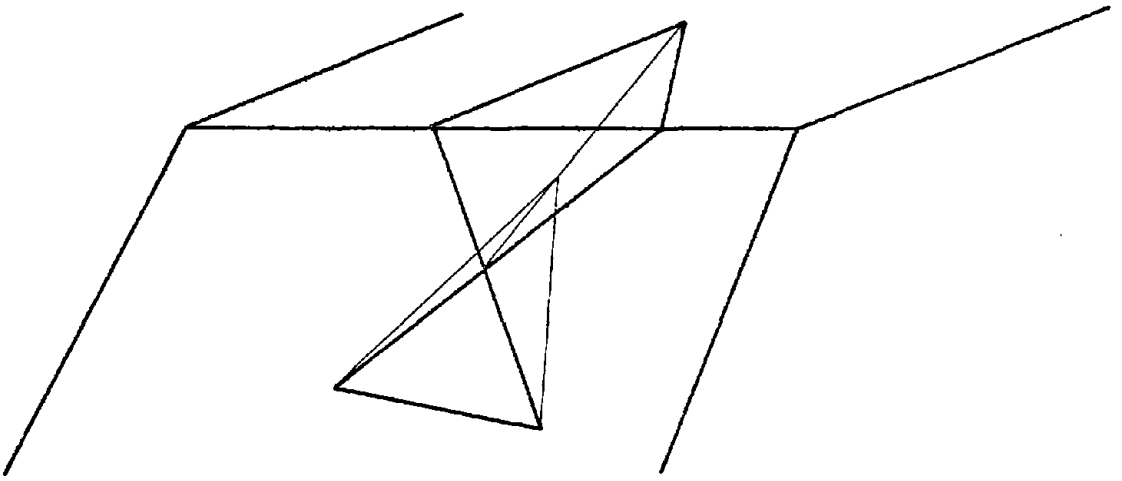

FIGURE 2.3 2- AND 3- JOINT WEDGES

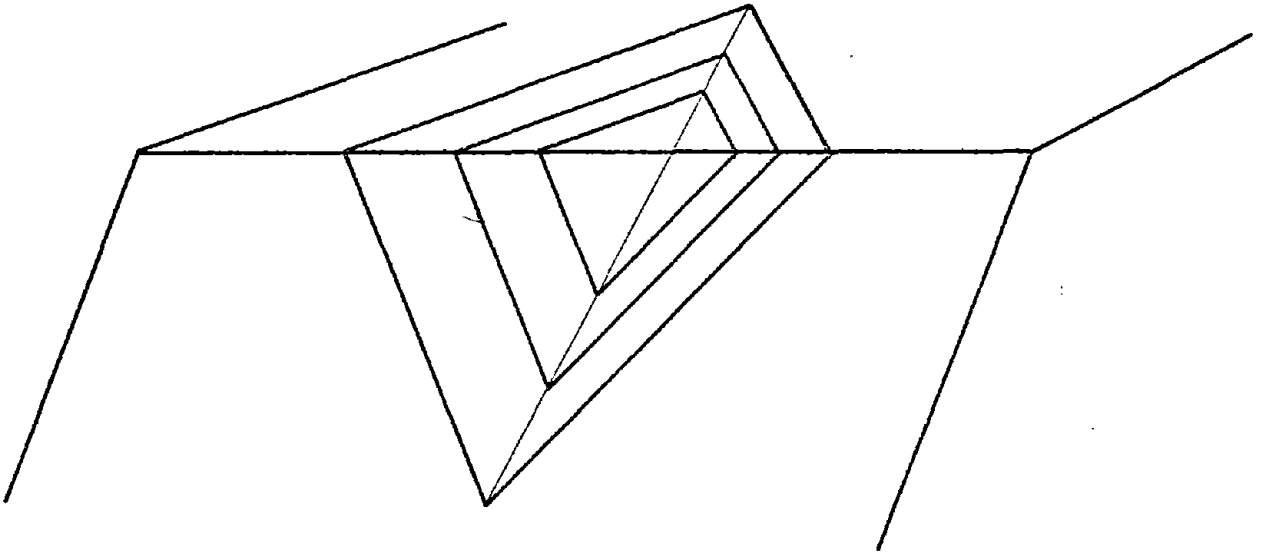

FIGURE 2.4 SETS OF JOINTS FORMING WEDGES

discontinuity at a specific location or it may be part of a joint set. A joint set usually consists of non-parallel or sub-parallel joints as was discussed in Part I Chapter ; a first and usual approximation in deterministic analyses is to assume parallelity of joints within a set).

Slope and joints combine to form typical wedges as shown in Figures 2.1 to 2.4. In addition to the wedges there are other typical bodies that can be formed like the blocks in Figures 2.5a,b.

- Weight: this is the prime driving force determined by wedge geometry and rock unit weight.
- Joint shearing resistance: the resistance (strength) of the joints can be expressed with the Coulomb parameters c, Φ for actually jointed parts and for intact rock bridges. (Joints are thus usually considered in a simplified manner to be a plane consisting of jointed parts and intact rock bridges.) This issue will be discussed extensively in Part III.
- Water: this factor has a significant effect reducing stability through increase of the driving forces and by decreasing the resistance (the effective stresses and thus the frictional component $\bar{\sigma} \tan \Phi$ of resistance). A problematic aspect regarding water pressure is the usually unknown distribution. A maximum is hydrostatic pressure distribution as shown in Figure 2.6a; this can occur if the joint exit on the slope is blocked e.g., through ice. A more frequently occurring distribution will be that of Figure 2.6b, but the location of the maximum is usually unknown. Sometimes uniform pressure along the entire discontinuity is assumed a convenient but often not realistic simplification.
- Other forces (Figure 2.7) : surcharges and earthquake contribute to instability while bolts or anchors are used to increase stability. Complicating the

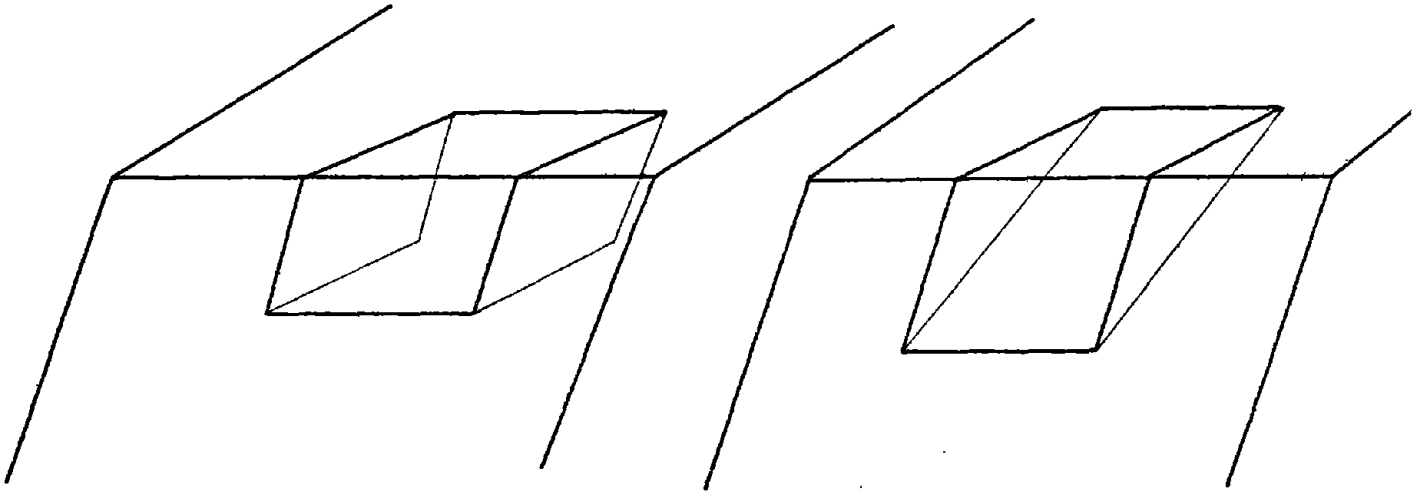

a) b)

FIGURE 2.5 a,b BLOCKS FORMED BY JOINTS

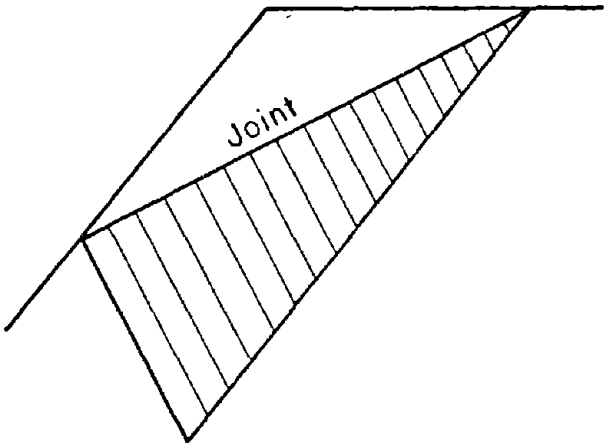

FIGURE 2.6a HYDROSTATIC WATER PRESSURE DISTRIBUTION

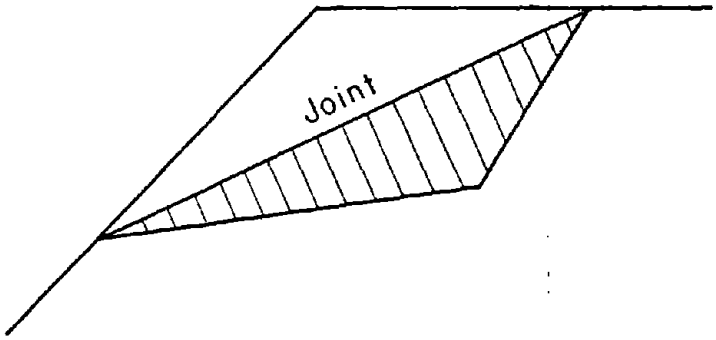

FIGURE 2.6b 'USUAL' WATER PRESSURE DISTRIBUTION

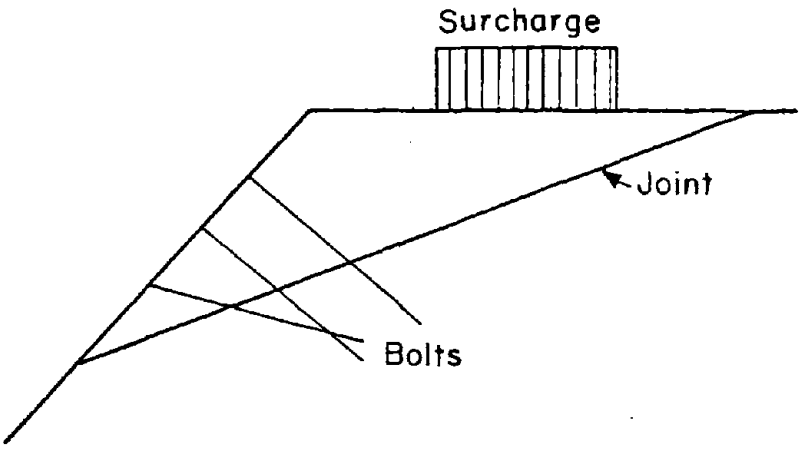

FIGURE 2.7 EXTERNAL FORCES

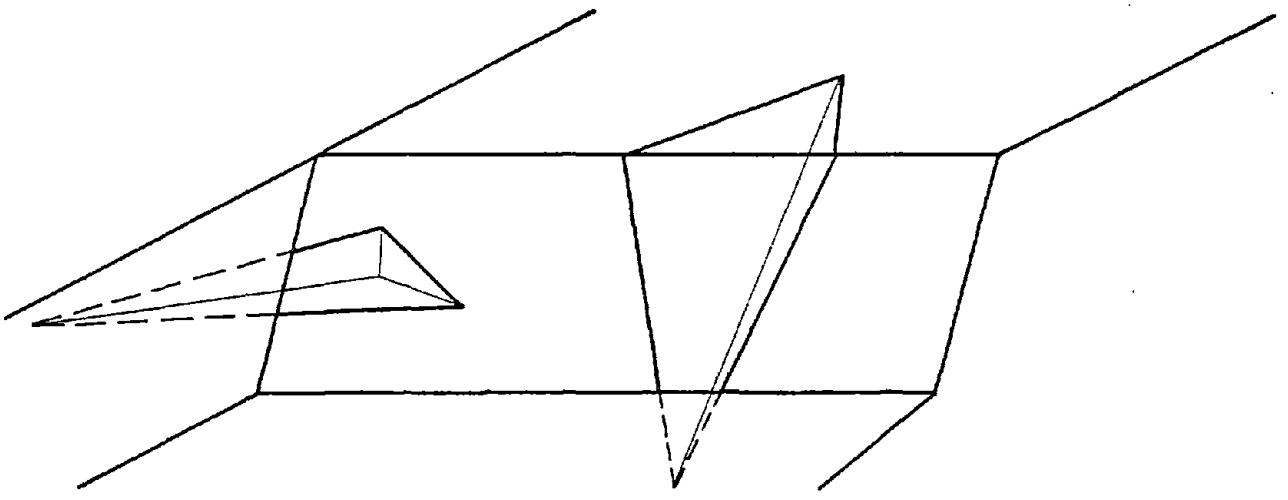

FIGURE 2.8 WEDGES THAT ARE KINEMATICALLY RESTRICTED BY THE SLOPE GEOMETRY

consideration of surcharges and bolt forces is the fact that they usually do not act through the center of gravity of the wedge. Earthquake forces act through the center of gravity but their direction and magnitude is not known.

There are thus a multitude of factors influencing stability of wedges or blocks. In addition, one has to be aware of the fact that wedges or blocks can become unstable in a variety of modes. This issue will be discussed extensively in Chapter 5 and other authors have done this to one extent also (Hendron et al., 1971; Wittke, 1965; Londe et al., 1969; Goodman et al., 1976). Briefly, wedges (or blocks) can either slide, topple about an edge or corner, or be lifted off. If sliding occurs it can be purely translational on one plane or on two planes (along the line of intersection); it can be rotational or a combination of rotation and translation. The stability analysis is usually conducted in two stages, the kinematic and kinetic stability analysis.

The kinematic analysis examines which movements can occur. First of all the lines of intersection of joint planes i.e., the wedge edges within the rock mass have to intersect the slope. Wedges whose apices are beyond the slope face (Figure 2.8) or that are tapered (Figure 2.9) cannot move. In a more refined consideration wedges with acute angles at the apex are restricted if not prevented from toppling moments and rotational sliding movements (for further discussion see e.g., Goodman (1976) or Wittke (1964)). An important point to be made here, is the fact that the rigid body assumptions makes many movements kinematically inadmissable that would be possible if relatively small deformations could take place. The kinematic analysis is basically used to reduce the number of bodies whose kinetic stability needs to be investigated.

In the kinetic analysis driving forces (weight, water, external driving forces, earthquake forces) are compared to the resisting forces (shearing resistance of joints and external resisting forces), i.e., the limit equilibrium analysis is conducted. Usually the ratio resisting/driving forces i.e., a factor of safety is computed, often also a safety margin (resisting forces minus driving forces). Although often not done,

moments should be considered in the limit equilibrium analysis and in the safety factor. A universally applicable wedge stability analysis procedure should thus, for a particular slope geometry:

- combine all joints to all possible wedge shapes
- compute the associated weights
- apply appropriate water and other forces
- check the critical mode of failure for each wedge
- compute the factor of safety or other indicator of stability (instability) for the wedge
- list stable and unstable wedges.

The user can then change slope geometry or stabilizing forces (e.g., bolts) or both and eliminate unstable wedges. (Recall that this is a purely deterministic approach, uncertainty in all influencing factors does thus not enter into the analysis). None of the available methods has the desired capabilities. Most require the input of specific geometries and forces and simply conduct the necessary vector computations. The furthest developed method, SWARS-2P permits the user to specify up to eight joints* and various force options, the procedure then goes through many possible combinations of forces and geometries and lists stable and unstable wedges. The method is however limited by considering only two joint wedges and translational sliding failure. Assuming the SWARS-2P procedure to be the most advanced one (others may have individual features that are better, but overall they do not reach the level of SWARS-2P), the following limitations can be identified.

- 2 joint wedges only (no 3 wedges, no blocks)
- maximum number of 8 joint (sets) that can be combined to form wedges
- consideration of translational sliding only
- forces have to go through the center of gravity

SWARS as described below will remove or reduce these limitations.

*A 'joint' represents a joint or a set of many parallel joints.

2.2 SWARS - Principle and Capabilities

(Details on the procedure and underlying analysis will be given in Section 2.3.)

Geometry:

SWARS combines up to eight (or if desired, more) joints (joint sets) into 2-joint and 3-joint wedges for a particular slope and top of the slope as shown in Figure 2.1 and 2.2. With appropriate analysis on the wedge forming joints (see Section 2.3) it is possible to derive directly combinations that can kinematically move in an infinite slope, i.e., tapered wedges (2.9) or wedges that would have to slide upward are automatically excluded. In a second step slope (and top of slope) size limitation can be introduced, specifically the crest length and slope height (Figure 2.10). This further reduces the number of kinematically possible wedges. Also, if desired, other size limitations may be introduced in order to define wedges that are smaller than the slope (2.11) would allow; this last capability is necessary for the study of remedial actions, like bolt application.

Comparing these capabilities with the above mentioned desirable ones, two restrictions remain: the maximum number of joints (8) from which wedges can be formed and the exclusion blocks. The number of available joints (sets) rarely exceeds eight and is usually smaller; thus this limitation has been kept as standard procedure. However the program is written such that only a card needs to be changed to accomodate a larger number. Blocks can be considered to be "truncated 2-joint or 3-joint wedges." Only if the effect of area dependent forces (cohesion, water) differs between a truncated and a complete wedge, will the simplification of considering only complete wedges introduce errors. A future version will have to include a specific block treatment, particularly when more is know about the failure mechanism (see Chapter 5). For the time being and in view of the uncertainty associated with the area dependent forces, the simplification is justified.

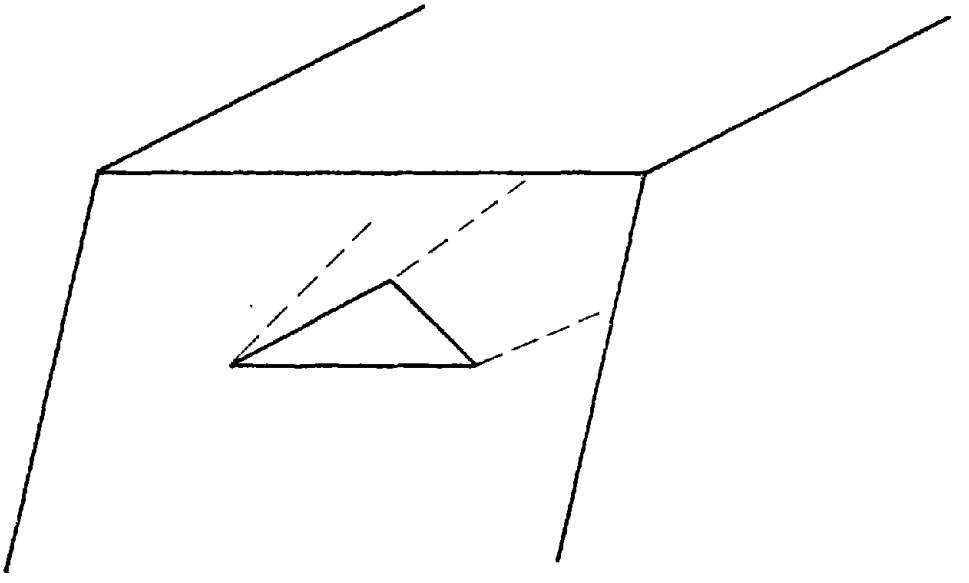

FIGURE 2.9 TAPERED WEDGE
(APEX OUTSIDE SLOPE)

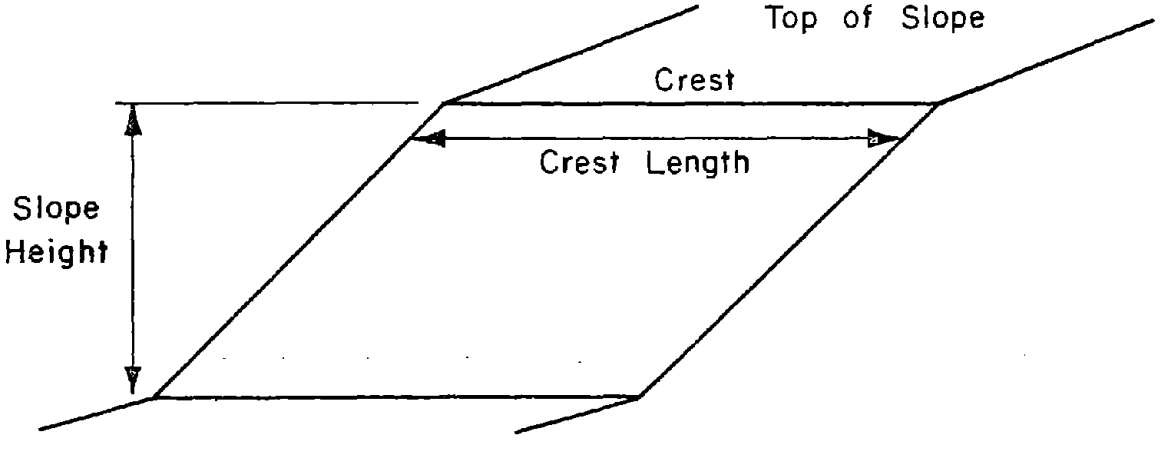

FIGURE 2.10 DEFINITIONS

Driving Forces:

In addition to weight, two water pressure options can be treated, a uniform water pressure acting on the entire respective joint plane and a hydrostatic water pressure below a user specified horizontal water level (see Figure 2.12). These water pressure options are approximations of the most likely pyramid-shaped distribution. Nevertheless the hydrostatic assumption is the extreme case that can occur if the joint exits are blocked.

Seismic effects can also be handled by SWARS. The present option is to specify direction and magnitude of a seismic force acting through the center of gravity. Caution should be exercised in chosing the acceleration values as discussed by Seed (1973). The 'seismic resistance option' by which the direction and magnitude of a seismic force is determined that just reduces the factor of safety to one, is a part of the program but not included in the standard output. Difficulties in interpretation make the use of this option problematic (Campbell 1974).

The most important innovation is the possibility to introduce point loads at arbitrary points and in arbitrary directions (not through the center of gravity) apart from or in addition to considering a uniform surcharge. A severe and unrealistic restriction has thus been removed.

Resisting Forces:

The resisting forces are of the Coulomb type consisting of a cohesion component, a friction angle component, an asperties angle component and including the possibility of considering the effect of persistence (through a multiplier of the cohesion components) i.e., $S=(1-p)\ C + N \tan (\Phi + i)$. An important feature of SWARS is the determination of two factors of safety for each wedge, one with the full Coulomb resisting forces (including friction angle, asperity angle and cohesion (persistence)), the other with only friction angle approximating the residual resistance. In this manner it is possible to consider the effect of small movements that may reduce the resisting forces to their residual value. Also depending on the purpose of the project under consideration a more or less conservative design may be based on these factors of safety.

In addition, bolt forces can be handled; they can be expressed similarly to the point loads above, i.e., acting in arbitrary locations and directions and not necessarily through the center of gravity. This again is a significant advance since it makes a realistic introduction of bolt action possible. It makes SWARS particularly attractive in connection with the aforementioned wedge size limitation. Bolts can be specified differently for different wedges and their effect can be analyzed separately. The danger of designing a bolting pattern for a large wedge that would allow a smaller internal wedge to become unstable is thus strongly reduced.

Mode of Failure:

Although still not considering all modes of failure, SWARS has been expanded beyond its predecessors to include for 2-joint wedges:

- Translational sliding along any one or both planes
- Lifting off both planes
- Toppling about the lower apex (point 0 Figure 2.1)
- Toppling about any of the edges

for 3-joint wedges:

- Translational sliding along any one plane
- Translational sliding along any combination of two planes
- Lifting off from all three planes

Not considered are thus the toppling of 3 joint wedges and rotational sliding modes. Toppling is relatively rare in case of 3 joint wedges (due to kinematic restraints except for wedges that are simultaneously very shallow and steep (Figure 2.13)). Rotational sliding will be discussed extensively in Chapter 5; it is often the critical mode if the forces not acting through the center of gravity are large compared to those acting through the center of gravity. Since rotation of wedges, if treated completely, involves additional kinematic constraints and double modes of failure (rotation in one plane, together in translation in the other) it was decided not to include it in SWARS. However Chapter 5 amongst other things provides an analytic approach and associated computer program to examine rotational modes of failure.

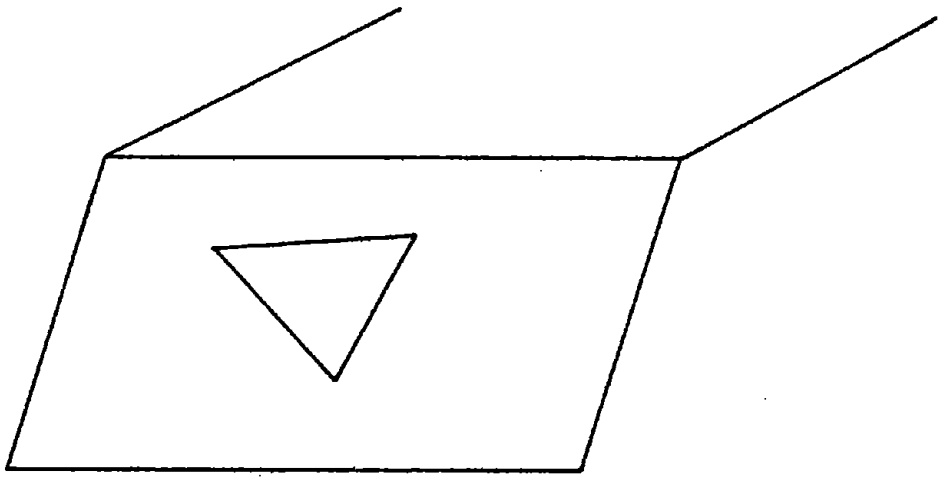

FIGURE 2.11 WEDGE SMALLER THAN SLOPE DIMENSIONS

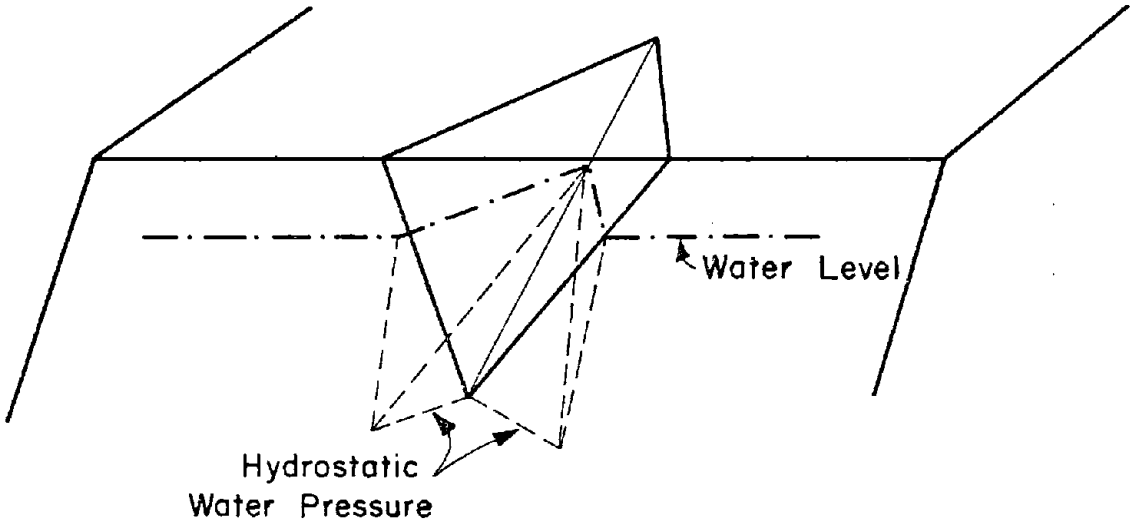

FIGURE 2.12 HYDROSTATIC WATER PRESSURE ON WEDGE

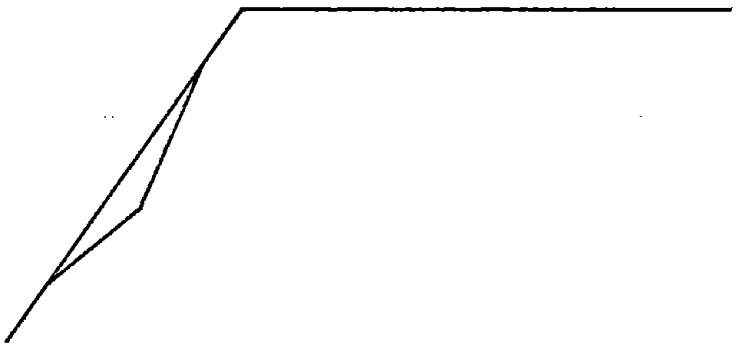

FIGURE 2.13 STEEP SHALLOW WEDGE

Also the criteria are given there, (Chap. 5), when rotation becomes critical. The user can check the output of SWARS, which lists wedge geometry and location, direction and magnitude of the resulting force, against these criteria and further examine wedges that are critical with regard to rotation. In this manner it was possible to keep the use of SWARS simple, while having the possibility to treat more complex modes of failure if necessary.

Results of Analysis with SWARS:

For the given joint sets and slope geometry SWARS computes the factors of safety for all possible wedges; these are wedges that can be geometrically formed and that are kinematically unconstrained. The user can specify water, external and earthquake loads on one hand and remedial measures in form of bolts (anchors) on the other hand. By varying the slope geometry and bolting-pattern and forces one obtains an optimum, although deterministic, design.

As mentioned previously some simplifying assumptions still remain in the interest of having a streamlined and efficient program for most practical applications. Limitations exist with regard to geometry (no blocks) and water pressure, although reasonably approximated in the present version. The other limitations, stress field and stiffness effects and additional modes of failure can be studied and analyzed by using the approaches listed in Chapters 4 and 5.

2.3 Swars-Detailed Procedure

While the previous section provided a general review of the capabilities of SWARS, this section will discuss the details. It is a somewhat expanded version of the algorithm discussion in Appendix UM7 and it is mainly intended to provide insight into the underlying analysis procedures. For actual application of the method, the user is referred to the user's manual and program documentation in Appendix UM7.

The user specifies the following:

number of joint sets: Any number up to and including eight

joint geometry: The strike and dip of each joint (set) in geologic notation but strike in the northern quadrant.

ex.: N25E, 60SE

slope geometry: Orientation in form of slope strike (like joint strike) and dip, where dip direction is always away from the slope (Figure 2.14). The slope can be overhanging. The crest of the slope is always assumed to be horizontal and to be parallel to the x- axis of the coordinate system (positive y-axis is horizontal into the slope, the positive z- axis upward (Figure 2.14). If there is a non-horizontal top of slope its angle has to be specified also (Figure 2.14b)· Slope size is defined by its length and height (see Figure 2.14). The additional optional size limitations shown in Figure 2.14 make it possible to define wedges of any desired size.

joint resistance: Friction angle, asperity angle, cohesion and joint continuity (persistence) for each joint.

driving forces: Unit weight of the rock. Water pressure can be introduced as a uniform pressure on a particular joint plane or as hydrostatic pressure below a user specified water level (see Figure 2.15). Two kinds of point forces can be applied one acting through the center of gravity and the other ('specific point load') acting at specific points and in specific directions. Uniform loads and seismic forces can be formulated as point forces of the first kind. Specific point forces require that the wedge on which they act be identified first, by listing the 2 or 3 joint sets which define the wedge (Note that it is possible with the aforementioned feature to limit wedge sizes, to specify the considered wedges even further).

bolt forces: Analogous to specific point forces. The output consists of a listing of wedges (see Appendix UM7). Each wedge is described by: its joint planes and its size, the direction and magnitude of the resulting force the mode of failure, the peak and residual factors of safety. The ouput can be limited to wedges having a factor of safety below a specified limit.

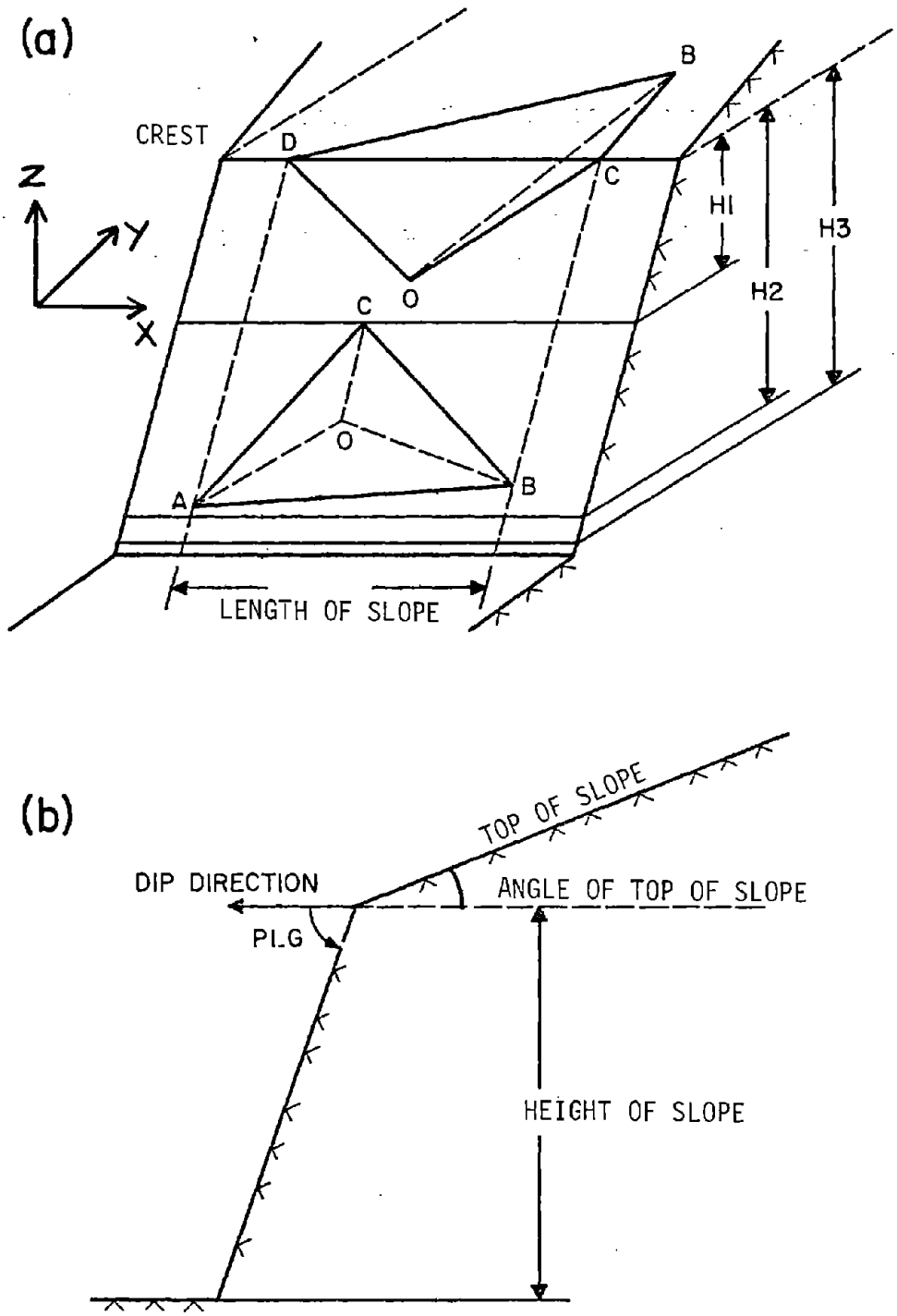

FIGURE 2.14 NOTATION FOR THE SLOPE

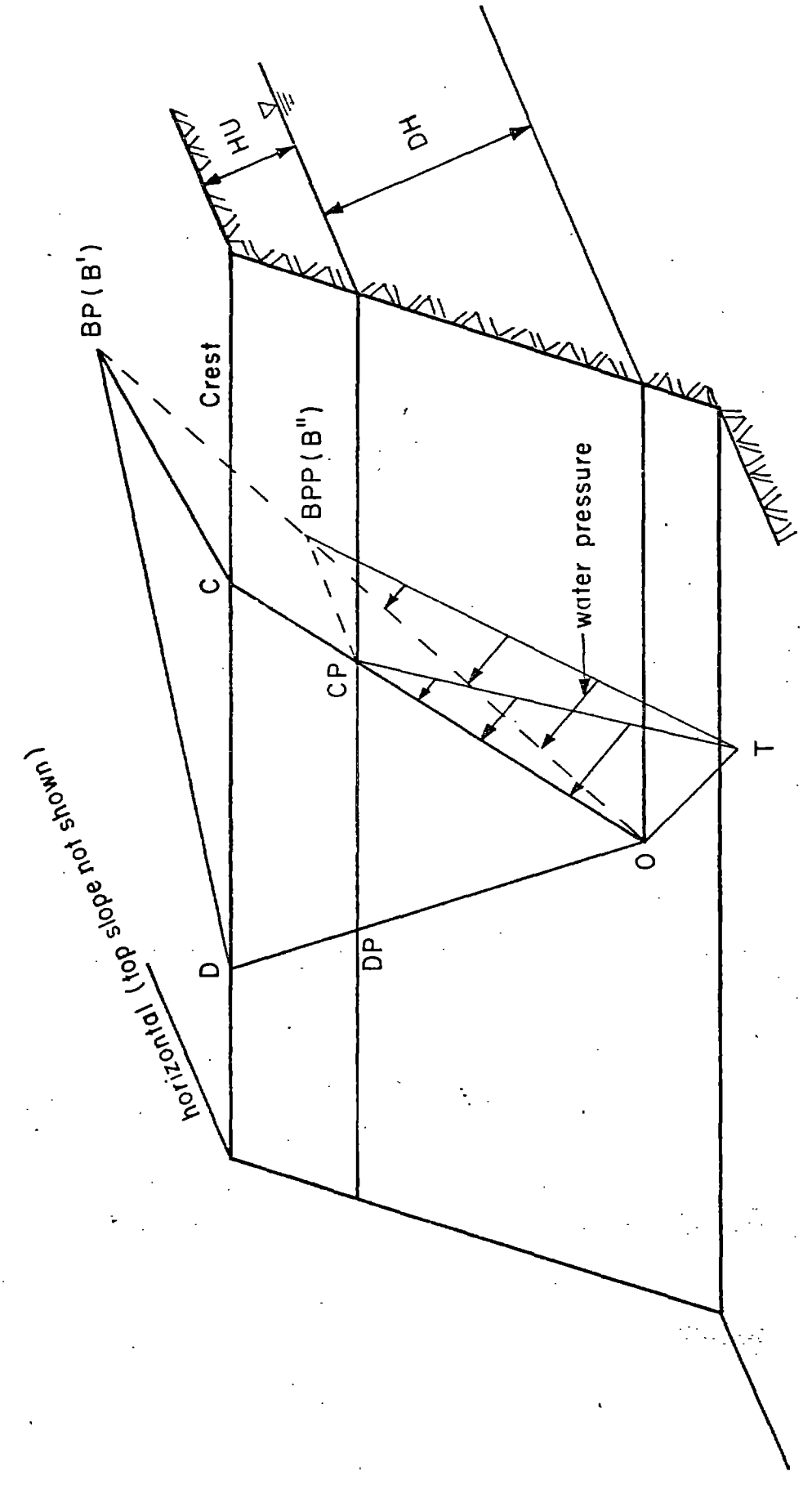

FIGURE 2.15 CALCULATION OF HYDROSTATIC WATER PRESSURE

The main algorithm is shown in Figure 2.16. It is basically the execution of the user's decision to analyze only 2 or 3-plane wedges or both. If a 2 plane analysis is required the joint planes are reordered in ascending order of their strikes. (This makes the computational procedure of forming 2 joint combinations easier.) The only other computation specifically associated with the main algorithm is the determination of the unit normal vectors $\bar{w}$ of each joint plane.

The 2 plane algorithm is listed in Figure 2.17. More of the details of the underlying analysis have been described by Campbell* (1974) and Campbell et al. (1976); they are also very similar to that by Hendron et al. (1971). The analysis first conducts a vector analytical check of the geometric feasibility (can a wedge be formed) and of the kinematics, excluding kinematically constrained wedges and defining the mode of failure. Wedge volume and weight are calculated with basic geometry. Finally the kinetic analysis is performed summing vectorially the driving and resisting forces to yield the factor of safety. There are however some innovative procedures in this analysis that are worthwhile mentioning: toppling failure can occur by toppling about the lower apex '0' (Fig. 2.1) or by toppling about one of the edges. Moments of the applied forces about point 0 are calculated, by first finding the applied force in vector form ($\bar{F}$) and the position vector of its point of application ($\bar{P}$), then the moment vector $\bar{M}$ is given by

$$\bar{M} = \bar{P} \times \bar{F}$$

For example, the moment vector ($\bar{M}_w$) of the weight ($\bar{W}$) is

$$\bar{M}_w = \overline{OS} \times \bar{W}$$

where $\overline{OS}$ is the position vector of the center of gravity of the wedge. For distributed loads, the resultant force vector and its point of application are used.

*A different convention compared to Campbell's regarding positive unit normals has been introduced: they are always pointing into the wedge. This makes the 2 joint and 3 joint analyses consistent.

Figure 2.16 Main Algorithm

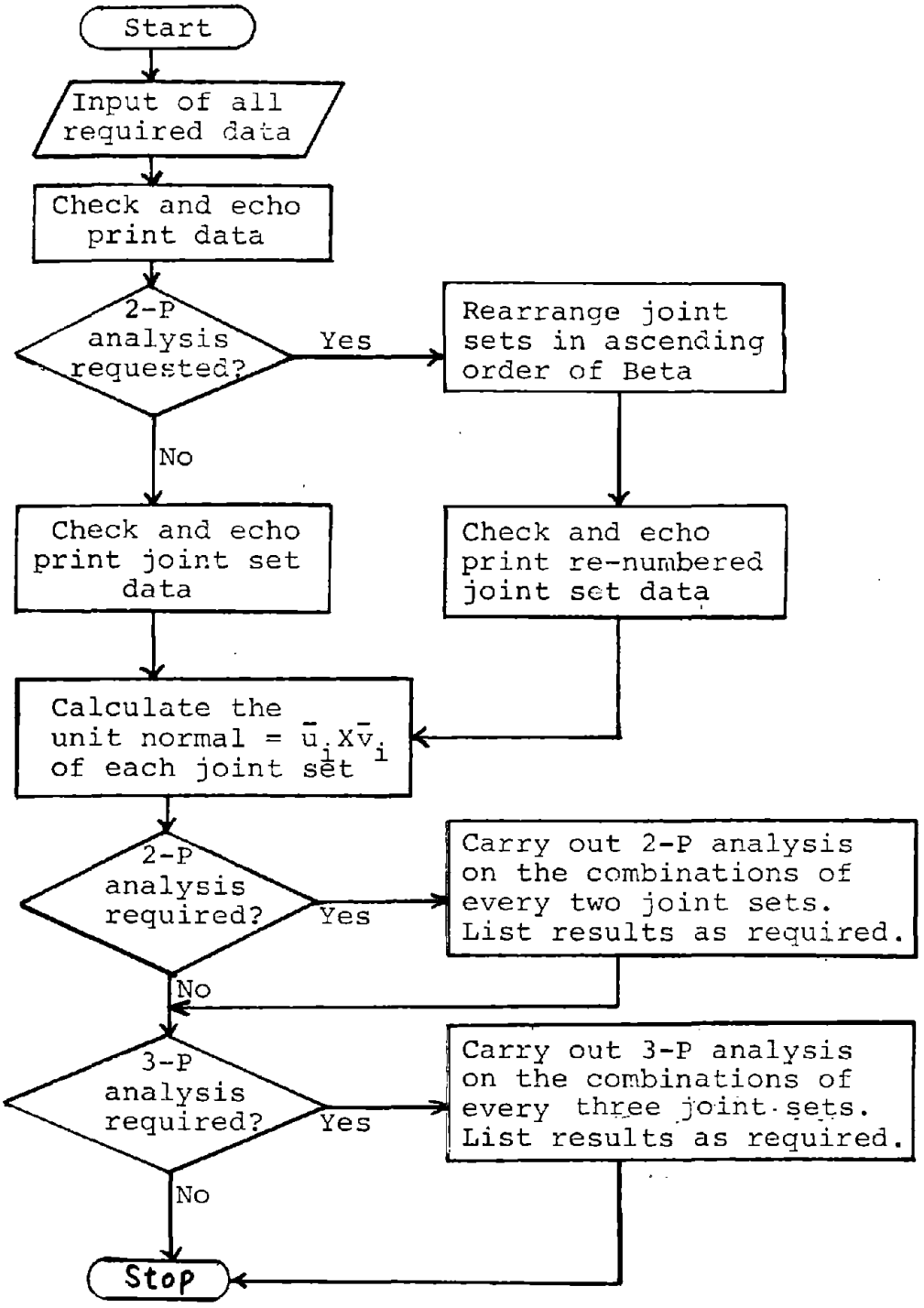

Figure 2.17 Algorithm of 2-P Analysis

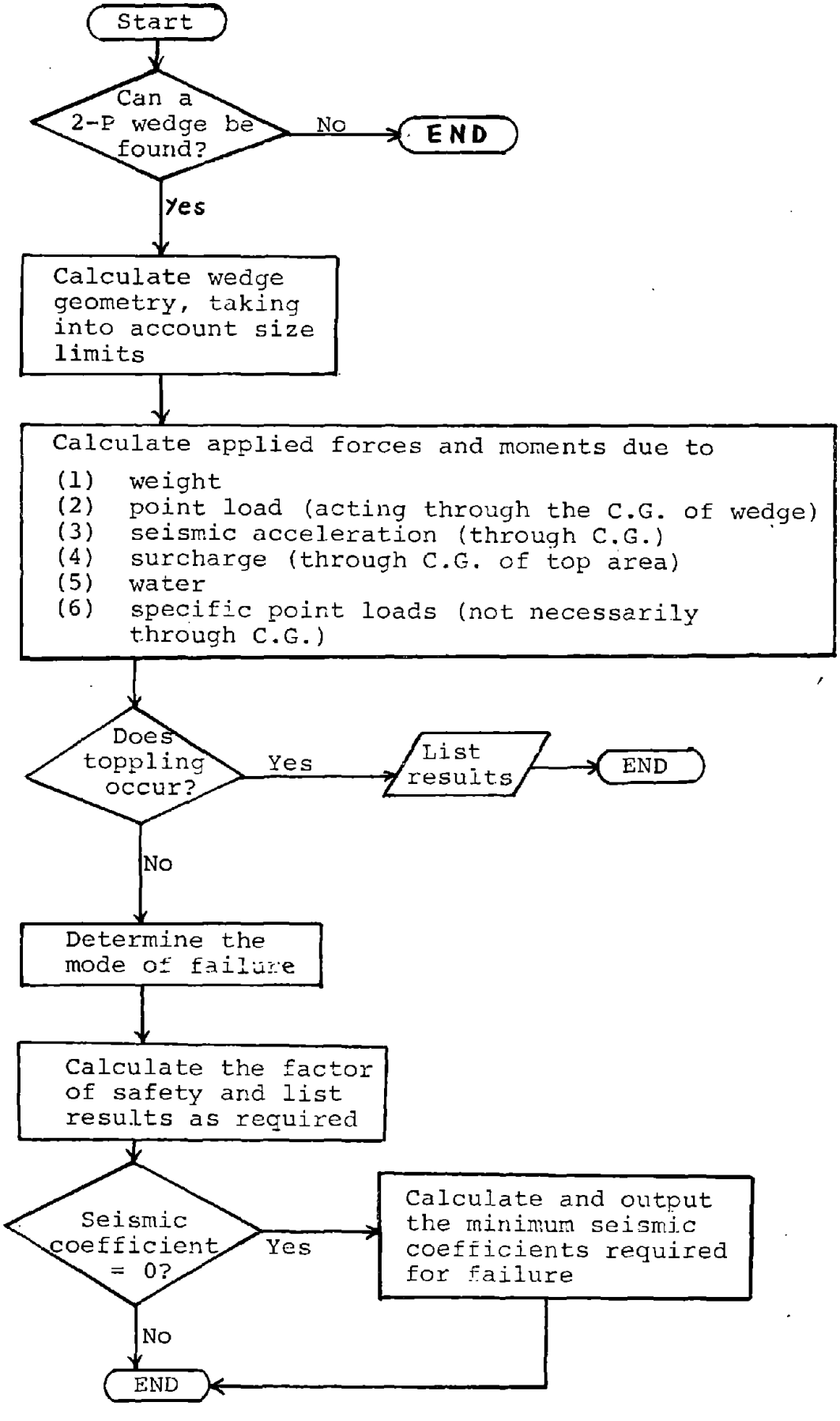

Toppling about an edge can occur when the reactions between the wedge and the base planes, which are assumed to be non-negative, cannot maintain moment equilibrium.

Taking the edge OD of the wedge in Figure 2.18a as an example, it will depend on the applied forces and their corresponding points of application whether the wedge will rotate out of the slope about the edge. However, one needs only to look at $\bar{R}$ (the resultant force vector which acts through the point 0) and $\bar{M}_o$ (the resultant moment vector of the applied forces about 0) since they are equivalent to the set of applied forces. Since $\bar{R}$ intersects the axis OD, it cannot cause a toppling moment about OD and the condition for toppling depends on $\bar{M}_o$ only: $\bar{M}_o \cdot \overline{OD} < 0$. Similarly, the condition for toppling about OC is: $\bar{M}_o \cdot \overline{OC} > 0$.

In contrast, the conditions for toppling about DB and CB depend on $\bar{R}$ too because it causes a moment about these edges. The respectve conditions are:

$$(\bar{R} \times \overline{OD} + \bar{M}_o) \cdot \overline{DE} < 0$$

$$(\bar{R} \times \overline{OC} + M_o) \cdot \overline{CB} > 0$$

It is important to note that there are kinematic conditions under which the wedge cannot topple. In the present version of SWARS it is assumed that if the angle between the two joint planes is less than 90 degrees, toppling about an edge is not considered.

The <u>three plane algorithm</u> (Figure 2.19) is analogous to that of the 2 plane analysis. The analysis follows the same procedure as before geometric feasibility and kinematic check -- wedge volume calculation -- kinetic analysis. The geometric calculations are now however quite complex and the associated method of analysis is one of the significant new developments.

<u>Formation of a 3-P Wedge</u>

The necessary and sufficient conditions for the formation of a 3-P wedge from joint planes (I), (J), and (K) and the slope face are that the three joints meet at a point and that any two of the joints and the slope face meet at a point. The shape of the 3-P wedge formed is unique (see Figure 2.20) once these conditions are satisfied. The

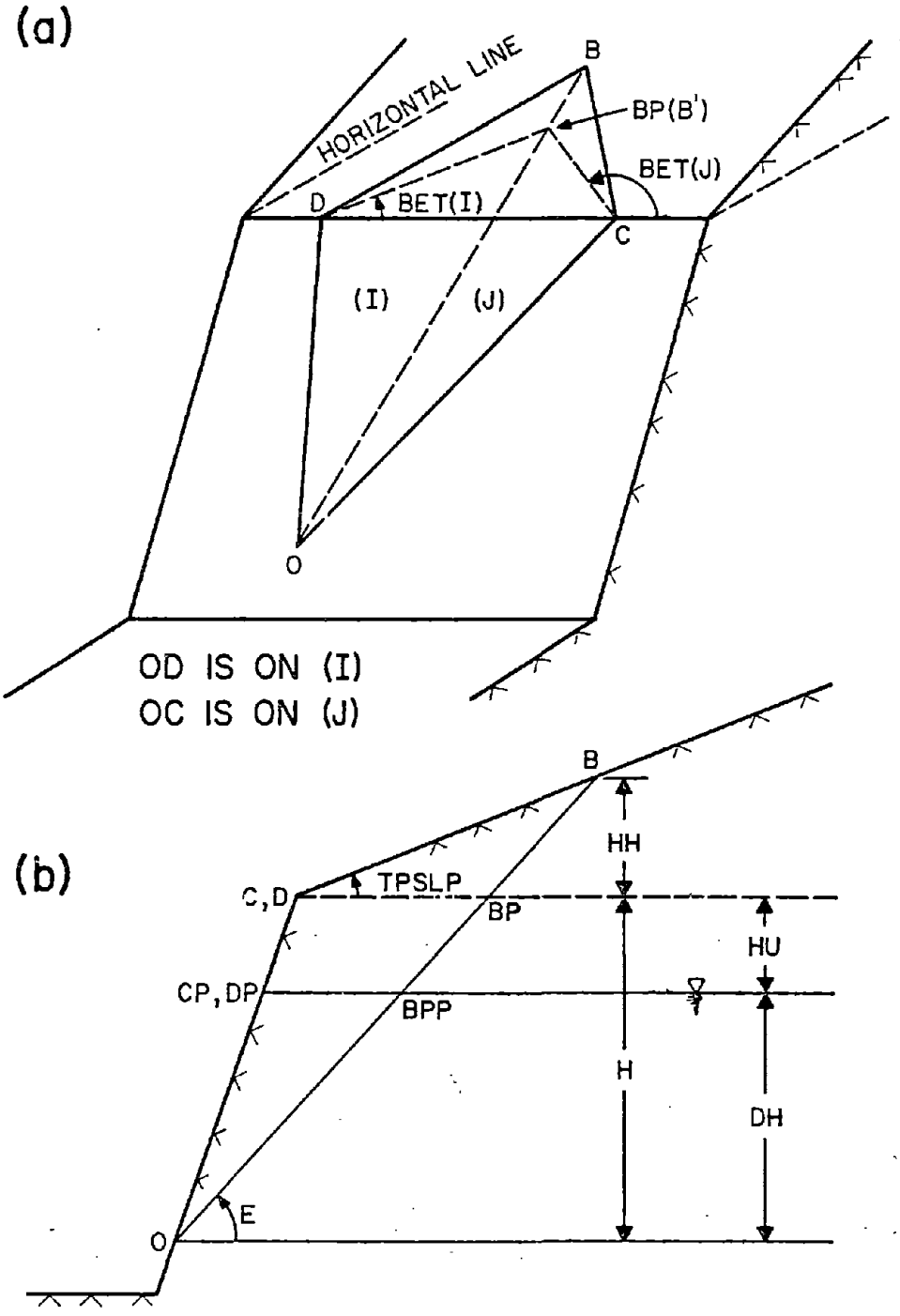

FIGURE 2.18 NOTATIONS FOR A 2P' WEDGE

Figure 2.19 Algorithm of 3-P Analysis

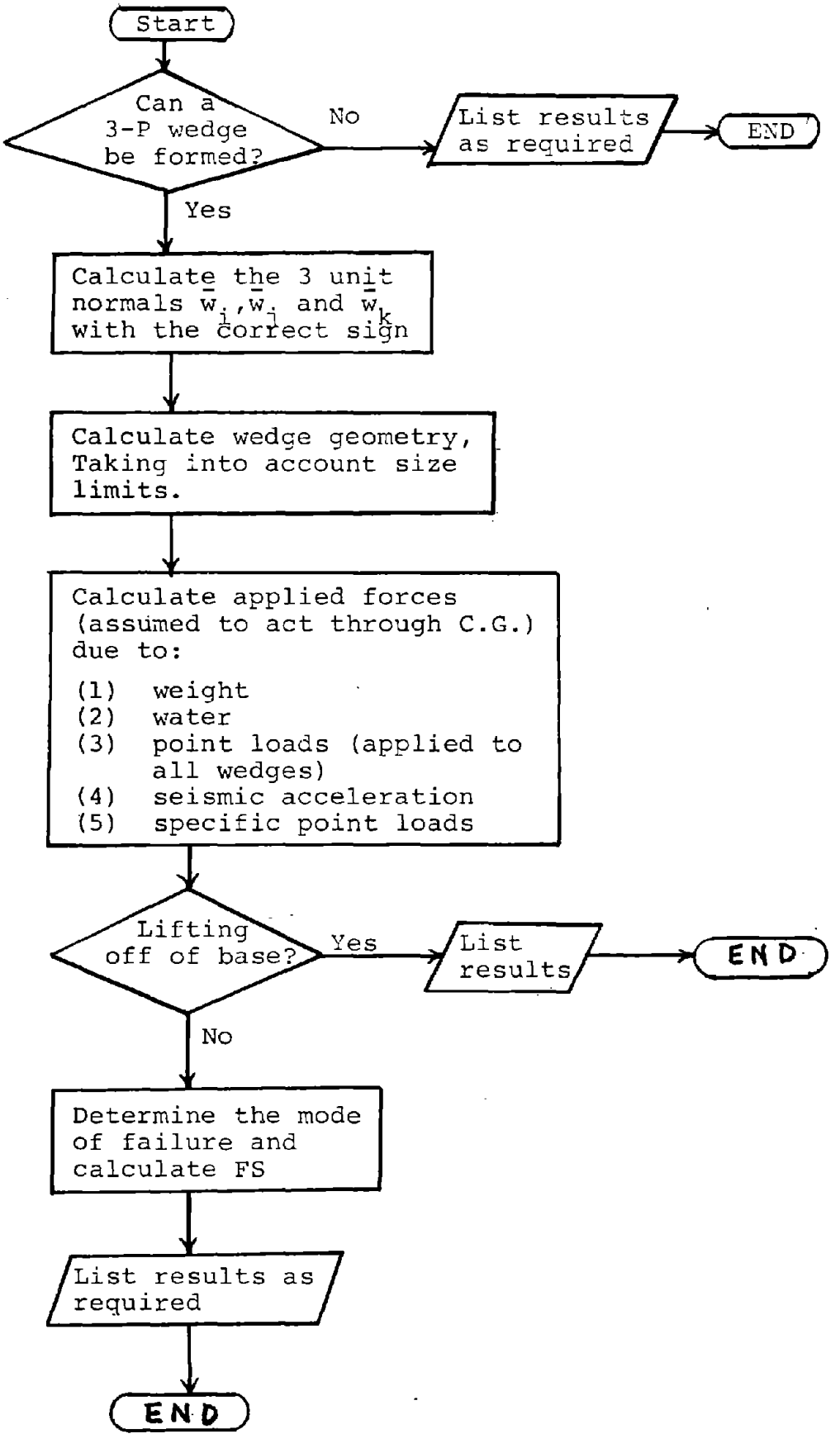

positions of the 3 joints and the slope face do not affect the shape of the wedge. Wedge geometry is defined by the intersection vectors $\bar{X}$, the unit normals $\bar{W}$ and the intersection normals $\bar{S}$ (see Figure 2.20). The intersection vectors $\bar{X}_{ij}$, $\bar{X}_{jk}$ and $\bar{X}_{ki}$ are defined such that they all point towards the slope face. The three unit normals $\bar{W}_i$, $\bar{W}_j$ and $\bar{W}_k$ all point into the 3-P wedge and the vectors $\bar{S}_{ij}$, $\bar{S}_{jk}$, $\bar{S}_{ki}$, $\bar{S}_{ji}$, $\bar{S}_{ik}$; $\bar{S}_{kj}$ are defined as shown in Figure 2.20. Algebraically the following holds:

$$\bar{X}_{ij} = \pm \bar{W}_i \times \bar{W}_j$$

$$\bar{X}_{jk} = \pm \bar{W}_j \times \bar{W}_k$$

$$\bar{X}_{ki} = \pm \bar{W}_k \times \bar{W}_i$$

$$\bar{S}_{ij} = \pm \bar{W}_i \times \bar{X}_{ij}$$

$$\bar{S}_{jk} = \pm \bar{W}_j \times \bar{X}_{jk}$$

$$\bar{S}_{ki} = \pm \bar{W}_k \times \bar{X}_{ki}$$

$$\bar{S}_{ji} = \pm \bar{X}_{ij} \times \bar{W}_j$$

$$\bar{S}_{ik} = \pm \bar{X}_{ki} \times \bar{W}_i$$

$$\bar{S}_{kj} = \pm \bar{X}_{jk} \times \bar{W}_k$$

When one faces the slope face and looks at the three joint planes (I), (J) and (K), the positive signs of all the above equations hold if (I), (J) and (K) are in anti-clockwise order. The negative signs hold if they are in a clockwise order.

However, the correct signs for the three unit normals are not known beforehand. The problem can be solved by first determining the correct signs for the intersection vectors $\bar{X}_{ij}$, $\bar{X}_{jk}$ and $\bar{X}_{ki}$. $\bar{X}_{ij}$ has the correct sign if

$$\bar{X}_{ij} \cdot \bar{W}_o < 0$$

where $\bar{W}_o$ is the unit normal of the slope face (Figure 2.20b). The correct signs for $\bar{X}_{jk}$ and $\bar{X}_{ki}$ are determined similarly by the inequalities:

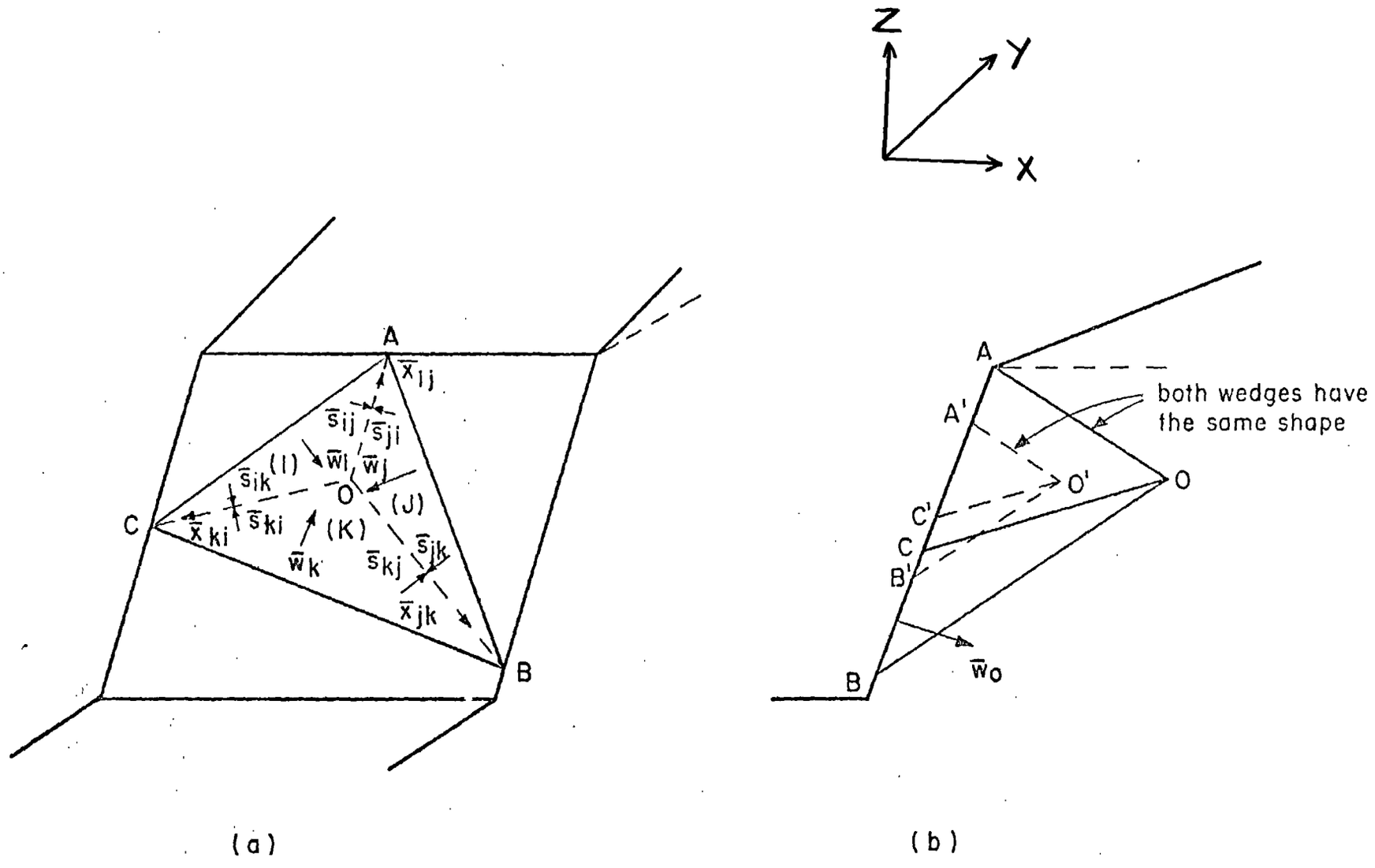

FIGURE 2.20 VECTOR NOTATIONS AND SHAPE OF A 3-P WEDGE

$$\bar{X}_{jk} \cdot \bar{W}_o < 0$$

$$\bar{X}_{ki} \cdot \bar{W}_o < 0$$

After the correct values for $\bar{X}_{ij}$, $\bar{X}_{jk}$ and $\bar{X}_{ki}$ are calculated, the following products are formed:

$$\bar{W}_j = \bar{X}_{ij} \times \bar{X}_{jk}/(|\bar{X}_{ij}| \cdot |\bar{X}_{jk}|)$$

$$\bar{W}_k = \bar{X}_{jk} \times \bar{X}_{ki}/(|\bar{X}_{jk}| \cdot |\bar{X}_{ki}|)$$

$$\bar{W}_i = \bar{X}_{ki} \times \bar{X} \quad /(|\bar{X}_{ki}| \cdot |\bar{X}_{ij}|)$$

These three vectors are the unit normals to the three joint planes and they are either all pointing into the wedge or all pointing out. If they all point into the wedge, $\bar{W}_k \cdot \bar{X}_{ij} > 0$. If not, their signs have to be reversed to yield the correct unit normals.

Once the three unit normals are known to be $\bar{W}_i$, $\bar{W}_j$ and $\bar{W}_k$, they are assumed to be in a clockwise order and the following products are formed:

$$\bar{S}_{ij} = \bar{X}_{ij} \times \bar{W}_i$$
$$\bar{S}_{jk} = \bar{X}_{jk} \times \bar{W}_j$$
$$\bar{S}_{ki} = \bar{X}_{ki} \times \bar{W}_k$$
$$\bar{S}_{ji} = \bar{W}_j \times \bar{X}_{ij}$$
$$\bar{S}_{ik} = \bar{W}_i \times \bar{X}_{ki}$$
$$\bar{S}_{kj} = \bar{W}_k \times \bar{X}_{jk}$$

Simultaneously with describing the wedge geometry, it is also necessary to satisfy the geometric feasibility and kinematic requirements. Geometric feasibility requires that the joint planes and the slope plane are not coplanar i.e.,

$$\bar{W}_1 \ (\bar{W}_2 \times \bar{W}_3) \neq 0$$

$$\bar{W}_o \ (\bar{W}_1 \times \bar{W}_2) \neq 0$$

$$\bar{W}_o \ (W_2 \times \bar{W}_3) \neq 0$$

$$\bar{W}_2 \ (W_3 \times \bar{W}_0) \neq 0$$

Kinematic constraints consist of several conditions:

1) Apex '0' should not be below A,B,C (Fig. 2.10) this can be fulfilled if at least one of the vertical (z-axis) components of the intersection vectors is equal or smaller than zero:

$$\text{at least one} \quad \begin{cases} \bar{X}_{12} \cdot \hat{k} \leq 0 \\ \bar{X}_{23} \cdot \hat{k} \leq 0 \\ \bar{X}_{31} \cdot \hat{k} \leq 0 \end{cases}$$

when $\hat{k}$ = unit vector in z - direction

Although 'upward movement' is under rare circumstances possible, (e.g., combination of seismic and water forces), it is not considered admissable in SWARS. If this condition needs to be relaxed it is possible to introduce other specific inclination limits).

2) At least one of the lines of intersection has to be inclined downward and has to intersect the slope:

0 < inclination of line of intersection < slope angle

$$0 < |\hat{k} \cdot \bar{X}_{12}| < |\hat{k}\bar{W}_o|$$

$$0 < |\hat{k} \cdot \bar{X}_{23}| < |\hat{k}\bar{W}_o|$$

$$0 < |\hat{k} \cdot \bar{X}_{13}| < |\hat{k}W_o|$$

3) The kinematic constraint due to slope size is introduced by comparing the maximum vertical and horizontal extent of the wedge to the height and length limits.

Static Water Pressure

To calculate the force acting on a joint plane of a 3-P wedge due to static water pressure, one first considers the general situations shown in Figure 2.21. OPQ in each of the three cases (a), (b) and (c) is the projection of the joint plane onto the Y-Z plane.

In each case the part of the joint plane under the water level ST is composed of a trapezoid and an inverted triangle. The total water force on the joint plane can be found by summing up the forces on the trapezoid and the triangle. The water force on the trapezoid ORST (see Figure 2.22 is calculated by

$$PVU = \int_0^{GW} GW*h*(\frac{HT - HS + h}{HT})*RL*dh = \frac{1}{6}(GW)(RL)(HS)^2(3HT-HS)/HT$$

where GW = unit weight of water and the other terms are defined in Figure 2.22.

The water force on the triangle RQ is given by

$$PVL = (GW)(HS)(\Delta ROQ) + (GW)(ZQO)(\Delta ROQ)/3$$

where (ZQO) = magnitude of the Z-component of $\overline{QO}$ and (ΔROQ) = area of the triangle ROQ.

Summing PVU and PVL yields PV (PV = PVU + PVL) the magnitude of the X - component of the water force on the plane. The water force vector is then given by

$$\overline{FW} = (PV/|WX|)\,\bar{W}$$

where WX = X - component of the unit normal $\bar{W}$.

If the intersection of the joint plane and the slope face is a horizontal line (i.e., WX = 0), the projection of the joint onto the Y - Z plane is a line and the above method cannot be used. In this case the projection of the plane on the X - Z plane may be considered where there are two possibilities shown in Figure 2.23; PV for the two possibilities is also given in Figure 2.23, and the water force vector is

$$\overline{FW} = (PV/|WY|)\,\bar{W}$$

where WY = Y - component of $\bar{W}$.

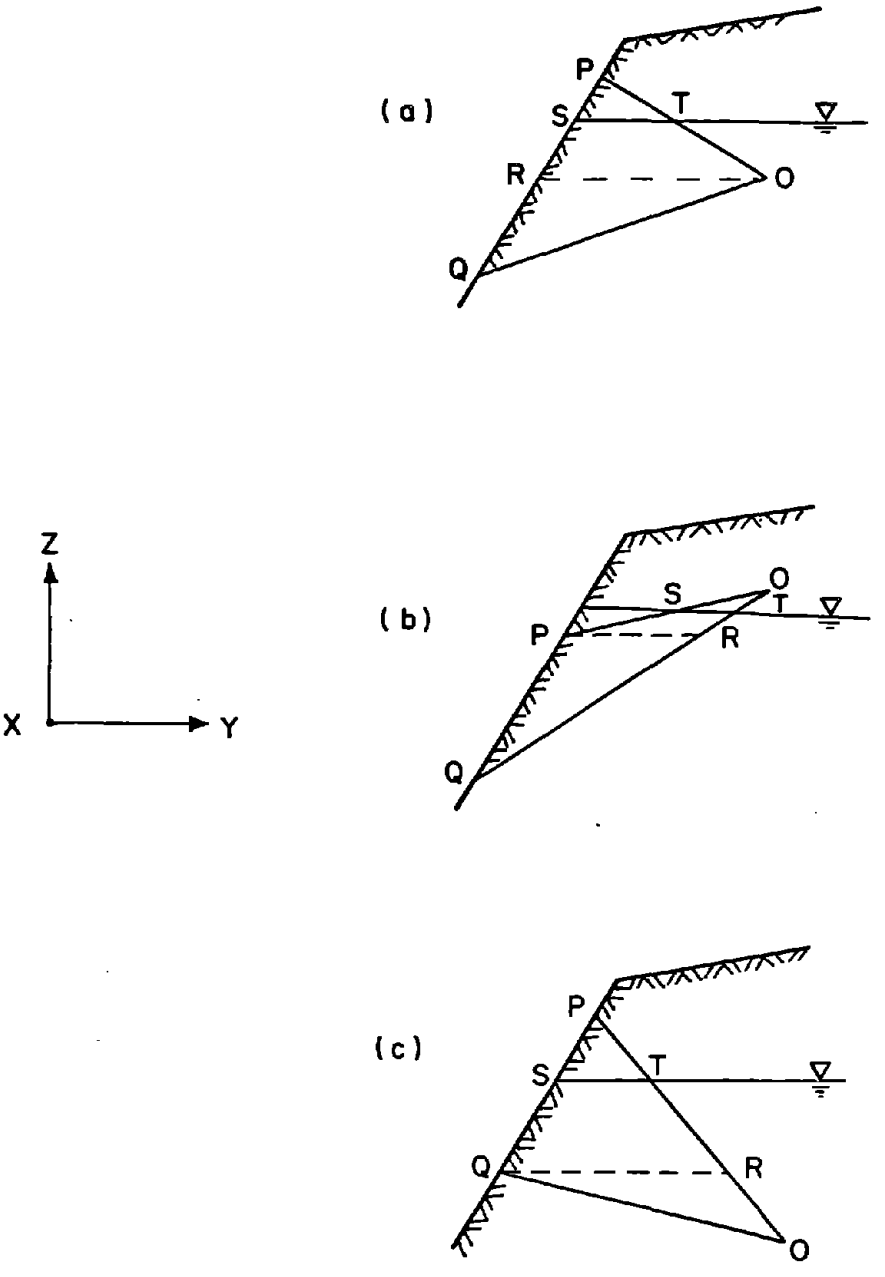

FIGURE 2.21 GENERAL STATIC WATER CONDITIONS

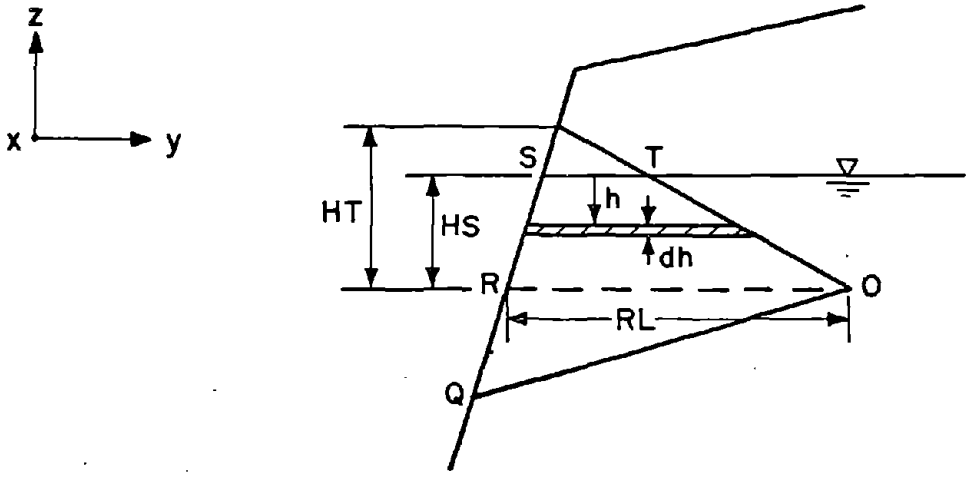

FIGURE 2.22 STATIC WATER PRESSURE

If both WX and WY equal zero, the joint plane is horizontal, and the static water pressure is a uniform pressure equal to $\overline{HS}$ x GW.

For a totally submerged joint plane, PV is found by assuming the water level to be at P and then sum the result and (GW)*(distance of actual water level above P)*(ΔPOQ).

The remainder of the three plane analysis consists of geometric calculations (wedge volume) and the kinetic analysis which are analogous to the 2 plane case, except for not considering toppling failure.

Details on the algorithm and on the program steps are given in Appendix UM7 together with the users' manual and an example output.

2.4 Conclusions and Outlook

SWARS provides the designer of rock slopes with an efficient tool for analyzing rock wedge stability. At the present time SWARS seems to be the most encompassing procedure and this without a loss in practicality. A first advantage is the fact that the slope geometry and the attitude of (up to eight) existing joint sets have to be specified and that the program automatically sorts out all geometrically and kinematically feasible wedges. This intermediate step however does not even have to concern the designer, who initially also specifies external loads, an approximate water pressure distribution and particularly stabilizing forces in form of bolt (anchor) forces and directions. The results, a listing of wedges having a factor of safety below a user specified value, does provide the basis for the actual engineering. The designer can vary slope geometry, bolt design and external loads to eliminate unstable wedges and to reduce the number of marginally stable ones. Naturally the opposite is also possible, for instance to steepen a slope if the wedges are overly safe. The efficiency and completeness of the approach makes it possible to study many alternatives.

In addition to these capabilities there are other specific advantages of SWARS: Wedges formed by 2 or 3 joint planes (and the slope) can be treated. Since it is possible to specify the wedge size, realistic stabilizing measures that consider individual wedges of all sizes can be designed. Translational sliding modes and (for 2 joint wedges only) toppling modes are investigated. Seismic effects can be also considered.

Looking at possible improvements of SWARS it seems that the consideration of additional shapes (mainly blocks) and of a greater variety of water pressure options would be desirable. The inclusion of additional failure modes, mainly toppling of 3 joint wedges and rotational sliding, may be another step, as is the treatment of stress field and stiffness effects. All these capabilities, which are now provided by separate analysis methods (see Chapters 4 and 5), may be incorporated in SWARS. The question of how SWARS should be further improved has to be studied very thoroughly in view of the fact that failure mechanisms have to be simplified to a certain extent and that the deterministic treatment of a strongly stochastic phenomenon is limited. Basically, the question is how far should a method which is by definition an approximation, be pushed to achieve an optimum between accurate representation and practicality.

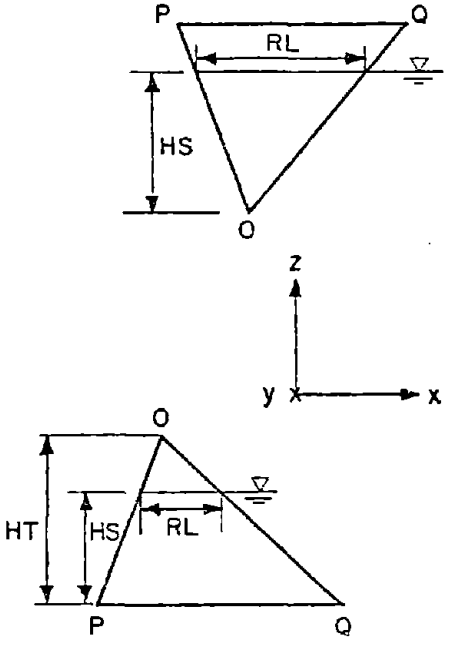

(a)

$$PV = \frac{1}{6} GW(HS)^2(RL)$$

(b)

$$PV = \frac{1}{6} GW(XPQ)(HS)^2(3HT - HS)/HT$$

FIGURE 2.23 STATIC WATER WHEN WX = 0

CHAPTER 3

SIMPLIFIED ANALYSIS FOR 2-JOINT WEDGES

Summary and Practical Applications

A simplified 2-joint analysis method for use with programmable pocket calculators has been developed. The routine works with three cards on HP 97/67 calculators. The user can specify the attitude of two joints, the slope geometry (attitude of face and top of slope) and wedge size and have the program calculate the wedge volume and areas of the wedge planes. The second step determines the wedge weight based on the geometry and water forces based on a user-specified water level. At this point the user can also specify other external driving or resisting forces. All forces are then assumed by the routine and the resulting force and failure mode is printed out. Sliding failure on each of the planes, on both planes or lifting off are considered. Finally a factor of safety for the potential failure mode is computed based on the previously derived resultant force and the joint resistance; the latter is specified in form of Coulomb parameters (c, Φ). The structure of the program makes an efficient parametric study of the effects of external forces, water forces, and resistance values possible. Nevertheless, the main intention of the method is to run a few stability checks on a reasonably well defined wedge. For instance, the analysis for a specific bolt design for a wedge that has been observed in the field can be performed easily and rapidly. The analysis method and program is thus an efficient practical tool, particularly in connection with the increasing use of observational design methods.

3.1 Introduction

Limit equilibrium analyses for wedges on rock slopes can be performed with relatively simple vector analytical and geometric computations at least as long as the geometry and failure modes are not too involved. This has first led to the development of design charts like those in Hoek and Bray (1974) relieving the user of most of the time consuming computations. The arrival of programmable pocket calculators has substantially increased the possibility for conducting stability analyses at the desk of the designer or in the field (without having access to a large computer). Bray et al. (1976) and Kovary et al (1975) have developed such programs for 2-joint wedges. Particularly, Kovary's et al. however, is quite restricted, allowing only sliding along the line of intersection. Bray's et al. program includes also sliding along single planes; it is however limited as far as external forces are concerned. Given these available procedures, the question has to be answered as toward what use should any further development of simplified wedge analysis methods be aimed.

In the design stage, the use of simplified analysis methods will be limited. Extensive parametric studies to consider uncertain natural characteristics and a variety of slope geometries and stabilizing measures will be conducted. This can only be handled by methods like SWARS requiring many analytical steps and significant storage capacity - pocket calculators; even anticipating further development cannot handle such approaches. On the other hand, the substantial development and price reductions of micro-computers will make it possible to handle programs like SWARS with such facilities. The use of pocket calculators in the design stage will then be even more limited. The main use of pocket calculators in design now and in the foreseeable future will be the investigation of specific wedges and of possibilities to stabilize them (reduce critical loads, apply bolts).

An increasing use of pocket calculator analysis can be foreseen in field applications. There is a distinct tendency to go to less conservative designs, particularly in conjunction with observational methods: By closely monitoring the performance of a slope and adapting the design if necessary, one can stay close to a factor of safety of 1 and achieve

an economical design. In such applications there will be a strong need to quickly determine the stability of an identified rock wedge e.g., to apply bolts before the lower apex is laid free (and thus the kinematic constraint is removed). Resistance characteristics will have been determined and water pressure alternatives will be known reasonably well. The user will like to vary external loads and stabilizing forces.

The requirements for the design and field use of simplified analysis methods are thus very similar:

- Computation of the geometry (vector characterization of all wedge planes, wedge volume) of an identified kinematically unconstrained wedge. (The calculator has to relieve the user from conducting the somewhat tedious calculations, but the decision on geometric and kinematic feasibility is made by the user). The geometries that can be handled should be reasonably realistic, i.e., a slope consisting of a slope face and a top of the slope (Fig. 3.1). 2-joint wedges should be treated as a minimum and if possible more complex wedge shapes.
- Computation of important driving forces. Magnitude and location of the weight value can be obtained from the geometric analysis above. The other important driving force is due to water and it is desirable that the user can simply specify a water level.
- Other external forces: uniform loads, driving point loads and bolt forces should be included. A quick investigation of the effect of such forces should be possible.
- Resistance values: The Coulomb (c,Φ) parameters description should be used to express the existence of a stress-dependent and a stress independent component.
- The output should be in the form of a factor of safety.

The pocket calculator program described below (Section 3.2) has been developed to satisfy these requirements; an example application is given in Section 3.3.

3.2 Pocket Calculator Program for 2-Joint Rock Wedges

The program is based on the 2-joint wedge analysis by Hendron et al.

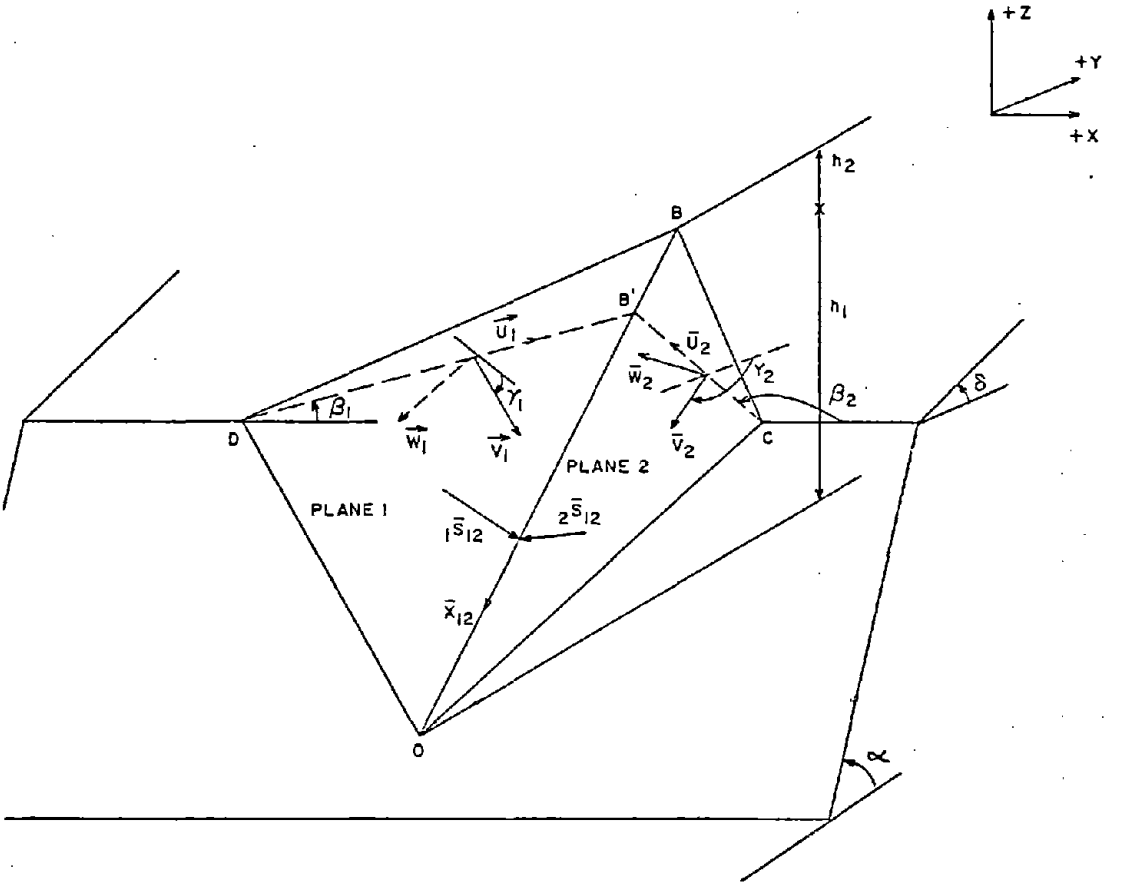

NOTE: $\vec{W}_1$ is directed into the joint plane.

$\vec{W}_2$ is directed away from the joint plane.

β_1 and β_2 are measured from the positive x direction, which is parallel to the strike of ths slope face.

γ_1 is measured downwards from an angle of (β_1-90^o) from the positive x axis.

γ_2 is measured downwards from an angle of (β_2-90^o) from the positive x axis.

FIGURE 3.1 SLOPE AND JOINT GEOMETRY

(1971) and Campbell (1974). The program has been developed for HP-97/67 calculators; it uses three (3) cards. A program listing and user guide is given in Appendix F. The sample appendix includes also some of the detailed analytical calculations. The method and calculator program includes most of the desirable features discussed in Section 3.1. Naturally, the limited number of programming steps in a pocket calculator required some restrictions. It was thus decided to only treat 2-joint wedges, but to include the other requirements, mainly the effect of forces in addition to weight.

3.2.1 Principles and Capabilities

The geometry of the wedge, i.e., its volume and the surface area and vector characterization of its planes, are computed from the slope geometry, joint attitude and size specification (see Figs. 3.1, 3.2). Slope geometry is defined by the angle α of the slope face and angle δ of the top of the slope. Joint orientation has to be specified by strike relative to the slope crest (the horizontally assumed slope crest is the x-axis of the coordinate system, (see Fig. 3.2) and dip from the horizontal. Wedge size is specified by the vertical distance (h_1) from Apex 0 to slope crest. Wedge geometry is then used to compute the weight vector and provides input for other force calculation.

The water force due to a hydrostatic pressure below a user specified water level (for no water effect $h_{water} = 0$ has to be entered) is automatically added (vector addition) to the weight to arrive at the resultant driving force vector. At this point the program stops and the user can enter additional external driving and resisting forces. These forces are entered in form of X, Y, Z components, i.e., magnitude and direction can be specified by the user; these (as well as other forces) are assumed however to act through the center of gravity.

The total resultant force is then obtained from weight, water and other forces. (Note that the resisting external force is deducted from the driving force, rather than to add it to the resisting force. This is a subject of controversy - neither assumption being entirely satisfactory.) With the resultant force the program determines the

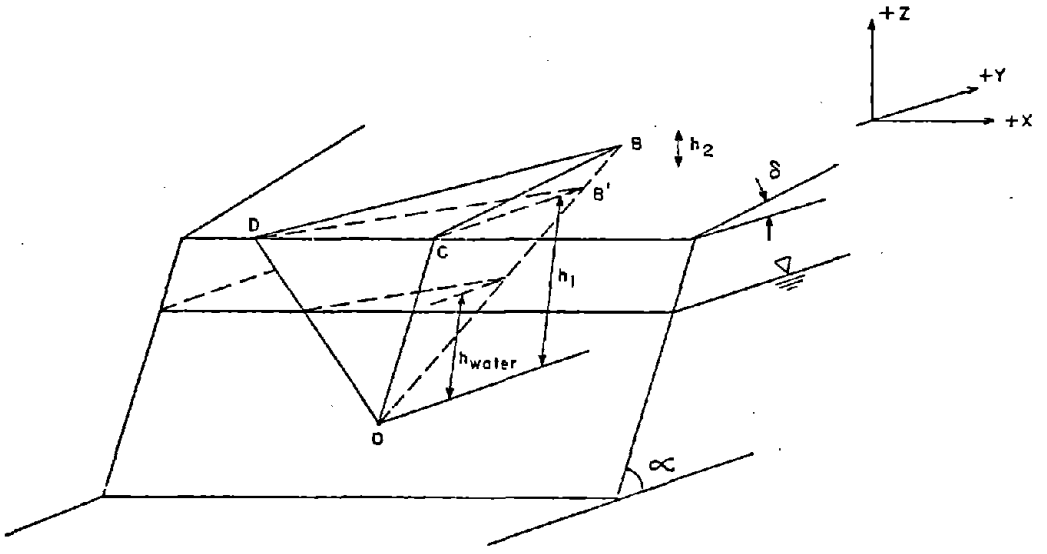

Percentage of the joint plane area below the water table

$$\text{PERCENT} = \left(\frac{h_{water}}{h_1}\right)\left(\frac{h_{water}}{h_1+h_2}\right) \qquad \text{(Ref. Campbell, 1974)}$$

Water force on wedge = $\frac{1}{3}\gamma_{water}h_{water}$ x PERCENT x Total Area of joint bounding the wedge

$$= \frac{1}{3}\gamma_w h_w \frac{h_w}{h_1}\quad\frac{h_w}{h_1+h_2} \quad \text{x Area of Joint Plane}$$

Acts normal to each of the two planes (i.e.,in the directions $\overline{W}_1$ and $\overline{W}_2$).

FIGURE 3.2 SIZE SPECIFICATION

mode of failure which can be translational sliding on either plane or on both planes (along the line of intersection) or lifting off from both planes. Rotational sliding and toppling are not considered.

Finally, the factor of safety is calculated for the particular mode of failure; the user has to select the appropriate subroutine based on the information on failure mode provided previously. The factor of safety is the ratio of the resisting tangential force over the driving tangential force, where resistance is expressed with the Coulomb parameters cohesion (c) and friction (Φ)

$$SF = \frac{|\bar{N}| \tan\Phi + c \times \text{Area}}{|\bar{R} - \bar{N}|}$$

where $\bar{N}$ = Normal Force Vector on plane, $\bar{R}$ = Resultant Force Vector.

3.2.2 Details of Procedure

Note that the program listing and some of the underlying analytical formulations are given in Appendix F.

User input (see also Figs. 3.1 and 3.2):

β_1, β_2	- strikes of joint plane 1 and joint plane 2, relative to routine x-axis, i.e., slope crest
γ_1,γ_2	- dip of joint plane 1 and joint plane 2
α	- inclination of slope face
δ	- inclination of top of slope
h_1	- vertical distance from wedge daylight at slope face (wedge apex 0) to crest
γ_{water}	- unit weight of water
γ_{rock}	- unit weight of rock
h_{water}	- vertical distance from wedge apex 0 to horizontal ground water level
F_x,F_y,F_z	- components of other forces (other than weight and water), e.g., seismic, surcharge, bolts

C_1 - cohesion of joint plane

ϕ_1 - friction angle of joint plane 1

C_2 - cohesion of joint plane 2 *

ϕ_2 - friction angle of joint plane 2

*Note that C can describe the effect of intact rock and that ϕ can include the asperity angle.

Sequence of computation (for steps marked with an asterisk more detailed formulations are given in Appendix F):

- unit normals, $\bar{W}_1$, $\bar{W}_2$
- line of intersection vector $\bar{X}_{12}$
- 'in plane' normal vectors to line of intersection, ${}_1\bar{S}_{12}$, ${}_2\bar{S}_{12}$
- volume and weight of wedge

$$\text{Volume} = \frac{1}{6}\left|\overline{DB} \times \overline{DC}\right| (h_1 + h_2) \qquad (3.1)$$

$$\text{where } h_2 = \frac{\tan\alpha - \tan\varepsilon_x}{\tan\varepsilon_x - \tan\delta} * \frac{\tan\delta}{\tan\alpha} * h_1$$

$$\text{where } \tan\varepsilon_x = \frac{X_{12z}}{X_{12y}}$$

- area of joint planes 1 and 2*

$$A_1 = \frac{1}{2}\left|\overline{OD} \times \overline{OB}\right| \quad , \quad A_2 = \frac{1}{2}\left|\overline{OC} \times \overline{OB}\right| \qquad (3.2)$$

- water forces F_{w1} and F_{w2} on joint planes 1 and 2

$$\text{e.g., } F_{w1} = \frac{1}{3}\gamma_w h_w \times \left[\frac{h_w}{h_1} \times \frac{h_w}{h_1+h_2}\right] \times A_1 \qquad (3.3)$$

(where $\frac{h_w}{h_1}\frac{h_w}{h_1+h_2}$ = % of area A_1 under water)

- resultant force $\bar{R}$

$$\bar{R} = \overline{\text{Weight}} + \overline{F_{wi}} + \overline{\text{Other Forces}} \qquad (3.4)$$

- Mode of Failure Determination

Mode 1: $\bar{R}\cdot W > 0$, $\bar{R}_1\cdot\bar{S}_{12} < 0$ slides on 1, separates from 2

2: $\bar{R}\cdot W < 0$, $\bar{R}_2\cdot\bar{S}_{12} < 0$ slides on 2, separates from 1

3: $\bar{R}_1\cdot W > 0$, $\bar{R}_2\cdot\bar{S}_{12} > 0$ slides on 1 and 2

4: $\bar{R}\cdot W < 0$, $\bar{R}\cdot W_2 > 0$ lifts off from planes 1 and 2

- Factor of Safety Determination:

Mode 1:

Conditions to be fulfilled $\bar{R}\cdot\bar{W}_1 > 0$

$$\bar{R}_1\cdot\bar{S}_{12} < 0$$

$$FS = \frac{N_1\tan\Phi_1 + C_1A_1}{T_1} = \frac{\bar{R}\cdot\bar{W}\tan\Phi_1 + C_1A_1}{|\bar{R} - (\bar{R}\cdot\bar{W}_1)\bar{W}_1|} \qquad (3.5)$$

Mode 2:

Conditions to be fulfilled $\bar{R}\cdot\bar{W}_2 < 0$

$$\bar{R}_2\cdot\bar{S}_{12} < 0$$

$$FS = \frac{N_2\tan\Phi_2 + C_2A_2}{T_2} = \frac{(\bar{R}\cdot\bar{W}_2)\tan\Phi_2 + C_2A_2}{|\bar{R} - (\bar{R}\cdot W_2)\bar{W}_2} \qquad (3.6)$$

where T_1 = tangential component of $\bar{R}$ to plane 1.

T_2 = tangential component of $\bar{R}$ to plane 2.

Mode 3:

Conditions to be fullfilled: $\bar{R}_1 \bar{S}_{12} \quad 0$

$\bar{R}_2 \bar{S}_{12} \quad 0$

$\varepsilon_x < \alpha$ if $0 < \alpha < \pi$

$\varepsilon_x < \delta$ if $\alpha = \pi$

Note that downhill sliding if $\bar{R} \cdot \bar{X}_{12} \quad 0$

uphill sliding if $\bar{R} \cdot \bar{X}_{12} < 0$

$$FS = \frac{N_1 \tan\Phi_1 + C_1 A_1 + N_2 \tan\Phi_2 + C_2 A_2}{T_{12}} \tag{3.7}$$

$$T_{12} = \frac{\bar{R}\,\bar{X}_{12}}{X_{12}} \tag{3.8}$$

$$N_1 = \frac{\bar{N}_{12y}\bar{W}_{2x} - \bar{N}_{12x}\bar{W}_{2y}}{\bar{W}_{1y}\bar{W}_{2x} - \bar{W}_{1x}\bar{W}_{2y}} \tag{3.9}$$

$$N_2 = \frac{\bar{N}_{12y}\bar{W}_{1x} - \bar{W}_{1y}\bar{N}_{12x}}{\bar{W}_{1y}\bar{W}_{2x} - \bar{W}_{1x}\bar{W}_{2y}} \tag{3.10}$$

where

$$\bar{N}_{12} = \bar{R} - \bar{T}_{12} \tag{3.11}$$

The program is structured such that the geometric calculations are performed with Card 1, the force calculations (weight, water, other user specified forces) with Card 2, and the factor of safety calculations with Card 3. This simplifies the performance of parametric studies: 1) for variation of water forces and study of various external forces only Cards 2 and 3 need to be used after the first run. (Before reusing Card 2 one has to

store h_1 in register A and h_1+h_2 in register E). 2) for variation of resisting forces, i.e., to study effect of uncertainties in c,ϕ only Card 3 needs to be used after the first run.

The procedure is thus straightforward and efficient, and even permits the user to conduct some parametric studies without repeating those computations that do not change. A short example will further illustrate the use of the program.

3.3 Example Application

A 2-joint wedge potentially sliding toward a vertical slope is investigated (see Fig. 3.3). No water is assumed.

The input information is:

$\beta_1 = 17°$	$\beta_2 = 63°$	$\alpha = 89.999°$	$C_1 = 0$
$\gamma_1 = 60°$	$\gamma_2 = 80°$	$\delta = 0°$	$\phi_1 = 30°$
		$h_1 = 12°$	$C_2 = 0$
			$\phi_2 = 30°$

P = 10 tons (20,000 lbs.) in the positive y direction.*

The geometric computations are conducted with the first card by performing the following steps:

```
    17  ENTER  60    A
    63  ENTER  80    A
                     B
 89.999 ENTER   0  ENTER  12  R/S
```

---

*Since program does not print the input external force (0,20,000,0), the user should mark it on the output paper.

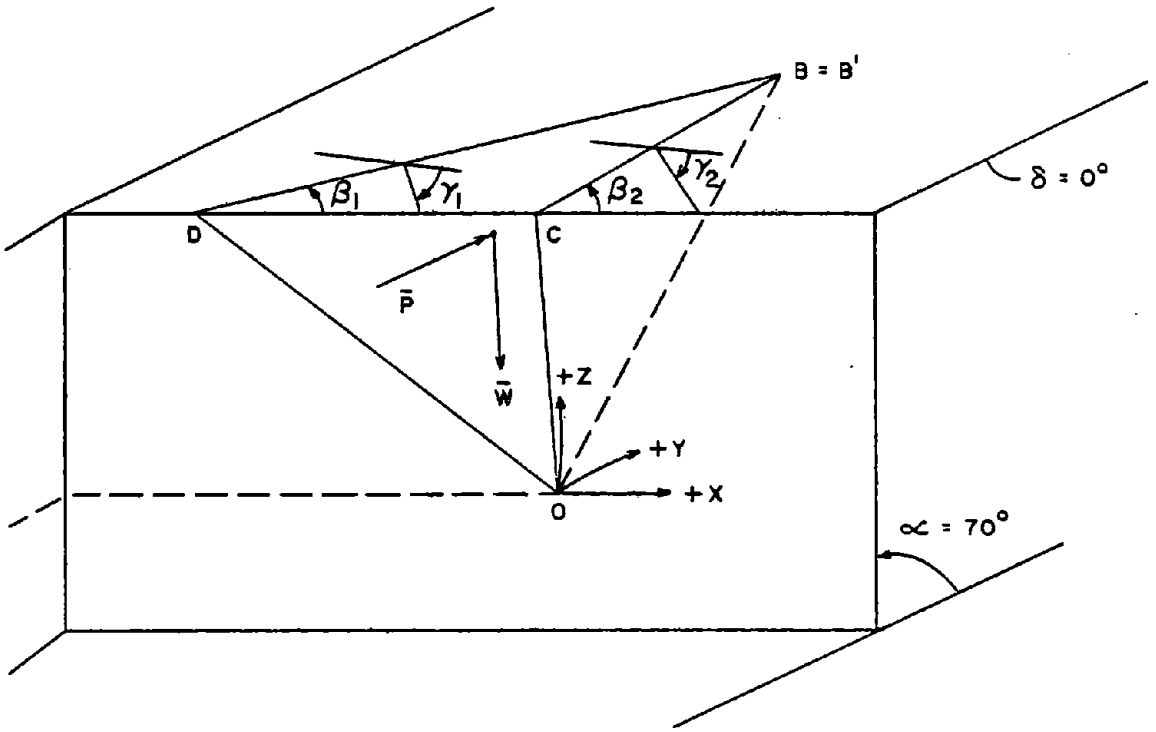

FIGURE 3.3 EXAMPLE CASE OF A 2-JOINT WEDGE

The geometric results are printed out:

β_1	17.00
γ_1	60.00
β_2	63.00
γ_2	80.00
α	90.00
δ	0.00
h_1	12.00
h_2	0.00

Force calculations with Card 2 require:

62.4 ENTER 160 ENTER 0 C

0 ENTER 20,000 ENTER 0 R/S

and result in:

R_w	0.00
Fraction water	0.00
Volume	329.26
Area 1	182.97
Area 2	52.00
$\bar{R}\cdot\bar{W}_1$	42904.33
$\bar{R}\cdot\bar{W}_2$	18089.88
$\bar{R}\cdot_1\bar{S}_{12}$	11054.02
$\bar{R}\cdot_2\bar{S}_{12}$	30616.30
ε_x	57.24

Since both $\bar{R}\ _1\bar{S}_{12}$ and $\bar{R}\ _2\bar{S}_{12}$ are positive and since $\varepsilon_x = 57.24$ is smaller than α sliding in failure mode 3 is potentially possible. The corresponding factor of safety calculation is performed with Card 3.

0 ENTER 30 ENTER 0 ENTER 30 f c

and the printed out results are:

C_1	0.00
ϕ_1	30.00
C_2	0.00
ϕ_2	30.00
FS	1.34

The considered wedge is thus stable.

3.4 Conclusions

A simple efficient analysis and program for HP 97/67 (or corresponding) pocket calculators has been created. The program which allows the user to examine 2-joint wedges subject to water and external driving and resisting forces satisfies the needs for rapid stability checks during the design phase and particularly in the field. It is thus possible to examine on site the effect of changing water conditions and the stabilizing effect of bolts. Also the effect of changing resistance parameters can be efficiently investigated. Although the program is structured to make these limited parametric studies efficiently possible it is not intended to provide the services of a complete method and procedure like SWARS. The pocket calculator program is aimed at cases where the wedge is reasonably defined and stability should be quickly checked. It is probably one of the most complete and efficient programs of this size and is particularly well suited for applications with observational design methods.

CHAPTER 4

STABILITY ANALYSIS FOR 2-JOINT WEDGES CONSIDERING THE STIFFNESS- AND STRESS FIELD EFFECTS

Summary and Practical Application

Limit equilibrium analysis with its rigid body assumption precludes deformation and thus any knowledge on stresses acting in the joint planes. Not being able to determine the stress distribution makes the problem indeterminate. In the normally employed force analysis, assumptions are required with regard to direction or even magnitude of forces to make unique solutions possible. As indicated in the previous chapters the exclusion of moments is a frequent assumption (consideration of moments in stability analysis will also be treated extensively in Ch. 5). The other common simplifying assumption and the subject of this chapter is the normality of reactions on the joint planes, an assumption that is often not explicitly stated. However, assuming normal reactions only can have severe consequences. Stability predictions can deviate considerably from the real situation and often on the unsafe side.

The normality assumption can be eliminated and more realistic force assumptions made if one considers the stiffness of joints or the state of stress in the slope (and wedge). Quite obviously these are artificial means to introduce the effect of stresses in a rigid body analysis method. They are however justified since the wedge itself is still considered to be a rigid body, but is acted upon by stresses (forces) determined via joint stiffnesses or related to the stress state in the slope. The standard normality assumptions for joint plane reactions imply that there is no shear stiffness (the ratio of normal stiffness to shear stiffness is infinite) and that the ratio of lateral to vertical "K" is 1. Stated in this way one becomes aware how far from reality one may be. Initial developments by other researchers for the stiffness and stress approaches were available but limited to simple geometries and frictional resistance only. Nevertheless, the state-of-the-art review and an investigation employing these approaches already show the possibility of significant discrepancies in stability predictions of "normal" and more realistic force assumptions.

In this chapter the stiffness and the stress approach are considerably expanded to be applicable to a broader range of 2-joint wedge geometries and particularly to include all the other capabilities of wedge stability analysis. These generalized approaches are used to again demonstrate the effect of the simplifying normality assumption. Using the stiffness approach one can show that, particularly for narrow wedges or wedges with one steep joint, considerable deviations in stability predictions result - the required friction angle (an expression of safety) can be up to 30° greater than for the normality assumption. A lateral

stress ratio different from K = 1 (implying non-normal reactions) is particularly significant if the wedges have relatively flat lying lines of intersection. K > 1 underestimates the factor of safety, while K < 1 overestimates it.

The definite need to eliminate the restrictive normality assumption in wedge stability analysis can thus be established.

Before developing a better analysis method it has,however,to be decided how the stiffness and stress approaches relate to each other. They evidently both represent the effect of a more correct force assumption, i.e., the underlying stress distribution. It can be shown that the stress approach correctly models the wedge in its natural environment. A state of stress has developed in the slope through a series of historical changes and the present stability is governed by the present state of stress. The joint stiffnesses in contrast can only be used to determine stress changes due to additional loads; stiffness cannot provide information on the present state of stress. The stiffness approach can therefore be used to make predictions on the effect of additional loads.

A method of analysis and computer program SWARS-2PM for 2-joint wedges was therefore developed incorporating the generalized stress and stiffness approaches and applying them in the correct sequence - stress approach to analyze the effect of weight, stiffness approach for the effects of other forces. Since the method and program is basically an extension of SWARS-2P, it includes all the powerful features of the latter: resistance descriptions with Coulomb parameters including persistence and asperity effect; water, seismic and external driving forces; bolt forces, possibility to determine all wedges formed by up to eight joint sets. These features, together with the realistic force assumption, which require however that stiffnesses and stress be determined, makes the analysis method and SWARS-2PM a highly effective tool for slope design.

4.1 Introduction

Limit equilibrium analysis is the usual approach to wedge stability analysis. Standard wedge analysis methods have been reviewed and advanced analysis methods and programs have been developed in Chapters 2 and 3 of this report. These approaches all follow the basic rigid body assumption of limit equilibrium analysis. The rigid body assumption i.e., the neglect of deformations, makes the problem indeterminate. Determinacy is implicitly or explicitly introduced by neglecting certain forces or by making assumptions on force directions. A well known example in the related field of soil mechanics is the interslice force in sliding circle analysis. As will be discussed in Section 4.2, the usual

simplifying assumption in wedge analysis is that the reactions of the wedge weight act perpendicularly to the joint* (discontinuity*) planes; also moments are often neglected (the consequence of the latter assumption and new methods considering moments will be discussed in Chapter 5.) Usually unknown to the common user, these simplifying force assumptions imply certain conditions regarding deformability or the stress field or both. As long as the real and the assumed conditions correspond to each other the solution will be correct. Deviating conditions may however considerably change this and result in failure where stable conditions were analytically determined or vice versa. Quite obviously, since the rigid body assumption excludes deformation considerations and, associated with it, effects of stress distribution, it is the deformability and the stress field that may cause significant errors if they do not comply with the assumptions.

This chapter therefore investigates the effect of discontinuity stiffness (discontinuity stiffness or deformability has normally a much greater effect than that of intact rock) and of the stress field in limit equilibrium analysis.

It will be shown how the results of wedge stability analysis change if the conditions are different from the standard assumptions. The methods and associated computer programs developed for this investigation can naturally be used by designers who like to include stress or discontinuity stiffness effects in their analyses. It should be pointed out however, that one still makes assumptions with regard to applied forces - although they are assumptions that are explicitly stated and related to underlying causes. Nevertheless they are still simplifications. One will be able to avoid some major mistakes by including stress field and stiffness effects, but caution is still necessary.

A good way to introduce the topic is by briefly reviewing the state-of-the-art.

---

*Terms joint and discontinuity are used interchangeably in this chapter.

4.2 State of the Art - Stiffness and Stress Effects

Most present approaches to rigid body analysis assume that the reactions between the wedge and the parent rock mass are perpendicular to the two* joint planes (Figure 4.1). Figure 4.2 shows a typical wedge and two sections - one perpendicular to the line AC, the line of intersection, and one parallel to line AC. The perpendicularity assumption regarding the reactions on the joint planes leads to the force diagram in Figure 4.3. The two reactions, R_1 and R_2, can be derived by solving two equations of force equilibrium:

$$W \cos \theta = R_1 \cos \beta_1 + R_2 \cos \beta_2 \tag{4.1}$$

$$R_1 \sin \beta_1 = R_2 \sin \beta_2 \tag{4.2}$$

If $\beta_1 = \beta_2 = \beta$:

$$R_1 = R_2 = \frac{W \cos \theta}{2 \cos \beta} \tag{4.3}$$

Assuming normality of the reactions simplifies the analysis, but is not entirely realistic. This has been investigated by considering non-normal reactions by Mahtab and Goodman (1970) and St. John (1971) through the use of joint shear and normal stiffnesses and by Steiner (1977)

*All the wedges discussed in this chapter are "two-joint wedges" i.e., tetrahedrons formed by two intersecting joints and two free surfaces.

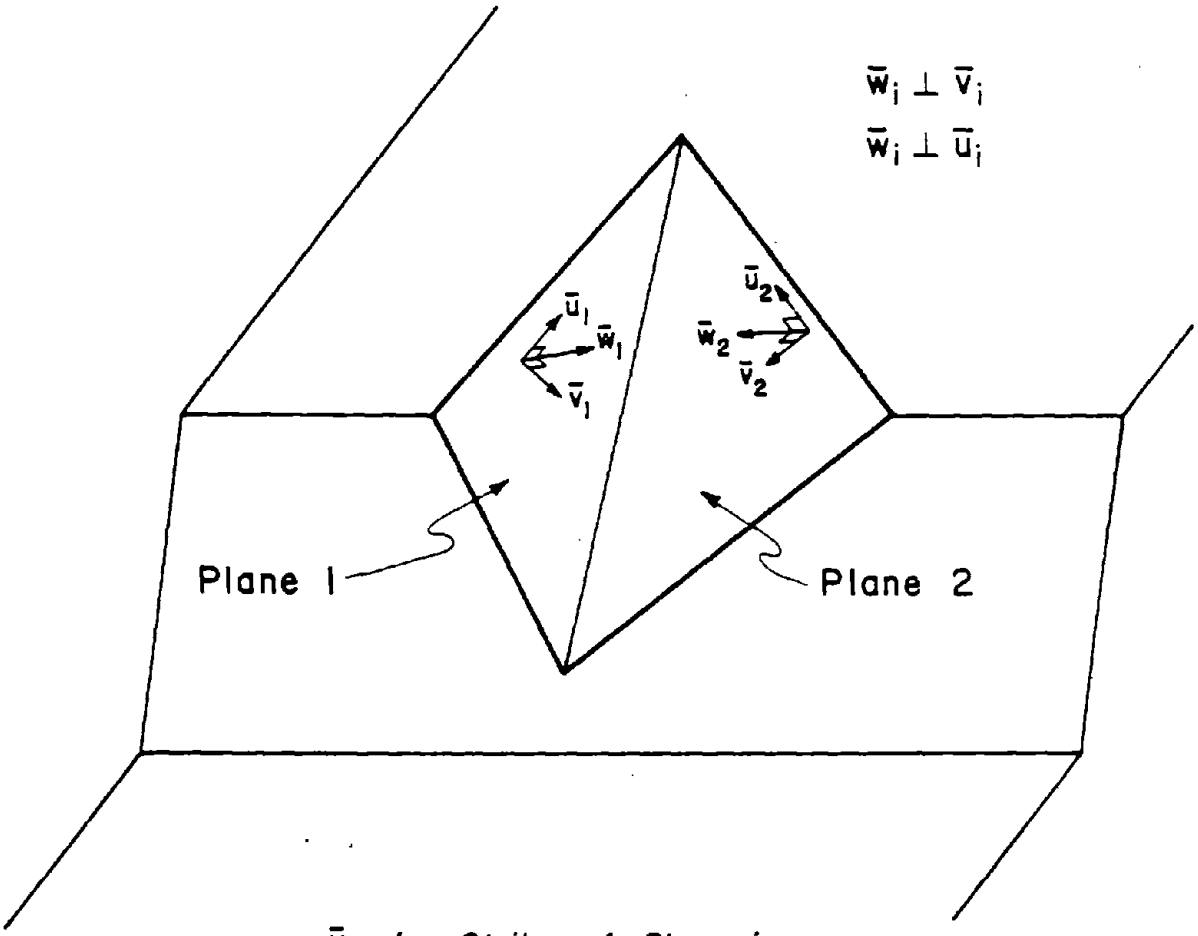

$\bar{u}_i$: Strike of Plane i

$\bar{v}_i$: Dip of Plane i

$\bar{w}_i$: Direction of Reaction from Plane i

Figure 4.1 Sliding Wedge--Reactions Perpendicular to the Joint Planes

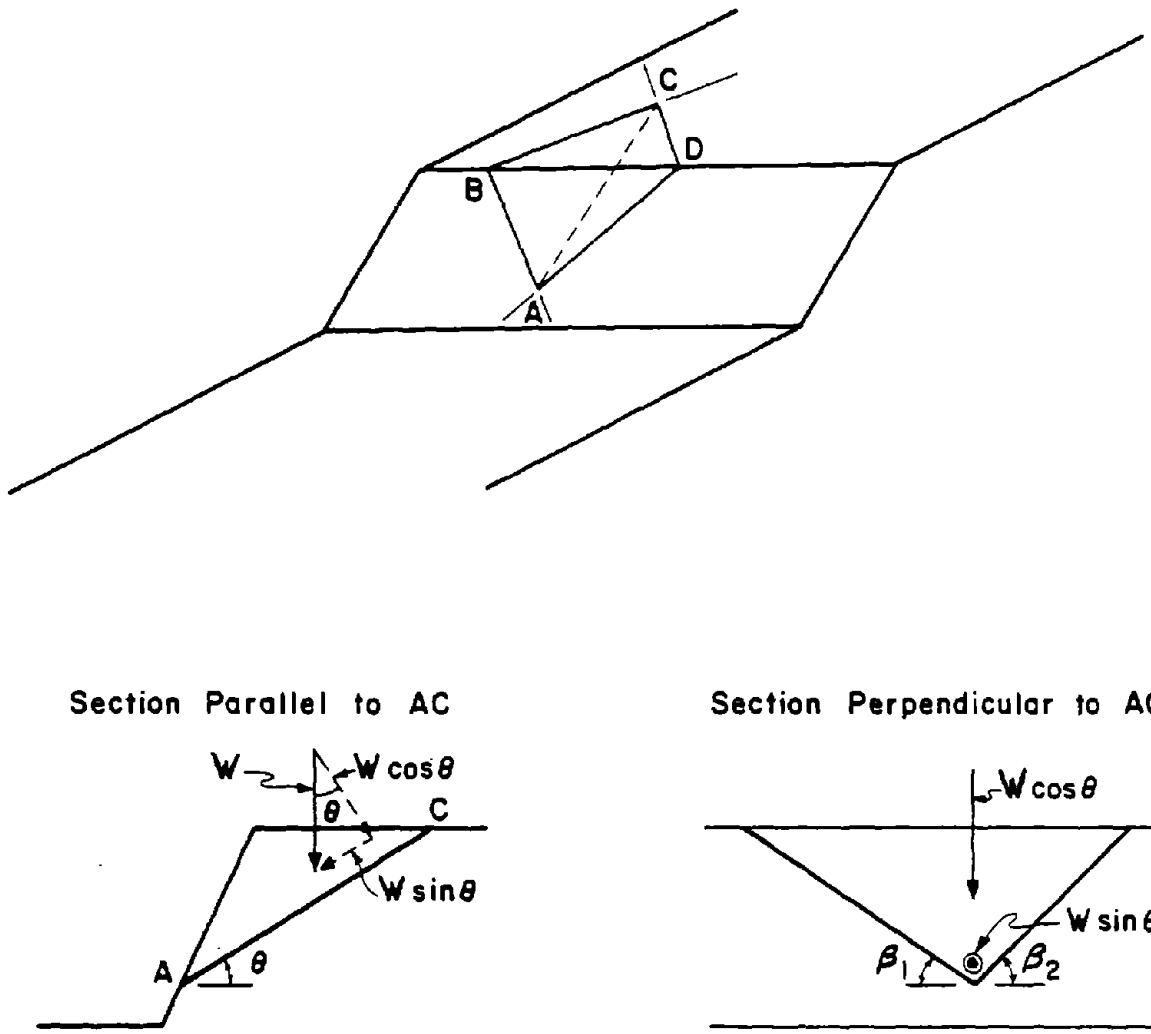

Figure 4.2 Resolution of Weight Vector into Components

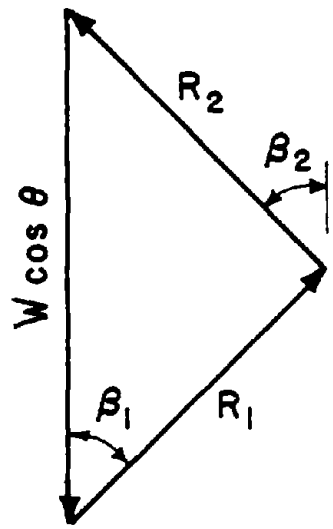

Figure 4.3 Force Diagram--Reactions Perpendicular to Joint Planes

through the use of the ratio of horizontal to vertical stresses, approaches that will now be briefly reviewed:

The stiffness approach introduces (Figure 4.4A) the tangential force T_i in addition to the normal forces N_i to represent the reactions on the sliding planes. N_i and T_i can be determined if the shear stiffness (k_s)* and normal stiffness (k_n)* of the joint or their ratio $R = \frac{k_n}{k_s}$ is known. For a symmetric wedge the ratio T_1/N_1 can be calculated as

$$\frac{T_1}{N_1} = \frac{\tau_1}{\sigma_{n_1}} = \frac{k_s (\sin \beta)\, \delta_r}{k_n (\cos \beta)\, \delta_r} = \frac{\tan \beta}{R} \tag{4.4}$$

From the force diagram shown in Figure 4.4C:

$$W \cos \theta = N_1 \cos \beta + N_2 \cos \beta + T_1 \sin \beta + T_2 \sin \beta \tag{4.5}$$

and

$$N_1 = N_2 = \frac{R \cos \beta}{2(\sin^2 \beta + R \cos^2 \beta)} W \cos \theta \tag{4.6}$$

$$T_1 = T_2 = \frac{\sin \beta}{2(\sin^2 \beta + R \cos^2 \beta)} W \cos \theta \tag{4.7}$$

For $R = \infty$, i.e., for zero shear stiffness:

$$N_1 = \frac{W \cos \theta}{2 \cos \beta} \quad \text{and} \quad T_1 = 0$$

---

* $k_s = \frac{\tau}{\delta_s}$; $k_n = \frac{\sigma_n}{\delta_n}$ where τ and σ_n are the shear and normal stresses; δ_s and δ_n are the shear and normal displacments.

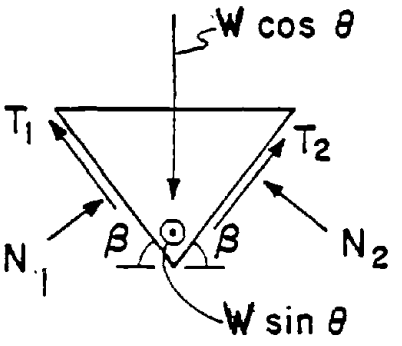

4.4 A

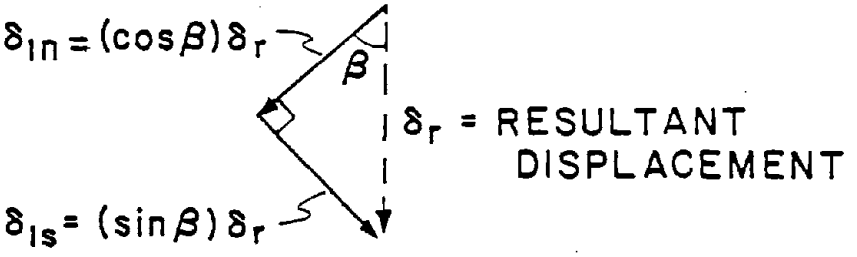

4.4 B

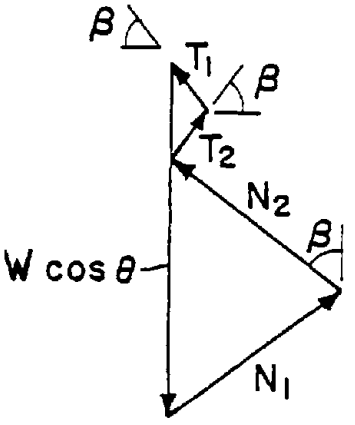

4.4 C

Figure 4.4 Symmetric Wedge--Reactions with Components Tangent to Joint Planes

These are the values derived earlier (Eq. 4.3) with the standard normality assumption.

The forces T_i and N_i can be used in the limit equilibrium equation for the wedge:

$$\text{Factor of Safety} = FS = \frac{2N_1 \tan \Phi}{T} \tag{4.8}$$

where $2N_1 \tan \Phi$ is the resisting factor (assuming only frictional resistance is present) and T is the driving force which is the vectorial addition of the shear forces perpendicular and parallel to the line of intersecting (Figures 4.4A and 4.2).

$$T = \sqrt{(2T_1)^2 + (W \sin \theta)^2} \tag{4.9}$$

If only the shear force in the direction of wedge movement, i.e., parallel to the line of interaction AD is considered,*

$$FS = \frac{2N_1 \tan \Phi}{W \sin \theta} \tag{4.10}$$

To show the effect of different shear and normal stiffnesses Φ_R (the "required friction angle" to obtain FS = 1.0) has been plotted versus the angle β (for a symmetrical wedge) in Figure 4.5. The most important conclusion from the figure is that decreasing R, i.e., increasing k_s relative to k_n, leads to a greater required friction angle.

*Section 4.4 examines the question of what constitutes failure and how to define the factor of safety.

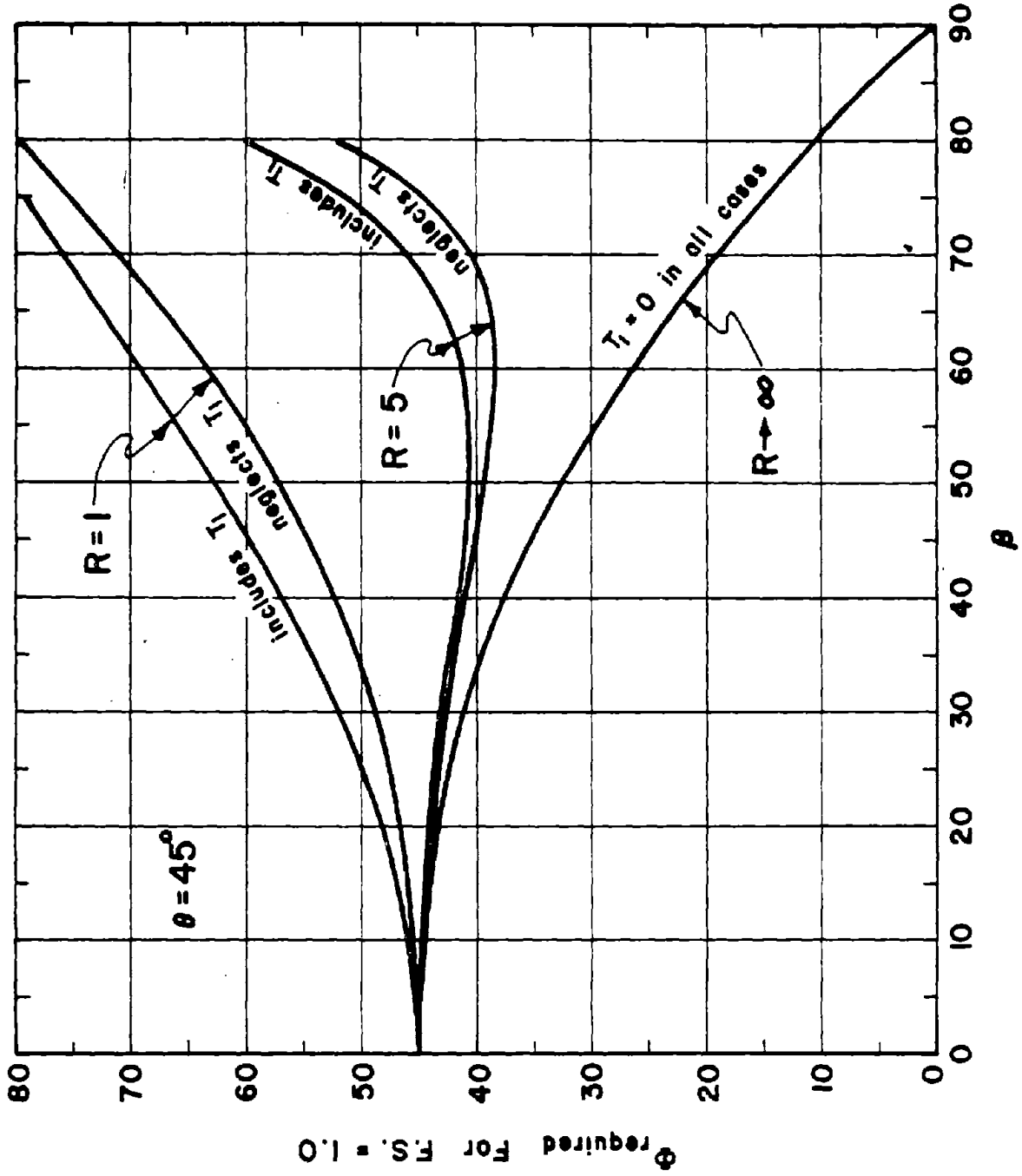

Figure 4.5 Φ Required For FS = 1.0 vs. β

The importance of R raises the question, What values of R do occur in nature? As was discussed in Part I of Chapter 6 several investigations have been conducted by Goodman (1972), Kulhawy (1975), Rosso (1976) and Barton (1972) in addition to the one by the MIT group. It has been shown there that it is not yet possible to correlate stiffness values with particular rocks, and only to a limited extent, with particular surface characteristics. Also R values range widely from 0.5 to 1000. Unweathered joints usually fall in the upper (500-1000) portion of the range while joints with fillers usually have R values below 50.

Several improvements of the stiffness approach should be made. The St. John model is based on a symmetric wedge with identical stiffness ratios on the two sliding planes. The strength of the joint is characterized solely in terms of frictional resistance with no provisions for cohesive resistance. Some of these limitations have been eliminated in an extended version of the model that will be discussed below.

The stress approach as introduced by Steiner relaxes the force direction assumptions by explicitly including the horizontal stress acting on the wedge. From the stresses acting on a small element of the wedge (Figure 4.6), one can establish a force equilibrium:

$$dN = (dW') \cos \beta(L_{CB}) + (KdW') \sin \beta(L_{CA}) \tag{4.11}$$

where L_{CB} = distance CB

and L_{CA} = distance CA,

when $L_{CB} = 1$

$$L_{CA} = \tan \beta \tag{4.12}$$

and thus

$$dN = dW' \cos \beta + KdW' \sin \beta \tan \beta \tag{4.13}$$

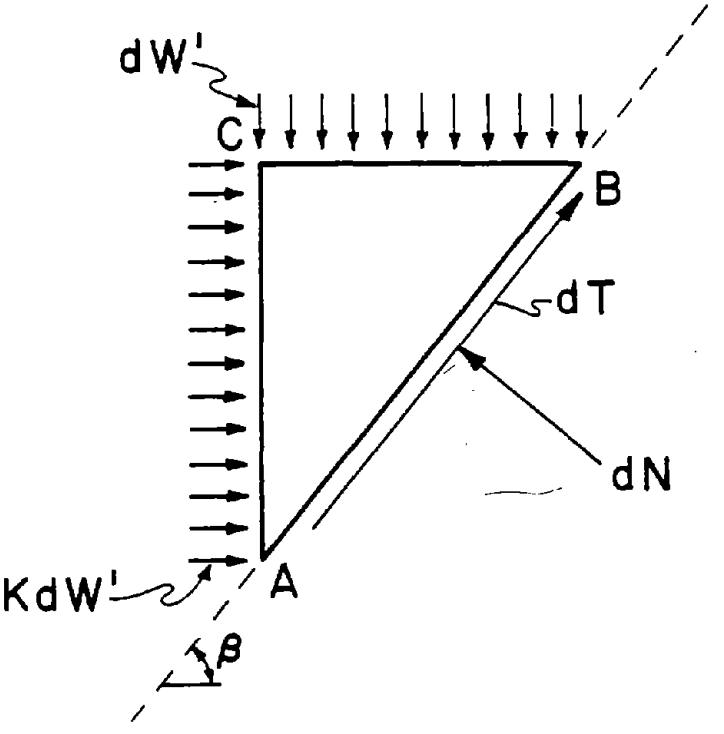

Figure 4.6 Stresses on Differential Area of the Joint Plane

Since dW' and kdW' are constant along the entire length of the joint the equation can be integrated to yield the normal force on the joint.

$$N = W' \quad (\cos \beta + K \sin \beta \tan \beta) \tag{4.14}$$

(Instead of the differential force equilibrium described above, one could arrive at the same result using the Mohr stress circle, Figure 4.7). If $W' = \frac{1}{2}W \cos \theta$, i.e., one-half the weight component in a direction perpendicular to the line of intersection (see Figure 4.3),

$$N_1 = N_2 = \frac{1}{2}W \cos \theta \ (\cos \beta + K \sin \beta \tan \beta) \tag{4.15}$$

and

$$T_1 = T_2 = \frac{1}{2}W \cos \theta \ (\sin \beta - K \cos \beta \tan \beta) \tag{4.16}$$

for K = 1, the forces become:

$$N_1 = \frac{W \cos \theta}{2 \cos \beta} \text{ and } T_1 = 0 \tag{4.17}$$

i.e., the values for the standard normal reaction assumption (Eq. 4.3). This standard assumption includes thus implicitly the equality of vertical and horizontal stresses.

Factors of safety can be derived either by considering the tangential forces parallel and perpendicular to the wedge movement direction or by only considering those parallel to the movement:

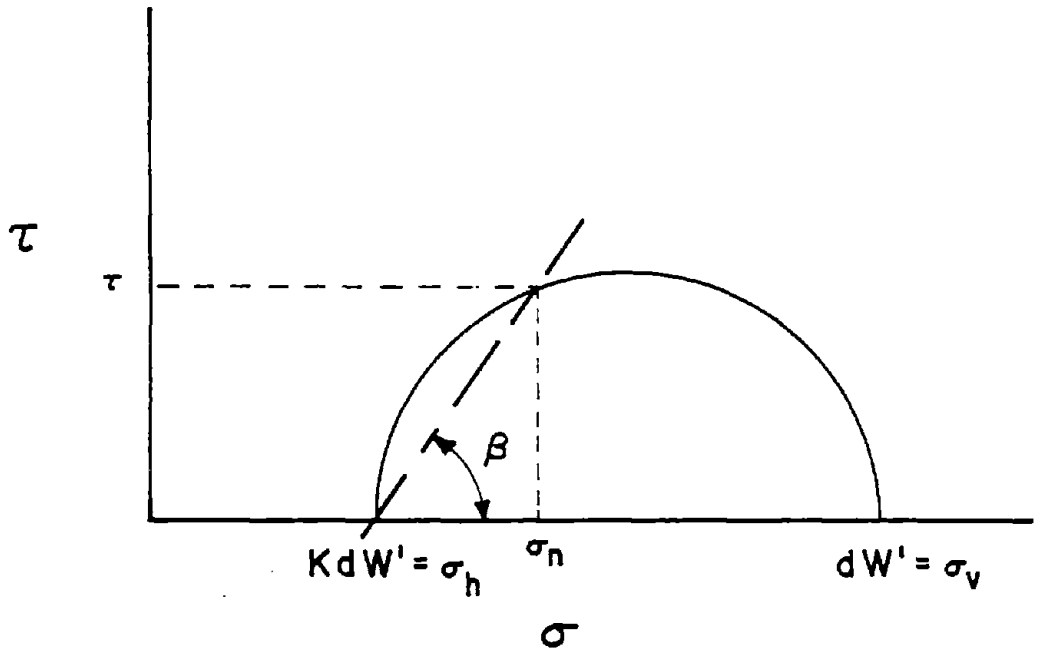

Figure 4.7 Mohr Stress Circle for the Stress State Shown in Figure 4.6

$$FS = \frac{2N_1 \tan \Phi}{\sqrt{(2T_1)^2 + (W \sin \theta)^2}} \tag{4.18}$$

$$FS = \frac{2N_1 \tan \Phi}{W \sin \theta} \tag{4.19}$$

The effect of introducing a factor $K \neq 1$ in the computation of factors of safety is presented in Figure 4.8, where

$$\frac{\text{FS with } K \neq 1}{\text{FS with } K = 1} = \frac{\frac{W \cos \theta}{W \sin \theta} \tan \Phi}{\frac{W \cos \theta}{W \sin \theta} \tan \Phi} \cdot \frac{\frac{1}{\cos \beta} (\cos^2 \beta + K \sin^2 \beta)}{\frac{1}{\cos \beta}} \tag{4.20}$$

$$= \cos^2 \beta + K \sin^2 \beta \tag{4.21}$$

Figure 4.8 shows that with $K > 1$ the traditional assumption $K = 1$ (and thus a reaction normal to the sliding plane only) underestimates the factor of safety and for $K < 1$ it overestimates it.

The notion of the stress ratio K needs some further clarification particularly in the context of a jointed rock mass. K used by Steiner refers to the state of stress within the wedge which may or may not be equal to the stress state in the remainder of the rock mass. A change or discontinuity in the material properties of a medium does not necessarily create a discontinuity in the state of stress existing in the medium. The question that arises is, what created the discontinuity in the first place or (more generally formulated) what is the stress history at the particular location? Depending on the stress history of the joint, K in the wedge may be or may not be identical to K in the entire rock mass.

The use of the stress ratio K in wedge stability analysis introduces the possibility of active or passive failure modes of a wedge in the direction perpendicular to the line of intersection. As shown in Figure 4.9A, the active case is:

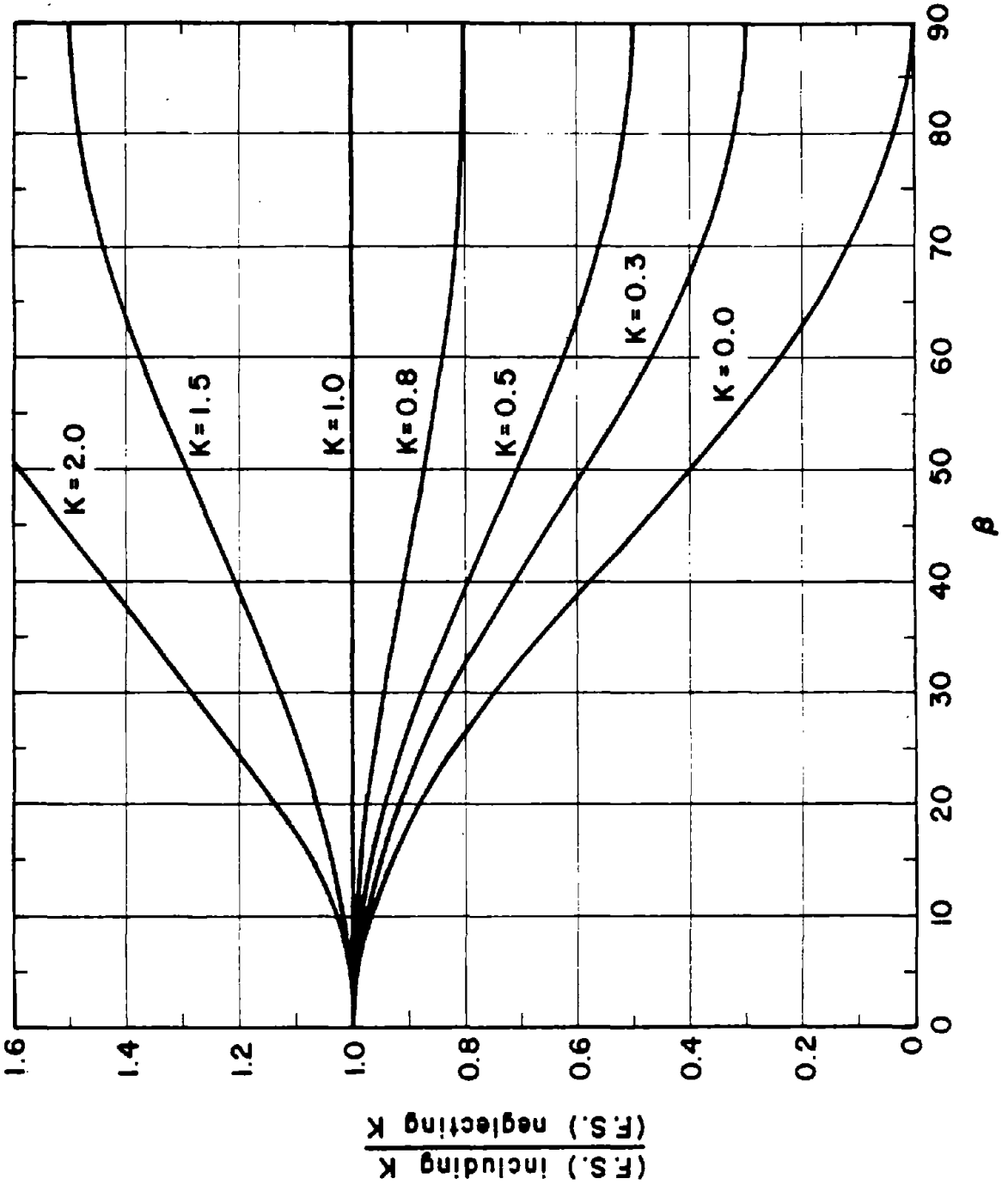

Figure 4.8 $\frac{\text{(FS) neglecting K}}{\text{(FS) including K}}$ vs. β

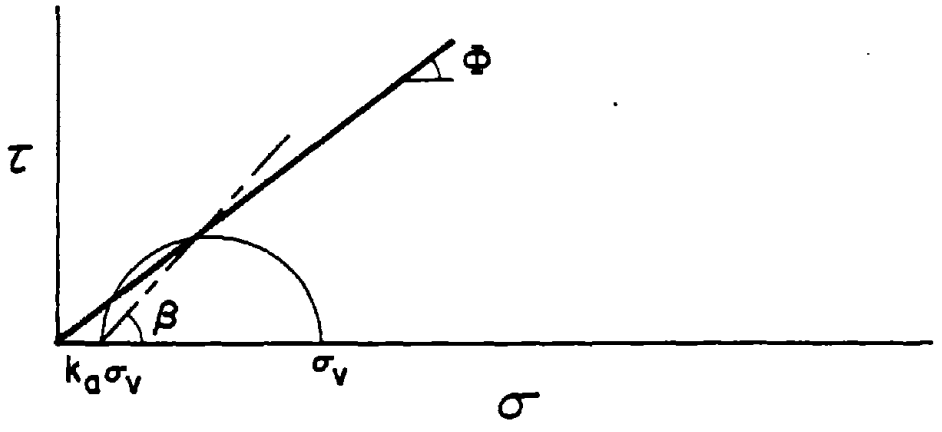

4.9 A

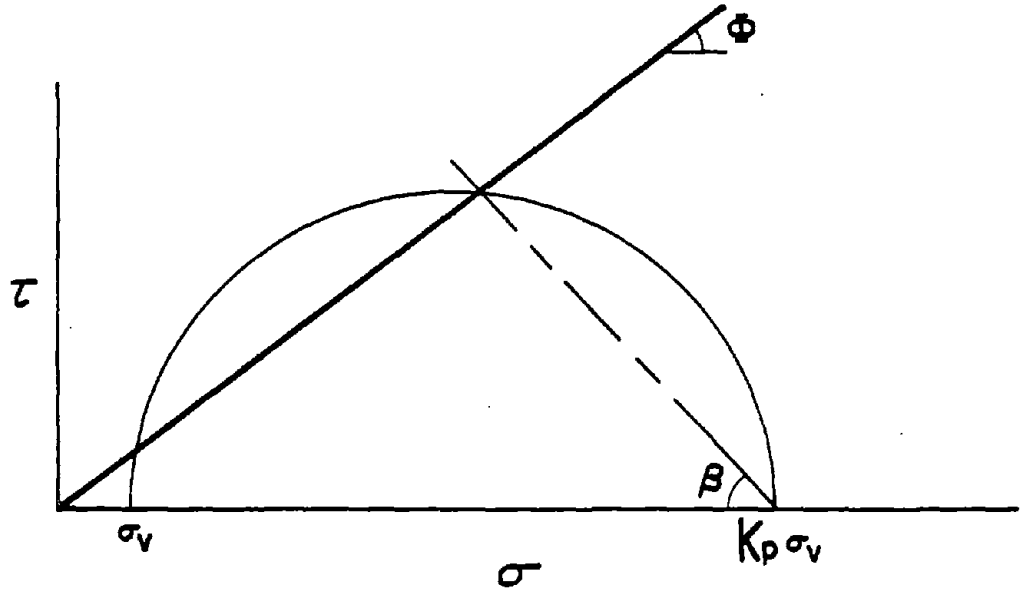

4.9 B

Figure 4.9 Mohr Stress Circles for Active and Passive Cases

$$\tan \Phi = \frac{\tau}{\sigma_n} = \frac{T}{N} = \frac{\sin \beta - K \sin \beta}{\cos \beta + K \sin \beta \tan \beta} = \frac{(1 - K)}{\operatorname{ctn} \beta + K \tan \beta} \tag{4.22}$$

Thus,

$$K_a = \frac{1 - \tan \Phi \operatorname{ctn} \beta}{1 + \tan \Phi \tan \beta} \tag{4.23}$$

In the passive case (Figure 4.9B) the direction of T reverses; therefore, a minus sign must be introduced into Equations 4.16 and 4.22.

$$\tan \Phi = \frac{-T}{N} = \frac{-(1 - K)}{\operatorname{ctn} \beta + K \tan \beta} \tag{4.24}$$

Thus,

$$K_p = \frac{1 + \tan \Phi \tan \beta}{1 - \tan \Phi \operatorname{ctn} \beta} \tag{4.25}$$

The practical significance of these two failure modes will be discussed in Section 4.5. Although the joint shear strength is exceeded in both cases it does not imply sliding failure along the line of intersection. It simply means that in the active case the wedge will settle in its niche and in the passive case the wedge will be lifted up until equilibrium is reached. If K in the rock mass is outside the range $K_p - K_a$, then the overall stress field in the rock mass will be different from the stress field in the wedge. In the wedge, K can only vary between the limits K_a and K_p as determined by Φ and β (see Equations 4.23 and 4.25) whereas in the rock mass K values smaller and greater respectively than these K_a and K_p can exist; K in such a rock mass will be inhomogeneously distributed.

The discussion above treated symmetric wedges. The concept can be extended to handle asymmetric wedges. Figure 4.10 is a section taken

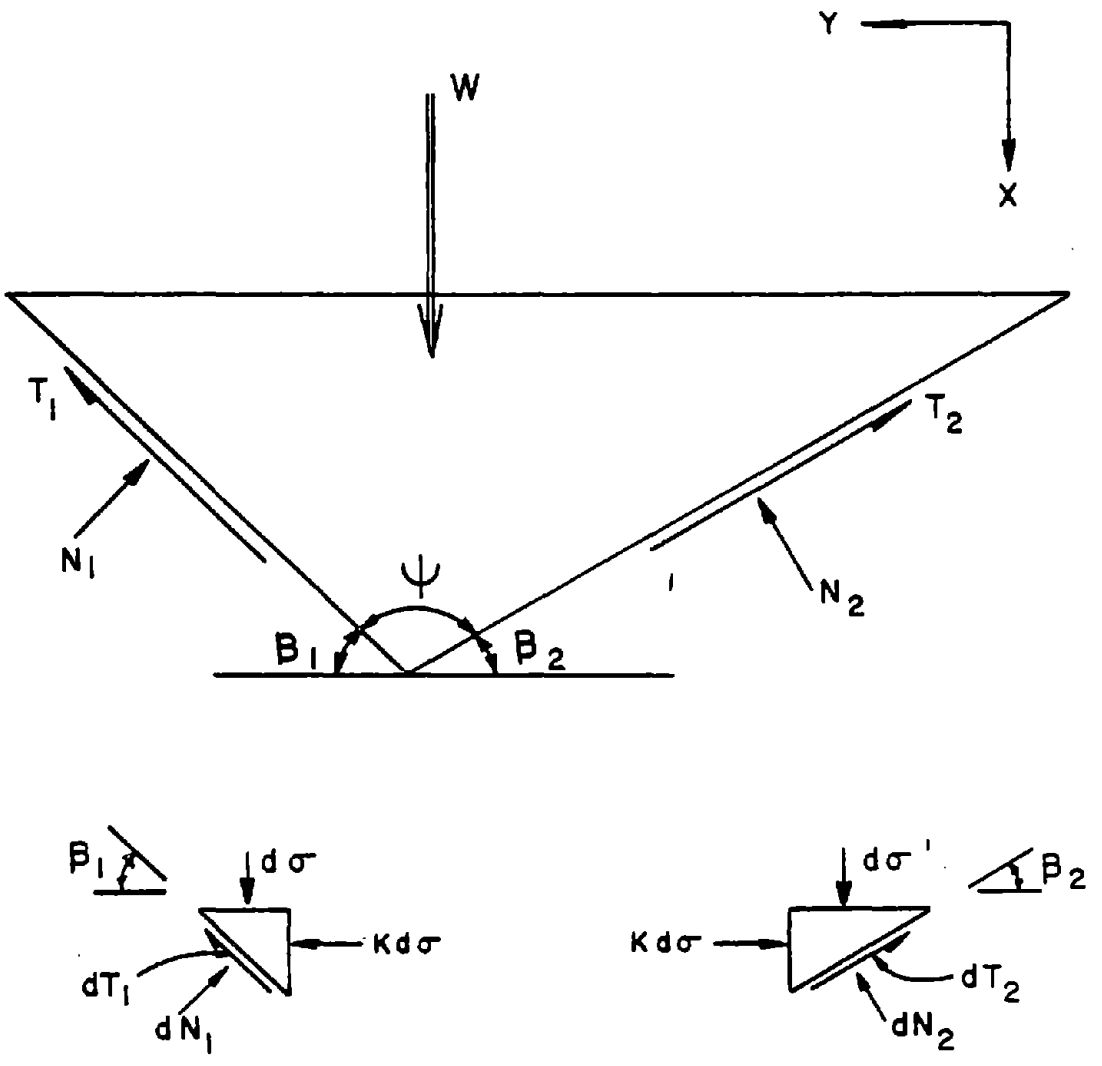

$$\frac{dT_i}{dN_i} = \frac{1 - K}{\operatorname{ctn} \beta_i + K \tan \beta_i}$$

Figure 4.10 Stresses on Differential Areas of the Joint Planes

perpendicular to the line of intersection of a typical asymmetrical wedge. Each differential segment along the joint plane can be treated like the element shown in Figure 4.6. The K parameter relates the shear and normal stresses on the joint planes (Equations 4.15 and 4.16). The stresses can be integrated to yield the following expressions:*

$$\frac{T_1}{N_1} = \frac{(1-K)}{\text{ctn } \beta_1 + K \tan \beta_1} = \lambda_1 \tag{4.26}$$

$$\frac{T_2}{N_2} = \frac{(1-K)}{\text{ctn } \beta_2 + K \tan \beta_2} = \lambda \tag{4.27}$$

Equations 4.26 and 4.27 can be used in conjunction with the equations of force equilibrium to evaluate N_1, T_1, N_2, N_2.

Summing forces in the x direction (Figure 4.10):

$$N_2 \cos \beta_1 + \lambda_1 N_1 \sin \beta_1 + N_2 \cos \beta_2 + \lambda_2 N_2 \sin \beta_2 = W^1 \tag{4.28}$$

W^1 is the component of the weight acting perpendicular to the line of intersection. As shown in Figure 4.2, $W^1 = W \cos \theta$. Summing forces in the y direction:

$$N_1 \sin \beta_1 - \lambda_1 N_1 \cos \beta_1 - N_2 \sin \beta_2 + \lambda_2 N_2 \cos \beta_2 = 0 \tag{4.29}$$

Rearranging Equation 4.29:

$$\frac{N_1}{N_2} = \frac{(\sin \beta_2 - \lambda_2 \cos \beta_2)}{(\sin \beta_1 - \lambda_1 \cos \beta_1)} = \lambda_3 \tag{4.29A}$$

* K may vary over the height of the wedge. If K does vary, the parameter shown in Equations 4.26 and 4.27 is the mean value of K for the entire height.

Equations 4.29A and 4.28 can be solved for N_2:

$$N_2 = \frac{W \cos \theta}{\lambda_3(\cos \beta_1 + \lambda_1 \sin \beta_1) + (\cos \beta_2 + \lambda_2 \sin \beta_2)} \tag{4.30}$$

Finally,

$$N_1 = \lambda_3 N_2 \tag{4.29B}$$

$$T_1 = \lambda_1 N_1 \tag{4.26A}$$

$$T_2 = \lambda_2 N_2 \tag{4.27A}$$

In this section both the stiffness and the stress approaches were presented but not the relations between these two methods for determining reactions at the joint planes. This important aspect will be discussed in Section 4.4 after the now following generalization of the stiffness approach.

4.3 Generalization of the Stiffness Approach

4.3.1 Derivation

The stiffness approach outlined by St. John can be generalized to include asymmetric wedges and arbitrary loads such as those shown in Figure 4.11. (The figure is a cross-section taken perpendicular to the line of intersection between two joint planes.) The generalized problem can be treated in a manner very similar to the one used by St. John. The fundamental assumption in the approach is that the wedge behaves as a rigid body resting on a deformable medium (the joint planes). The deformational characteristics of the joints can be expressed in terms of two stiffness values: k_n and k_s.

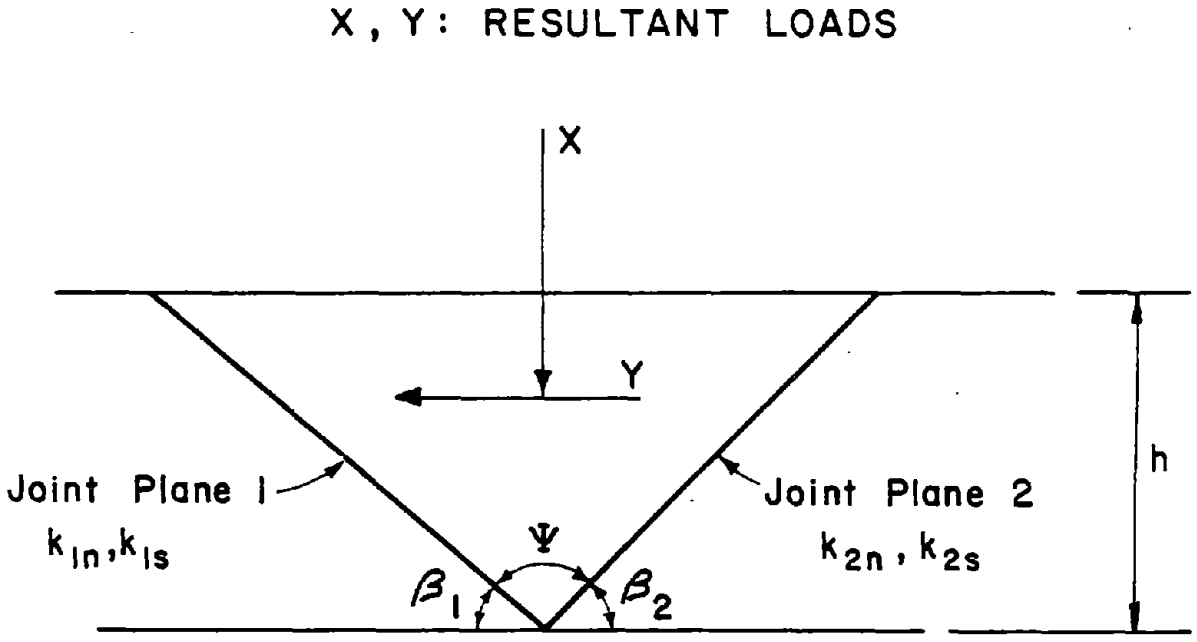

Figure 4.11 Generalized Stiffness Approach--Known Parameters

$$K_n = \frac{\text{normal stress}}{\text{normal displacement}} = \frac{\sigma_n}{\delta_n} \tag{4.31}$$

$$k_s = \frac{\text{shear stress}}{\text{shear displacement}} = \frac{\tau}{\delta_s} \tag{4.32}$$

k_n and k_s are material properties which are assumed constant throughout the range of stresses encountered in engineering practice. The method implicitly assumes that σ_n and δ_s as well as τ and δ_n are unrelated, i.e., the off-diagonal terms in the stiffness matrix are zero.

$$\begin{pmatrix} \sigma_n \\ \tau \end{pmatrix} = \begin{bmatrix} k_n & 0 \\ 0 & k_s \end{bmatrix} \begin{pmatrix} \delta_n \\ \delta_s \end{pmatrix} \tag{4.33}$$

As indicated in Figure 4.12, the problem involves six unknowns: N_1, T_1, N_2, T_2, δ_t and α. There are also six independent equations. Two equations are the force equilibrium equations in the x and y directions:

$$N_1 \cos \beta_1 + T_1 \sin \beta_1 + N_2 \cos \beta_2 + T_2 \sin \beta_2 = X \tag{4.34}$$

$$N_1 \sin \beta_1 - T_1 \cos \beta_1 - N_2 \sin \beta_2 + T_2 \cos \beta_2 = Y \tag{4.35}$$

where X and Y are the resultants of the applied load in the vertical and horizontal directions respectively (see Figure 4.11 and 4.12).
The other four equations relate the shear and normal stresses to the magnitude and direction of the resultant displacement:

$$\delta_t h = \frac{N_1}{(\sin \alpha + \cos \alpha \operatorname{ctn} \beta_1) k_{1n}} \tag{4.36}$$

$$= \frac{T_1}{(\cos \alpha - \sin \alpha \operatorname{ctn} \beta_1) k_{1s}} \tag{4.37}$$

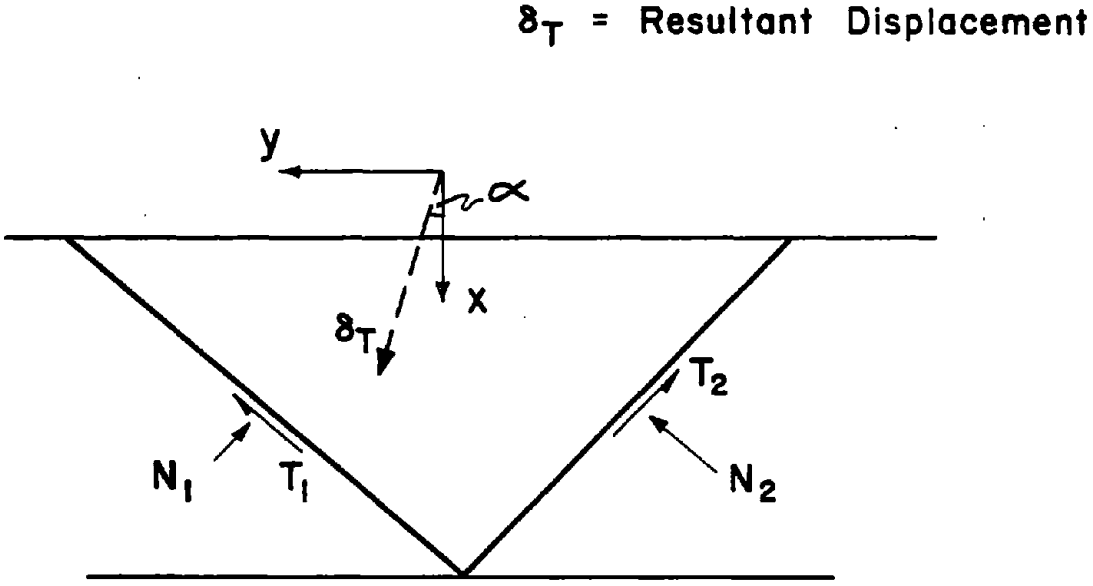

Figure 4.12 Generalized Stiffness Approach--Unknown Parameters

$$\delta_t h = \frac{N_2}{(\cos \alpha \operatorname{ctn} \beta_2 - \sin \alpha)k_{2n}} \tag{4.38}$$

$$= \frac{T_2}{(\cos \alpha + \sin \alpha \operatorname{ctn} \beta_2)k_{2s}} \tag{4.39}$$

All of the above expressions are derived in Appendix D.

The six equations can be reduced to two if T_1, T_2 and N_2 are expressed in terms of T_1 and substituted into the force equilibrium equations:

$$\cos \beta_1 + \frac{ak_{1s} \sin \beta_1 + bk_{2n} \cos \beta_2 + ck_{2s} \sin \beta_2}{(\sin \alpha + \cos \alpha \operatorname{ctn} \beta_1)k_{1n}} = \frac{X}{N_1} \tag{4.40}$$

$$\sin \beta_1 - \frac{ak_{1s} \cos \beta_1 + bk_{2n} \sin \beta_2 - ck_{2s} \cos \beta_2}{(\sin \alpha + \cos \alpha \operatorname{ctn} \beta_1)k_{1n}} = \frac{Y}{N_1} \tag{4.41}$$

where $a = \cos \alpha - \sin \alpha \operatorname{ctn} \beta_1$

$b = \cos \alpha \operatorname{ctn} \beta_2 - \sin \alpha$

$c = \cos \alpha + \sin \alpha \operatorname{ctn} \beta_2$

The two equations involve only two unknowns (N_1 and α). They can solved for α:

$$\alpha = \tan^{-1}\left[\frac{YB - XA}{XC - YA}\right] \tag{4.42}$$

$$A = (K_{1n} - k_{1s})\cos\beta_1 + (k_{2s} - k_{2n})\cos\beta_2$$

$$B = k_{1n}\frac{\cos^2\beta_1}{\sin\beta_1} + k_{1s}\sin\beta_1 + k_{2n}\frac{\cos^2\beta_2}{\sin\beta_2} + k_{2s}\sin\beta_2$$

$$C = k_{1n}\sin\beta_1 + k_{1s}\frac{\cos^2\beta_1}{\sin\beta_1} + k_{2n}\sin\beta_2 + k_{2s}\frac{\cos^2\beta_2}{\sin\beta_2}$$

All the remaining unknowns can be found by substituting back into the various equations. The solution procedure is a cumbersome operation to perform by hand, but it can be easily programmed for a computer. (They have been included in the program SWARS-2PM described in Appendix UM5.)

All the expressions shown above were based on a two dimensional cross section; hence, the analysis implicitly assumed the wedge has a length of unity along the line of intersection. Strictly speaking, the equations are valid only for cases involving an infinitely long wedge of constant dimensions in an infinitely high rock slope (Figure 4.13). The joint planes bounding the wedge form a notch in the slope; X and Y correspond to loads per unit length along the notch. All of the reactions at the joint planes are constant along the slope. Obviously, these conditions are seldom even approximated in the field.

Fortunately, the physical interpretation of the results need not be quite so restrictive. The left side of Equations 4.40 and 4.41 depend only on stiffnesses and the shape of the wedge (β_1,β_2); they do not contain any terms involving h, the height of the wedge. Thus, the ratios X/N_1 and Y/N_1 are constant for geometrically similar cross sections even though X, Y and N_1 may each be functions of h. This independence can be used to generalize the applicability of Equations 4.40 and 4.41. They are valid for finite wedges as long as all cross sections

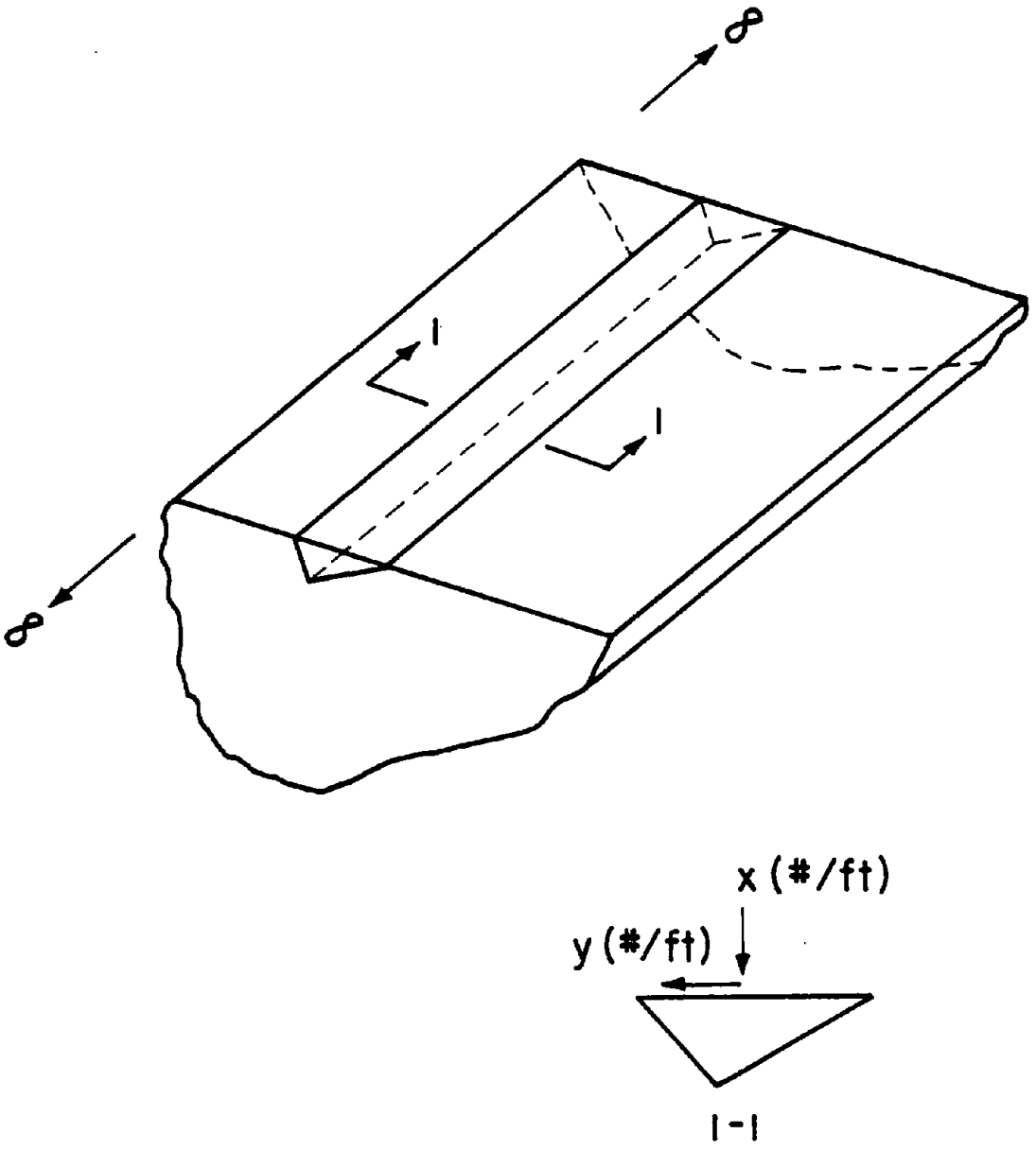

Figure 4.13 Notch in Infinite Slope

perpendicular to the line of intersection are geometrically similar. This situation occurs whenever the line of intersection of the joint planes intersects the slope at a right angle (Figure 4.14). The proof of this generalized relationship is relatively straightforward:

Equation 4.40 can be rewritten in terms of differentials

$$dN_1 = \frac{dX}{e} \tag{4.43}$$

$$\text{where } e = \left(\cos \beta_1 + \frac{ak_{1s} \sin \beta_1 + bk_{2n} \cos \beta_2 + ck_{2s} \sin \beta_2}{(\sin \alpha + \cos \alpha \operatorname{ctn} \beta_1)k_{1n}}\right)$$

N_1 is the total force in joint plane 1.

$$N_1 = \int_{\substack{\text{entire}\\\text{wedge}}} dN_1 = \frac{1}{e} \int_{\substack{\text{entire}\\\text{wedge}}} dX \tag{4.44}$$

$$N_1 = \frac{X}{e} \tag{4.45}$$

Similarly,

$$N_1 = \frac{Y}{f} \tag{4.46}$$

$$\text{where } f = \left(\sin \beta_1 - \frac{ak_{1s} \cos \beta_1 + bk_{2n} \sin \beta_2 - ck_{2s} \cos \beta_2}{(\sin \alpha + \cos \alpha \operatorname{ctn} \beta_1)\, k_{1n}}\right.$$

Equations 4.45 and 4.46 are mathematically identical to 4.40 and 4.41; however, X and Y represent the <u>total</u> applied forces in the x and y direction rather than unit loads as in Equations 4.40 and 4.41.

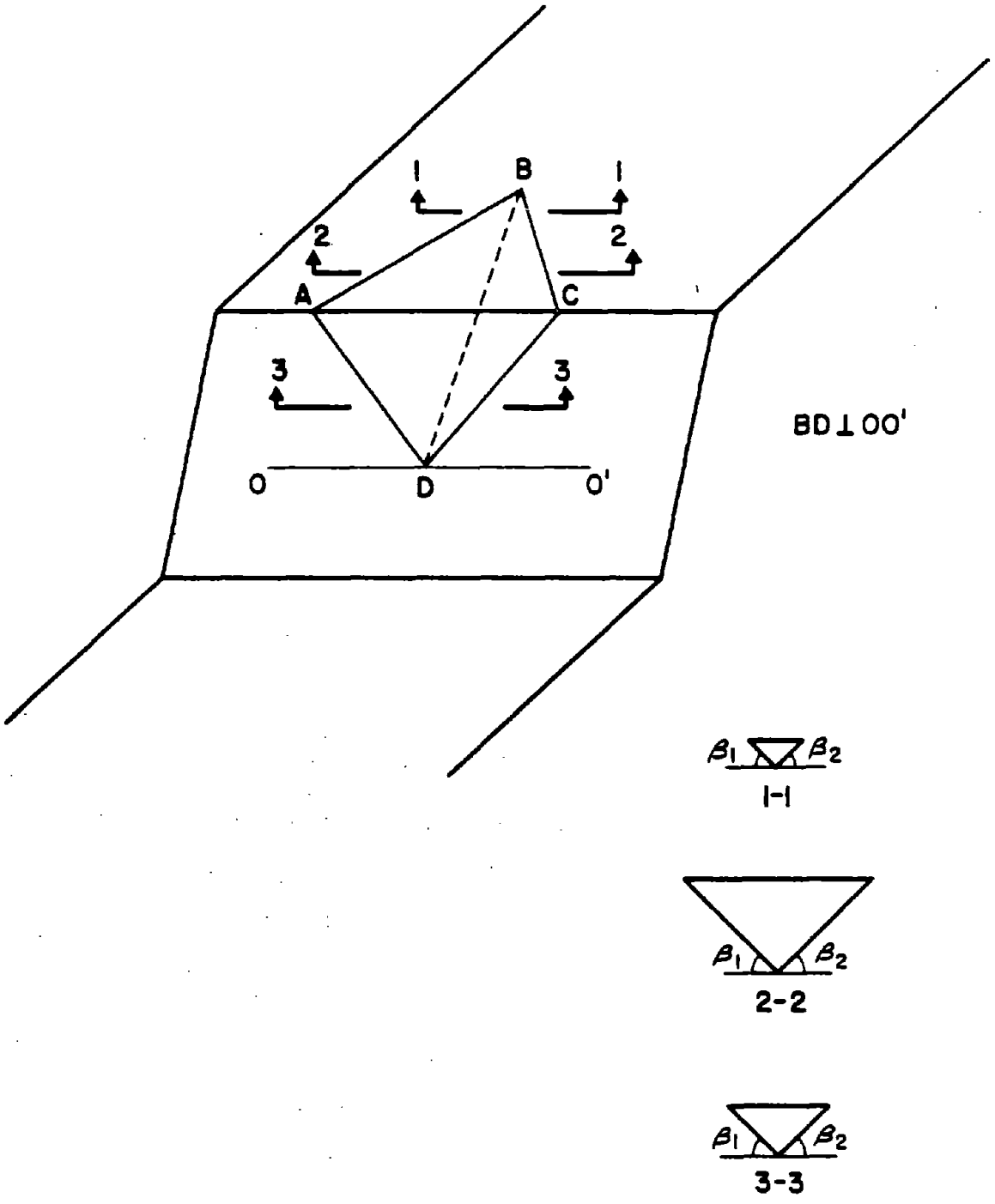

Figure 4.14 Wedge With Geometrically Similar Cross Sections

Analyses involving asymmetrical wedges must be handled on an individual basis. The gross contact areas between the wedge and its parent rock mass must be calculated for each joint plane. As will be discussed later, the analysis can easily be programmed for computerized solutions.

4.3.2 Applications Under Special Conditions

There are some special situations where it is possible to simplify the analysis. If there is no load in the y direction, i.e., Y = 0 the expression for α (Equation 4.42) simplifies to:

$$\alpha = \tan^{-1}\left[\frac{(k_{1s} - k_{1n})\cos\beta_1 + (k_{2n} - k_{2s})\cos\beta_2}{k_{1n}\sin\beta_1 + k_{1s}\frac{\cos^2\beta_1}{\sin\beta_2} + k_{2n}\sin\beta_2 + k_{2s}\frac{\cos^2\beta_2}{\sin\beta_2}}\right] \tag{4.47}$$

Case 1: $Y = 0 \quad k_{1n} = k_{2n} = k_{1s} = k_{2s}$

When all the stiffnesses are equal the numerator of the equation reduces to 0 and α becomes 0. The equality of stiffness (together with Y = 0 implies that the resultant displacement of the wedge will be in the x direction ($\alpha = 0$).

Case 2: $Y = 0 \quad k_{1n} = k_{2n} >> k_{1s} = k_{2s}$

These conditions correspond to the assumptions implicitly made in conventional stability analyses. The equation for α becomes:

$$\alpha = \tan^{-1}\left[\frac{\cos\beta_2 - \cos\beta_1}{\sin\beta_1 + \sin\beta_2}\right] = \frac{\beta_1 - \beta_2}{2} \tag{4.48}$$

Thus, the resultant displacement will occur at an inclination equal to half the difference between β values (Figure 4.15).

4.3.3 Discussion of Results Obtained with Generalized Stiffness Approach

The solution procedure outlined above has been used to develop several plots that illustrate the sensitivity of the results (particularly N_1 and N_2) to changes in the input parameters (β_1, β_2, k_{1n}, k_{2n}, k_{1s}, k_{2s}). The results are valid for a wedge in a infinitely long notch or a wedge whose line of intersection is orthogonal to the strike of the slope face. In all cases, it has been assumed that Y = 0 and X = weight of the wedge. The results are expressed in the same manner as those presented in Section 4.1 i.e., the dependent variable is Φ_R (the value of Φ required to produce a factor of safety equal to 1.0):

$$\Phi_R = \tan^{-1} \left(\frac{W \sin \theta}{N_1 + N_2} \right)^* \qquad (4.49)$$

θ = angle between the line of intersection of joint planes and the horizontal (Figure 4.16).

W = weight of wedge

Figure 4.16 shows a typical wedge and identifies the parameters selected for study in the sensitivity analyses.

Case 1: $k_{1n} = k_{2n}$; $k_{1s} = k_{2s}$; $\psi = 90°$

$0° \leq \beta_1 \leq 90°$

$0° \leq \beta_2 \leq 90°$

*Tangential driving force parallel to line of intersection only.

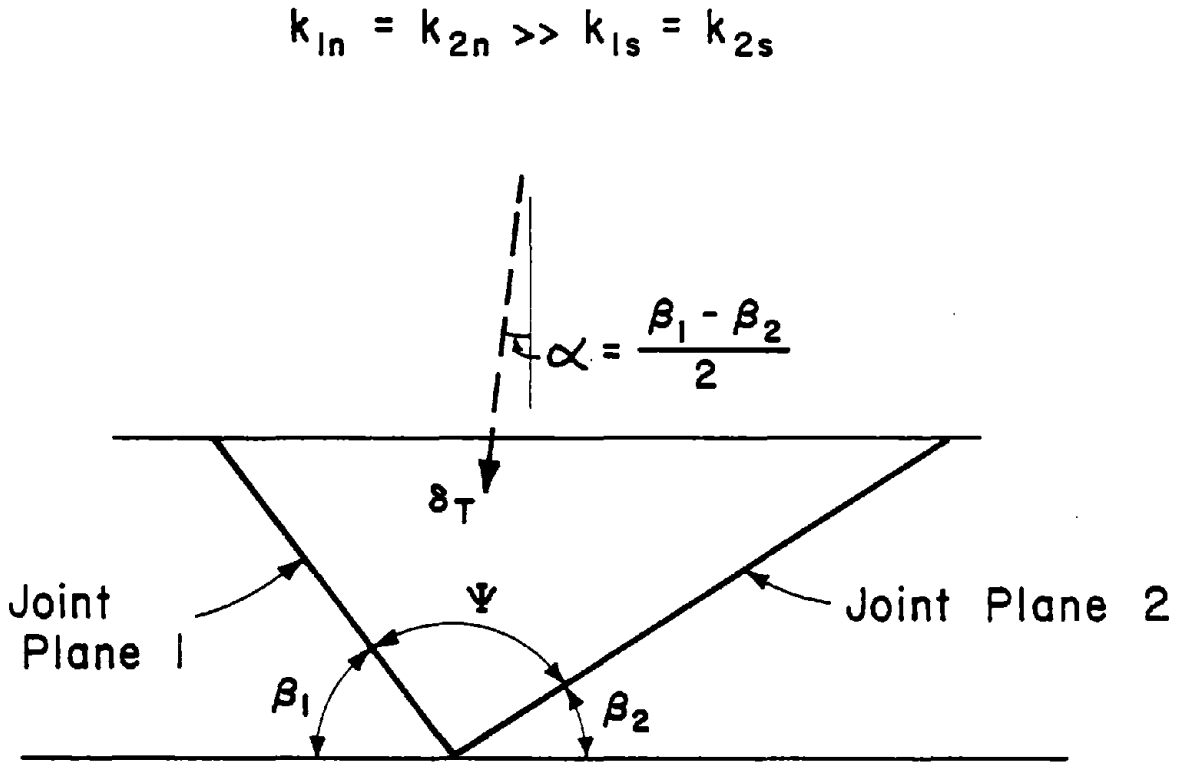

Figure 4.15 Direction of Displacement When $K_{1n} = K_{2n} >> K_{1s} = K_{2s}$

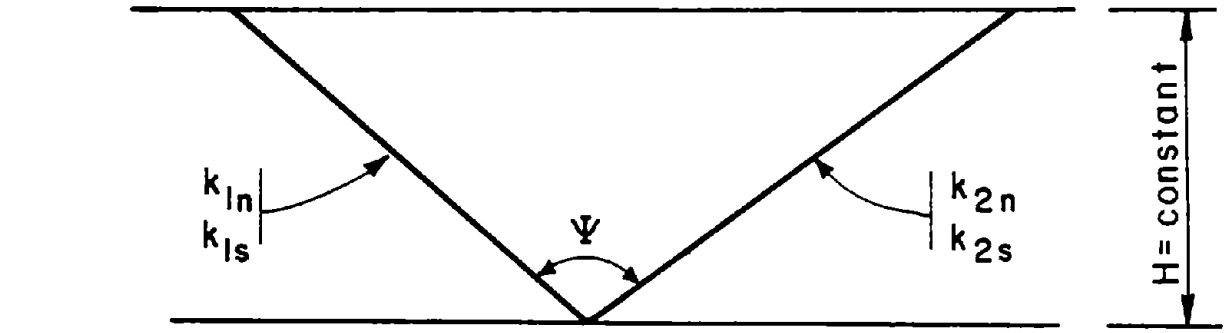

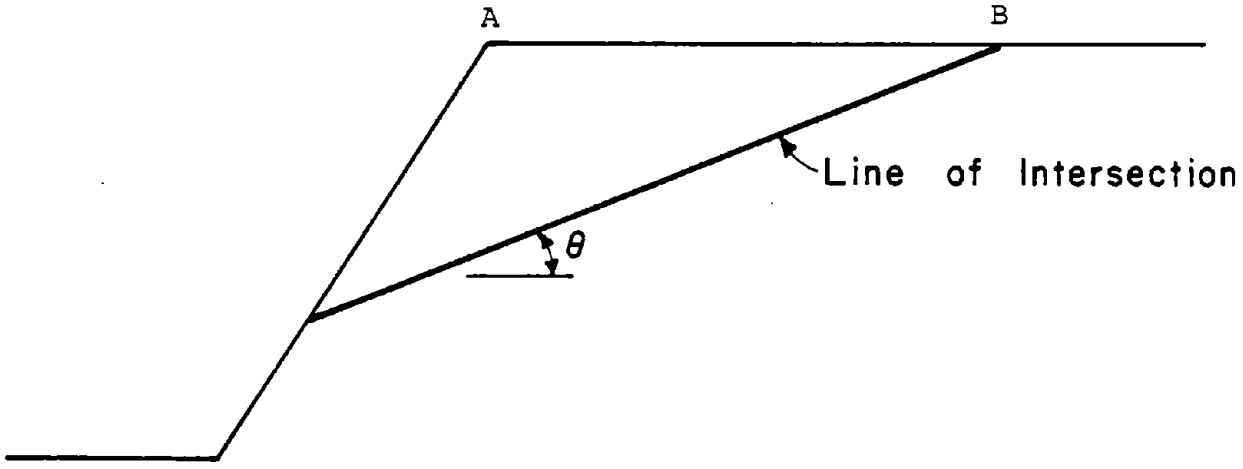

Figure 4.16 Parameters Varied in Sensitivity Analyses

Figure 4.17 illustrates the functional relationship between β_1 and ϕ_R (β_1 and β_2 are complementary angles as $\beta_2 = 180° - \psi - \beta_1 = 90° - \beta_1$). Two families of curves were developed for $\theta = 30°$ and $\theta = 45°$ respectively. Each family is composed of several members that represent different values of R, the stiffness ratio:

$$R = \frac{k_{1n}}{k_{1s}} = \frac{k_{2n}}{k_{2s}} \tag{4.50}$$

All the curves are symmetrical about the line $\beta_1 = \beta_2 = 45°$.

$R = \infty$ and $R = 1$ represent conditions that are tentatively considered to be the upper and lower bounds for natural rock joints. The curve for $R = \infty$ reflects the effect of "wedging" (Hoek and Bray, 1972) as Φ_R decreases with increasing β_1. The curve for $R = 1$ shows just the opposite trend as Φ_R increases strongly with β_1. (The two curves seem to be symmetrical about the line $\Phi_R = \theta$. However, this apparent symmetry has not been analytically proven. There is no readily discernible explanation for this effect from a mechanical standpoint). A stiffness ratio of 2.5 yields a virtually constant value of friction angle that is approximately equal to θ.

Case 2: $k_{1n} = k_{2n}$; $k_{1s} = k_{2s}$ $\psi = 120°$.

$0° \leq \beta_1 \leq 60°$

$0° \leq \beta_2 \leq 60°$

The curves for $\psi = 120°$ (Figure 4.18) look quite similar to those for $\psi = 90°$ (Figure 4.17). They have an axis of symmetry and they diverge as β_1 increases. However, the divergence is not as pronounced for $\psi = 120°$. The difference in Φ_R values is approximately 8.2° at $\beta = \beta_1 = 30°$. Once again, a value of $R = 2.5$ yields $\Phi_R \sim \theta$ regardless of the value of β_1.

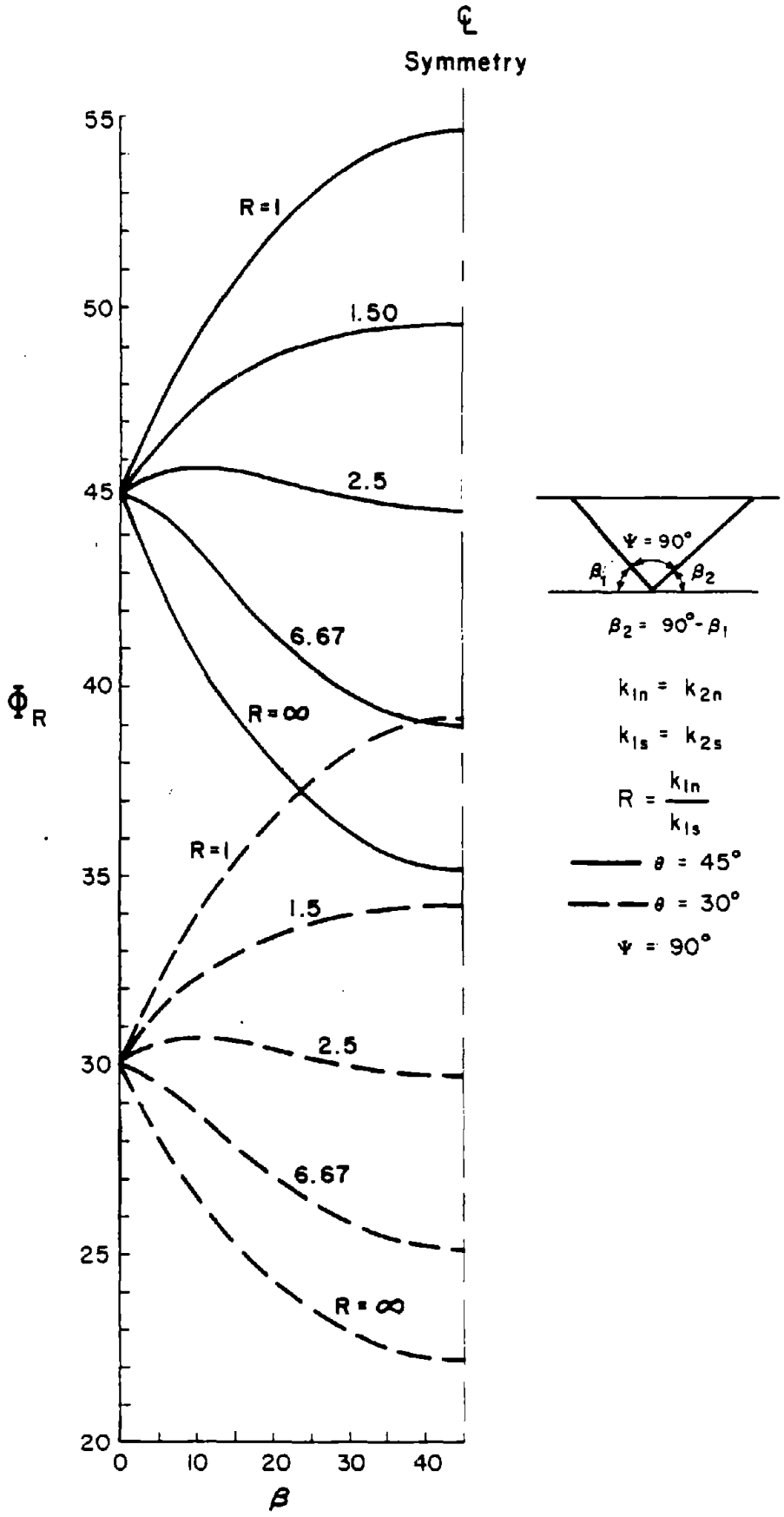

Figure 4.17 Φ_R vs. β_1 For $\Psi = 90^\circ$

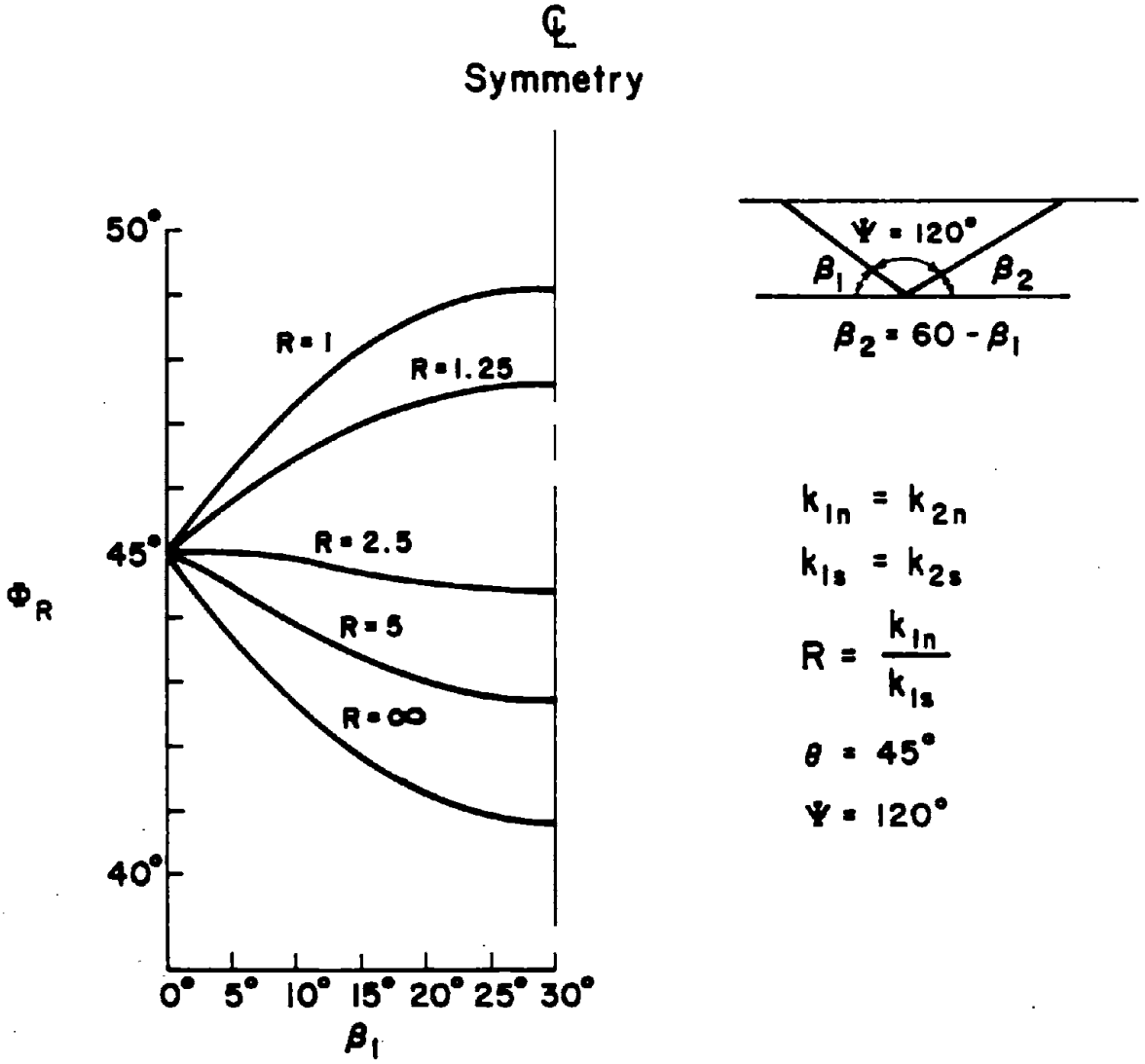

Figure 4.18 Φ_R vs. β_1 For $\Psi = 120^\circ$

Case 3: $k_{1n} = k_{2n}$; $k_{1s} = k_{2s}$; $\psi = 60°$

$0° \leq \beta_1 \leq 120°$

$0° \leq \beta_2 \leq 120°$

Figure 4.19 presents results for the case $\psi = 60°$. Near the axis of symmetry ($\beta_1 = 60°$) the curves behave much like the ones examined earlier. However, as β_1 approaches 0 the curve become irregular. A problem arises in that region because β_2 ($\beta_2 = 120° - \beta_1$) becomes greater than 90°, i.e., joint plane 2 overhangs the wedge (Figure 4.20). The overhang does not pose any difficulties from an analytical standpoint; however, the physical interpretation of the results demands closer scrutiny: for every R there is a critical value of β_1 (defined as β_{1cr}) such that for all $\beta_1 < \beta_{1cr}$ the normal force on joint plane 2 is tensile. This value β_{1cr} occurs when the direction of the wedge's resultant displacement δ_T is parallel to joint plane 2 (Figure 4.20). Figure 4.21 shows the relationship between β_{1cr} and R. If $\beta_1 \leq \beta_{1cr}$ the wedge tends to pull away from joint plane 2. Continuous rock joints cannot sustain a tensile load so the $\beta_1 - \Phi_R$ curves must be modified to reflect the change in N_2. The exact form of the curve depends on the shape and deformational characteristics of the asperities in the joint plane. It is conceivable that even in the absence of a normal force some asperities may interlock and generate a shear force in the overhanging joint plane. On the other hand, if the plane is relatively smooth, T_2 (as well as N_2) may reduce to 0 as soon as β_1 is less than β_{1cr}. Figure 4.22 illustrates schematically some of the typical forms that the curve for R = 1 may assume. Curve B ignores the tension problem. It is merely a mathematical extension of Curve A into tensile region of N_2. Curve C represents the other extreme. A severe discontinuity occurs at $\beta_1 = \beta_{1cr} = 30°$ as both N_2 and T_2 drop to 0. The portion of Curve C that lies to the left of point 0 represents sliding along a single plane--plane 1. The estimated curve D recognizes the existence of some shear forces in the joint plane for $0 < \beta < \beta_{1cr}$. Most natural joint

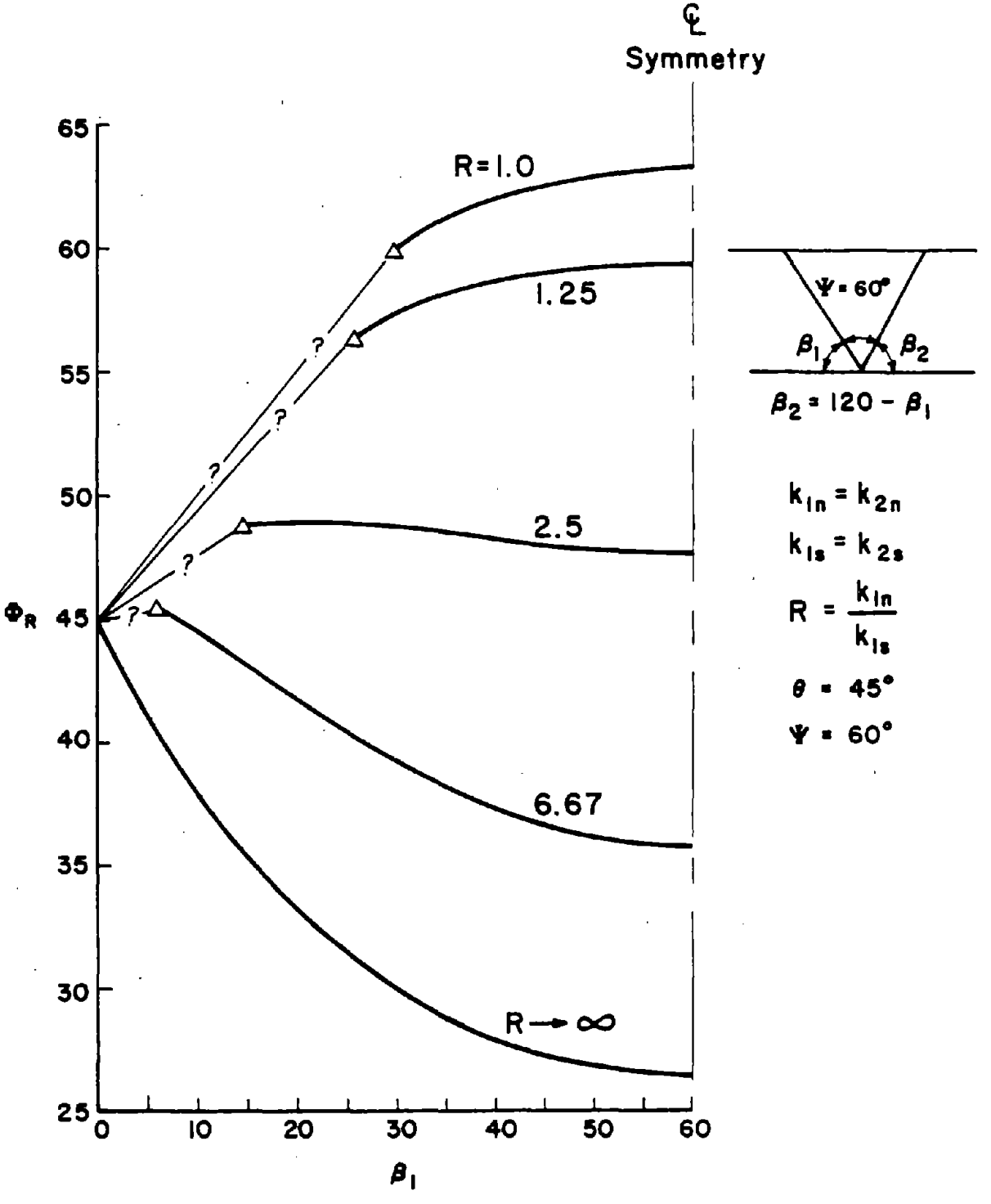

Figure 4.19 Φ_R vs. β_1 For $\Psi = 60^\circ$

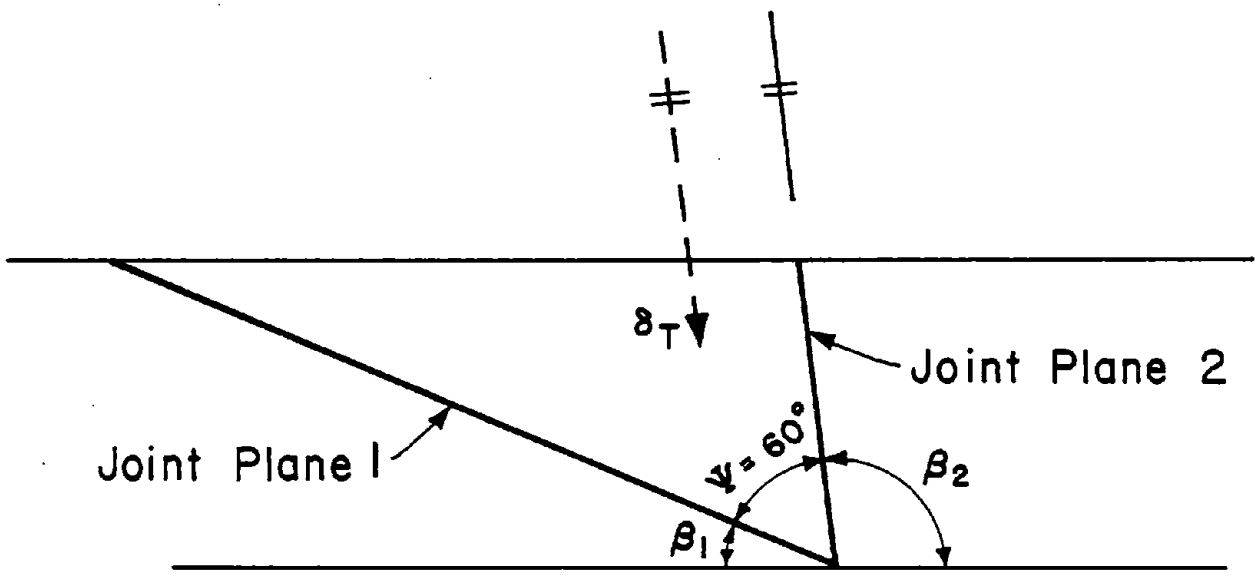

Figure 4.20 Overhanging Joint Plane

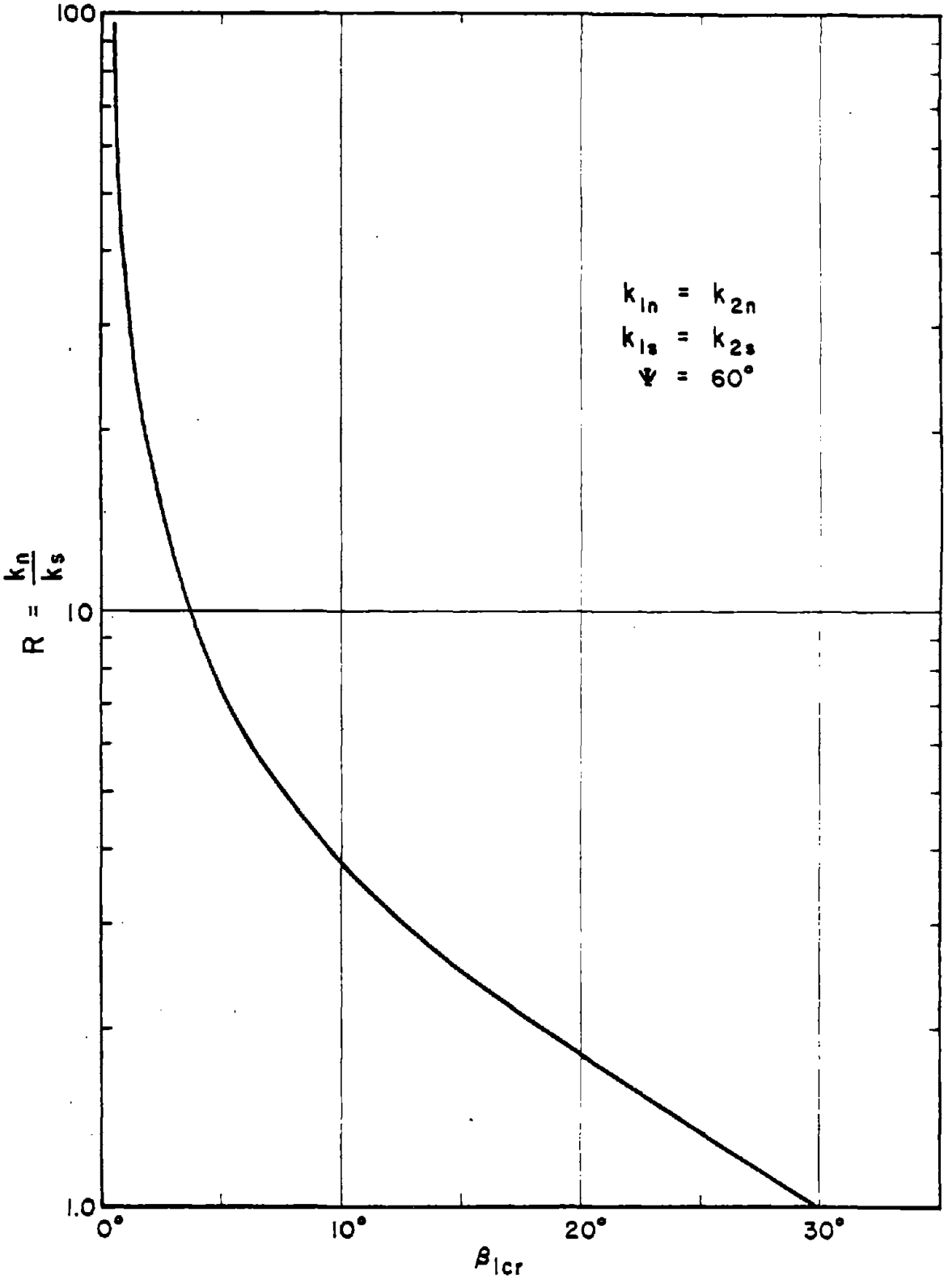

Figure 4.21 R vs. β_{1cr} for $\Psi = 60^{\circ}$

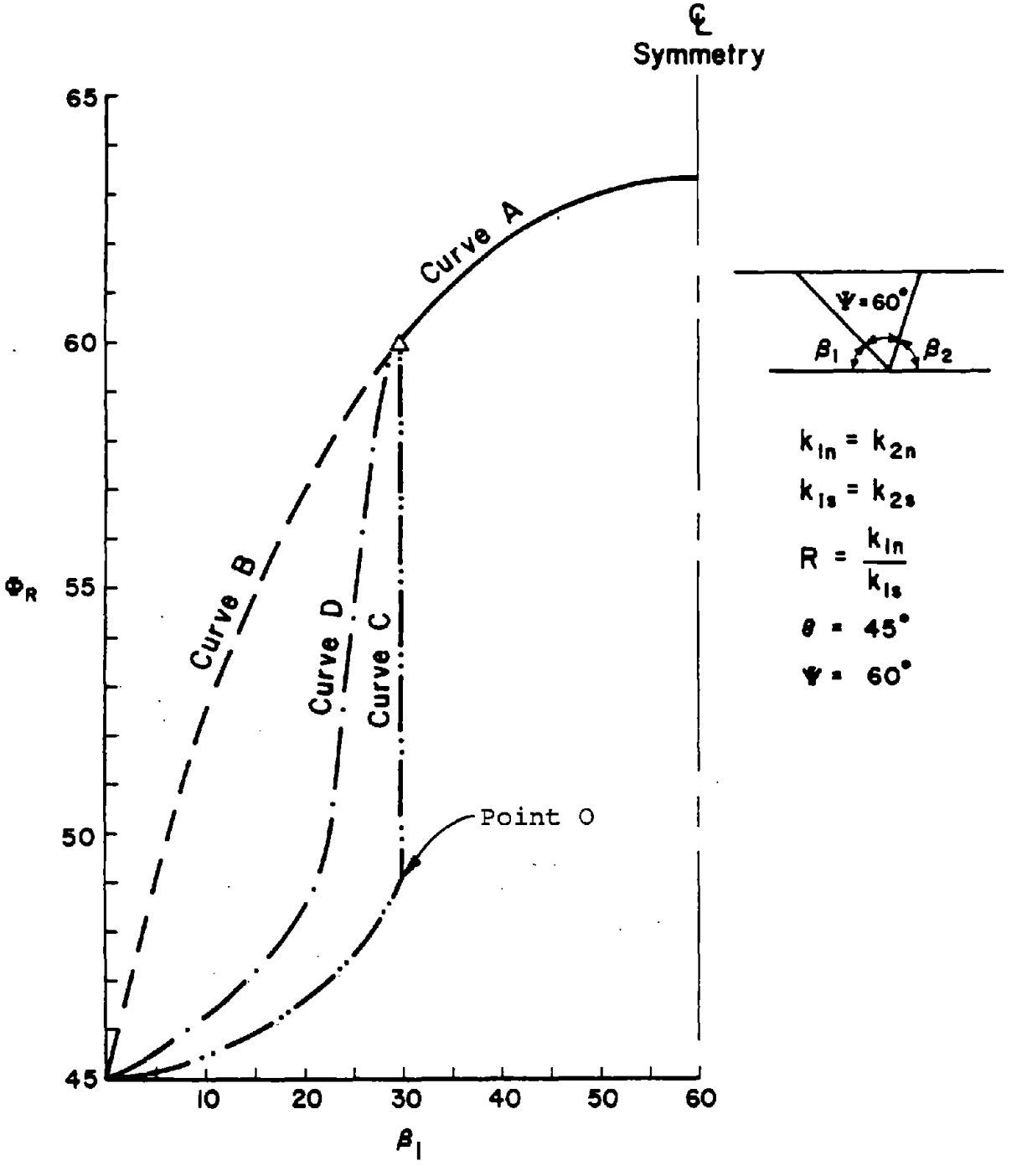

Figure 4.22 Φ_R vs. β_1 For $\Psi = 60^\circ$ and R = 1--Curves Reflect Different Reactions on Joint Plane 2

planes would probably have curves that plot between C and D.

When $\beta_1 > \beta_{1cr}$, the curves for R = 1 and R = ∞ seem to be symmetrical (Figure 4.19), a property which is apparently shared by all such pairs of curves (Figures 4.17, 4.18). For $\psi = 60°$, the maximum difference ($\Delta\Phi_{R\,max}$) between the curves is 30°. This difference always reaches a maximum at $\beta_1 = \beta_2$ (symmetry) and is a function of ψ. Figure 4.23 shows that $\Delta\Phi_{R\,max}$ is a very strong function of ψ and decreases rapidly as ψ increases.

Case 4: $k_{1s} = k_{1n}; k_{2n}$

$0° \leq \beta_1 \leq 90°$

$0° \leq \beta_2 \leq 90°$

$$S = \frac{k_{2s}}{k_{1s}} = \frac{k_{2n}}{k_{1n}}$$

The effect of different stiffnesses in the joint planes is shown in Figure 4.24. The curves become more skewed as S increases. The changes in shape reflect the fact that in Equation 4.49 the numerator (W sin θ) is a constant while the denominator ($N_1 + N_2$) varies with geometry of the wedge. A high value of S suggests that joint plane 2 bears a disproportionately large share of the weight of the wedge. The reaction at joint plane 2 consists of N_2 and T_2. Since β_1 and β_2 are complementary angles, β_1 values near 0° are associated with β_2 values near 90°. When β_2 approaches 90° most of the reaction is supplied by T_2. Under these conditions (low β_1 and high S), N_1 and N_2 are low and a high Φ_R is required to maintain equilibrium. The argument can be reversed for cases involving β_1 near 90°. β_2 near 0° implies a high N_2 and a correspondingly low Φ_R.

All of the curves pass through the point $\beta_1 = 45°$ and $\Phi_R = 54.75$. Since ψ equals 90°, β_1 of 45° defines a symmetrical wedge. Under this special condition, the sum $N_1 + N_2$ is a constant regardless of the value of S.

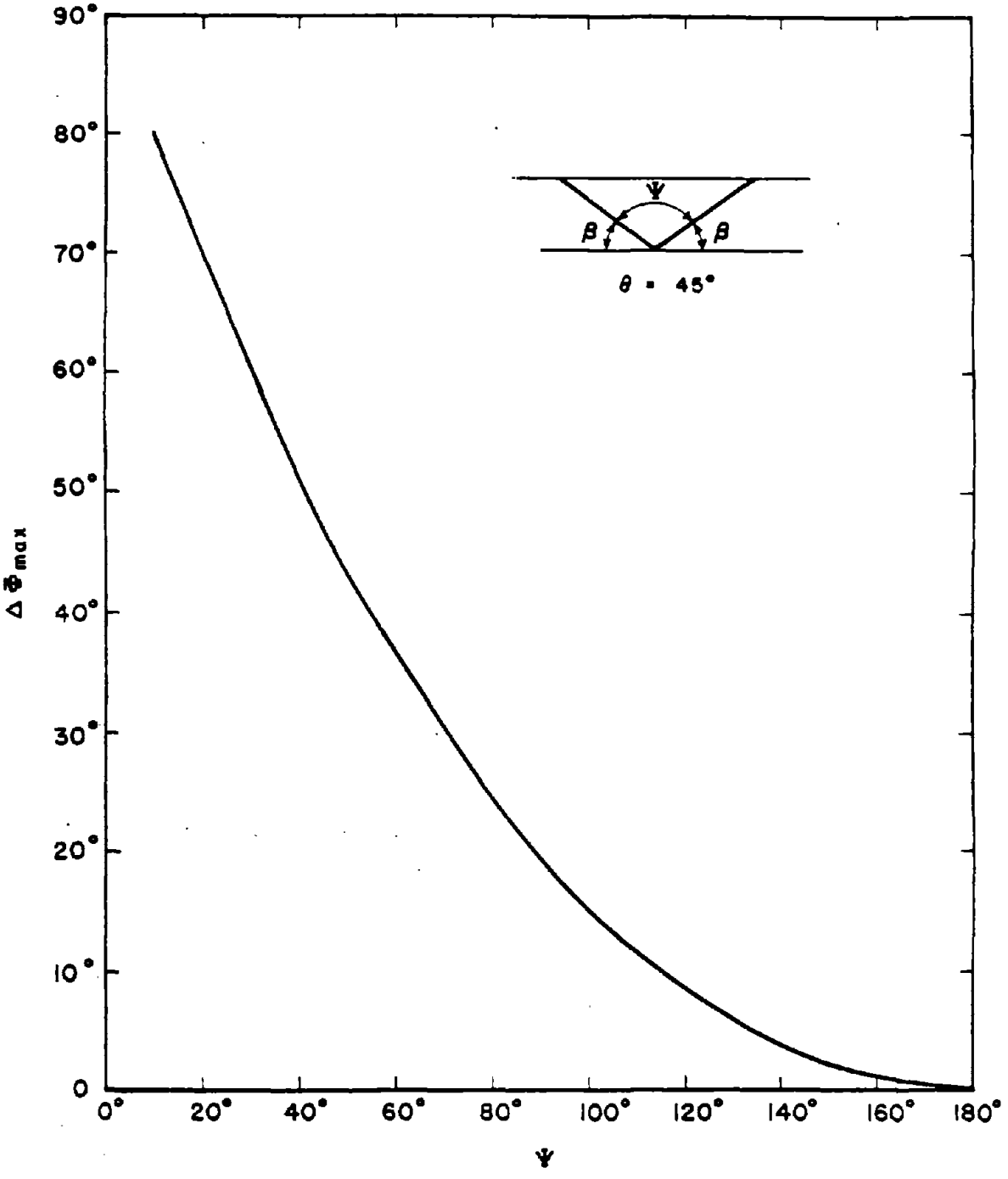

Figure 4.23 $\Delta\Phi_{max}$ vs. Ψ for $\theta = 45^{\circ}$

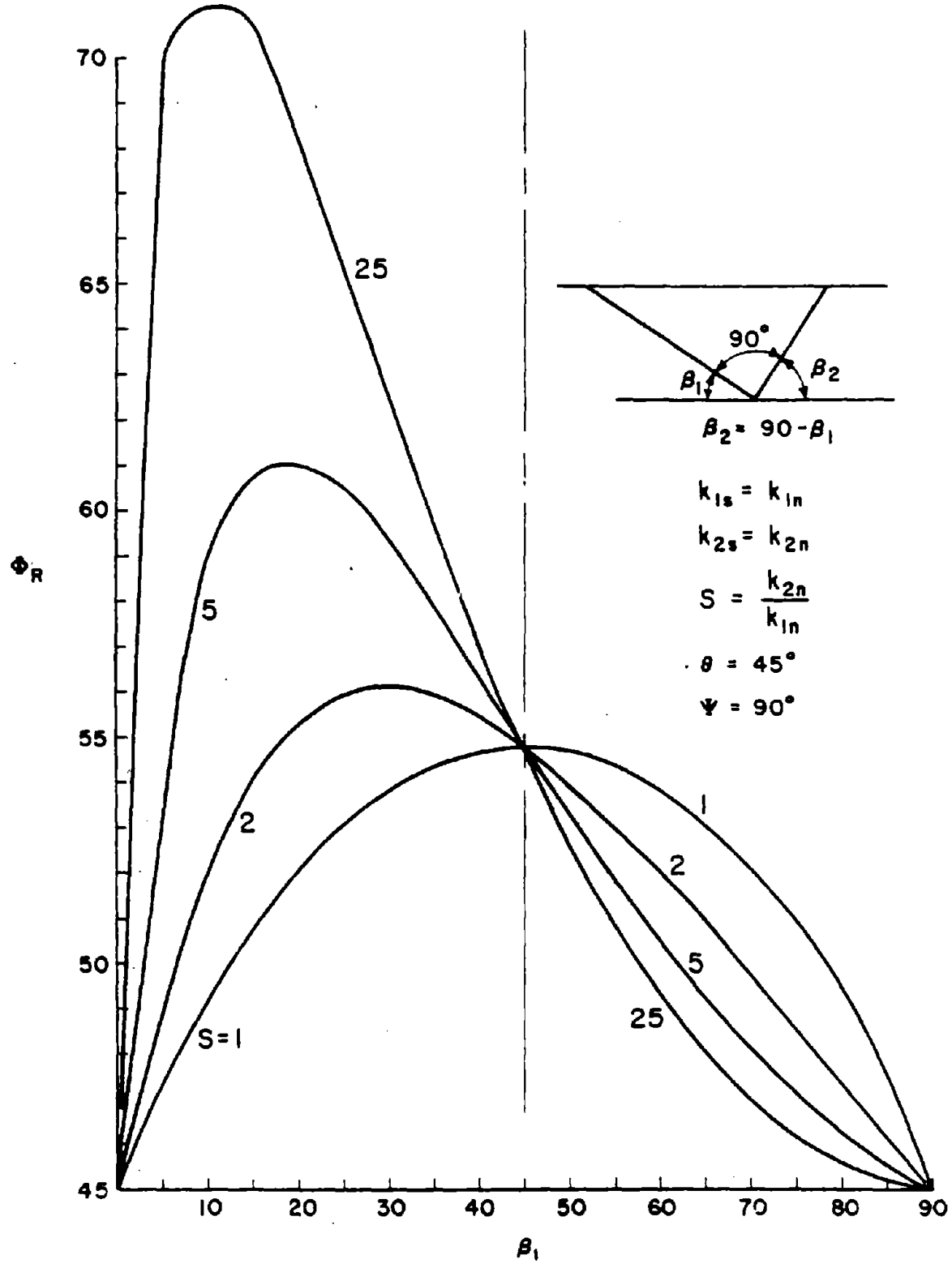

Figure 4.24 Φ_R vs. β_1 For $\Psi = 90^\circ$ and Varying S

All of the results summarized in this section are based on wedges that have geometrically similar cross sections along their entire lengths. The physical significance of this assumption was discussed earlier. The method can however be generalized to handle wedges with arbitrary geometries. The technique is discussed in Section 4.6 in connection with the computer program SWARS-2PM.

4.4 Stress Approach Vs. Stiffness Approach

Section 4.2 showed that assumptions regarding force acting on planes critically affect stability analysis. That same section discussed the "stress" and "stiffness" approaches as two alternate methods to more correctly consider the actual conditions. As mentioned there and in the introduction (Section 4.1) (usually simplifying) assumptions have to be made because the rigid body conditions do not consider stress distributions which in turn govern the forces. An obvious question arises: Is it possible to know the stresses on the joint planes? The question is difficult to answer because the stresses depend on cumulative effects of loads and joint stiffnesses - both of which can change as time progresses. Figure 4.25 illustrates the concept. It is a schematic representation of the temporal variations in loads, joint stiffnesses and stresses that occurred during the existence of a hypothetical wedge.

The stresses are a function of the loads and stiffnesses. During any small time increment Δt there is a direct relationship between incremental loads (ΔL) and incremental stresses (ΔS). ΔS is related to ΔL through the stiffness equations presented in Section 4.4. The precise relationship between ΔS and ΔL depends on the values of the stiffnesses during that interval. An incremental load applied at t_1 will not necessarily produce the same change in stresses as the same load applied at t_2 because the stiffnesses at t_1 and t_2 may be different. The stresses at any time t reflect the original stresses (at t_0) plus all the changes that have occurred since t_0. (The model presumes that the principle of superposition is valid at least in a crude sense.) Thus, S_p, the present state of stress, is a function of the cumulative interaction between loads and stiffnesses; S_p is not directly related to the current stiffnesses.

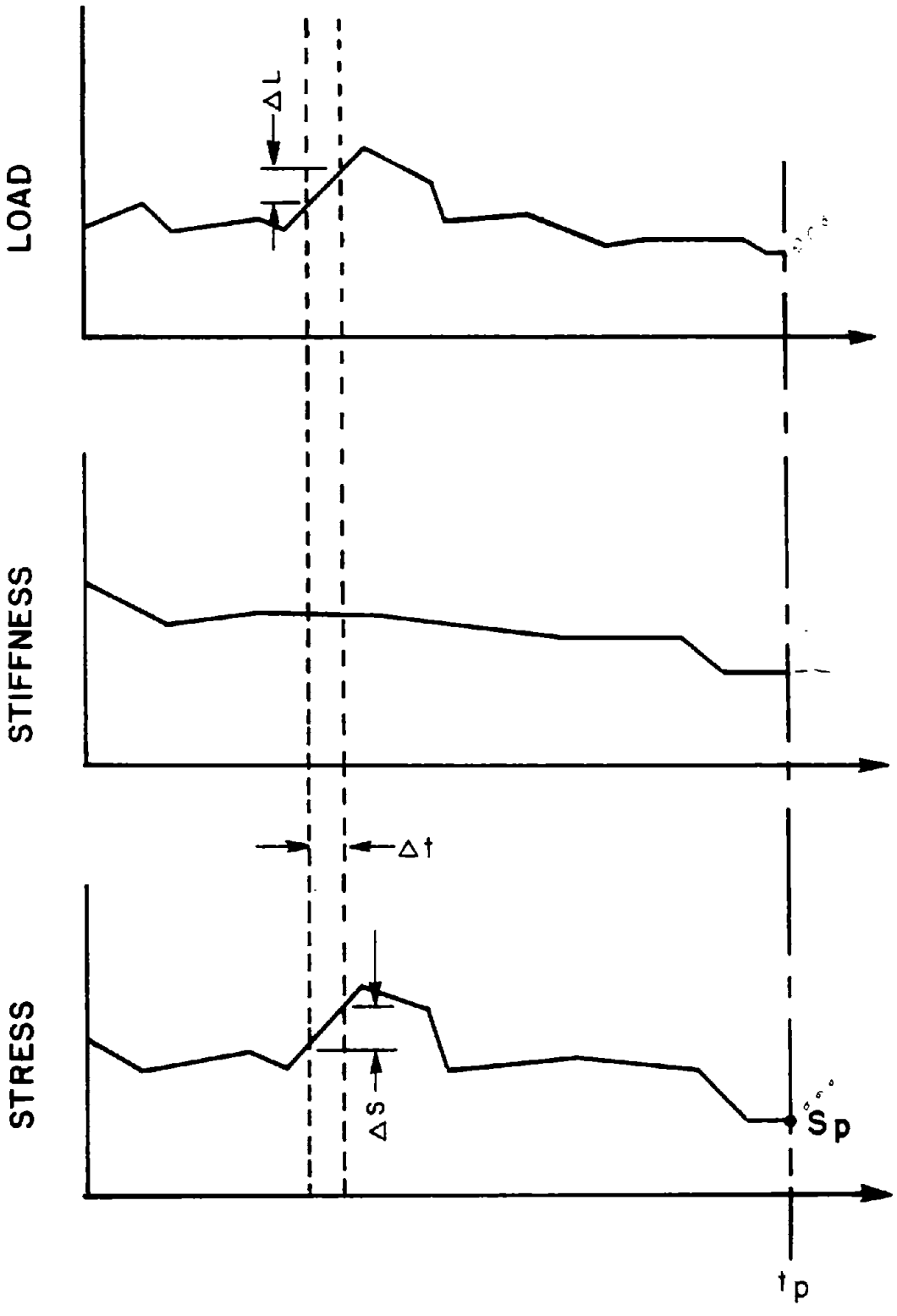

Figure 4.25 Load, Stiffness and Stress vs. Time

The lateral stiffnesses are instrumental in determining the effects of additional loads, but yield no information concerning S_p.

The lateral stress ratio K is an expression of the present state of stress S_p. As a consequence of the conclusions just drawn, K reflects the original state of stress and any changes since then, including the stress that created the discontinuities. The stress state may however have further changed after creation of the joints (within the limits K_p and K_a as explained in Section 4.2). Two important conclusions can be drawn from the fact that the present stress state and K reflect the entire history.

- K within the wedge can be different from K in the slope. (K in the wedge can only vary between K_a and K_p; K in the slope can vary over a wider range).
- The stability analysis of a wedge only subject to its weight should be considered with "stress approach" and not the stiffness approach. (The present joint stiffness has only effect on the last stress increment but not on the stress state - see Figure 4.24.)

A practical note needs to be made here. Although the stress approach is analytically correct, it may be problematic to perform since K is difficult to measure, particularly if the stresses are absolutely small.

Joint stiffness has, however, to be considered if the present (natural) state of stress S_p is changed. If, again referring to Figure 4.25, a load is added at T_p (dotted line in Figure 4.25) the new stress state can be derived only through the joint stiffnesses. One would naturally measure the stress state or K after application of the load, this is however practically difficult (and expensive) as mentioned before; more importantly, however, it would not allow predictive analyses, the normal use of analysis. These considerations on stiffness lead thus to the conclusion

- Stability analyses of wedges subject to loads in addition to their weight have to be considered with the "stiffness approach".

The complete stability analysis has thus to combine stress and stiffness approaches in the following manner:

1. The stress approach is used to calculate the reactions (N_1, N_2, T_1, T_2) due to the weight of the wedge.
2. The stiffness approach is used to calculate the reactions due to all other additional loads, particularly if the analysis is used to make stability predictions.

The procedure is admittedly a simplification of actual conditions but it does present a consistent methodology for treating rock wedges.

As mentioned, the weight of the wedge should be analyzed through the stress approach. The stiffness plots shown as Figures 4.17 to 4.19 are a direct violation of this principle. These plots describe the highly idealized situation portrayed in Fig.4.26; the wedge weight is treated as an external load that is applied only after the stiffnesses have revealed their current values. As discussed earlier, the stiffness approach should however only treat "current" loads. Although the plots should not be used to examine gravitational loads they can be used to examine any other loading that is directly proportional to the size of the wedge. The plots were based on cross sections with different shapes (β_1 varied) but with a constant height (Figure 4.16). N_1 and N_2 are directly proportional to the weight of the unit cross sections (Equation 4.45); $X = W \cos \theta$. Equation 4.49 indicates that Φ_R, the ordinate of the plots, is a function of $\frac{W}{N_1 + N_2}$; hence, any loading that is directly proportional to the weight should yield the same values of Φ_R. Since the wedges have a constant height, the distance AB in Figure 4.16 is directly related to the area or to the weight of the action. Thus a uniform loading along AB would be directly related to the weight of the wedge. Therefore, Figures 4.17 to 4.20 show the effect of a uniform surcharge on the top (and front) faces of the wedge.

4.5 The Factor of Safety

The presence of shear forces on the joint planes in a direction perpendicular to the line of intersection presents some difficulties in defining the factor of safety (FS). This problem was alluded to in

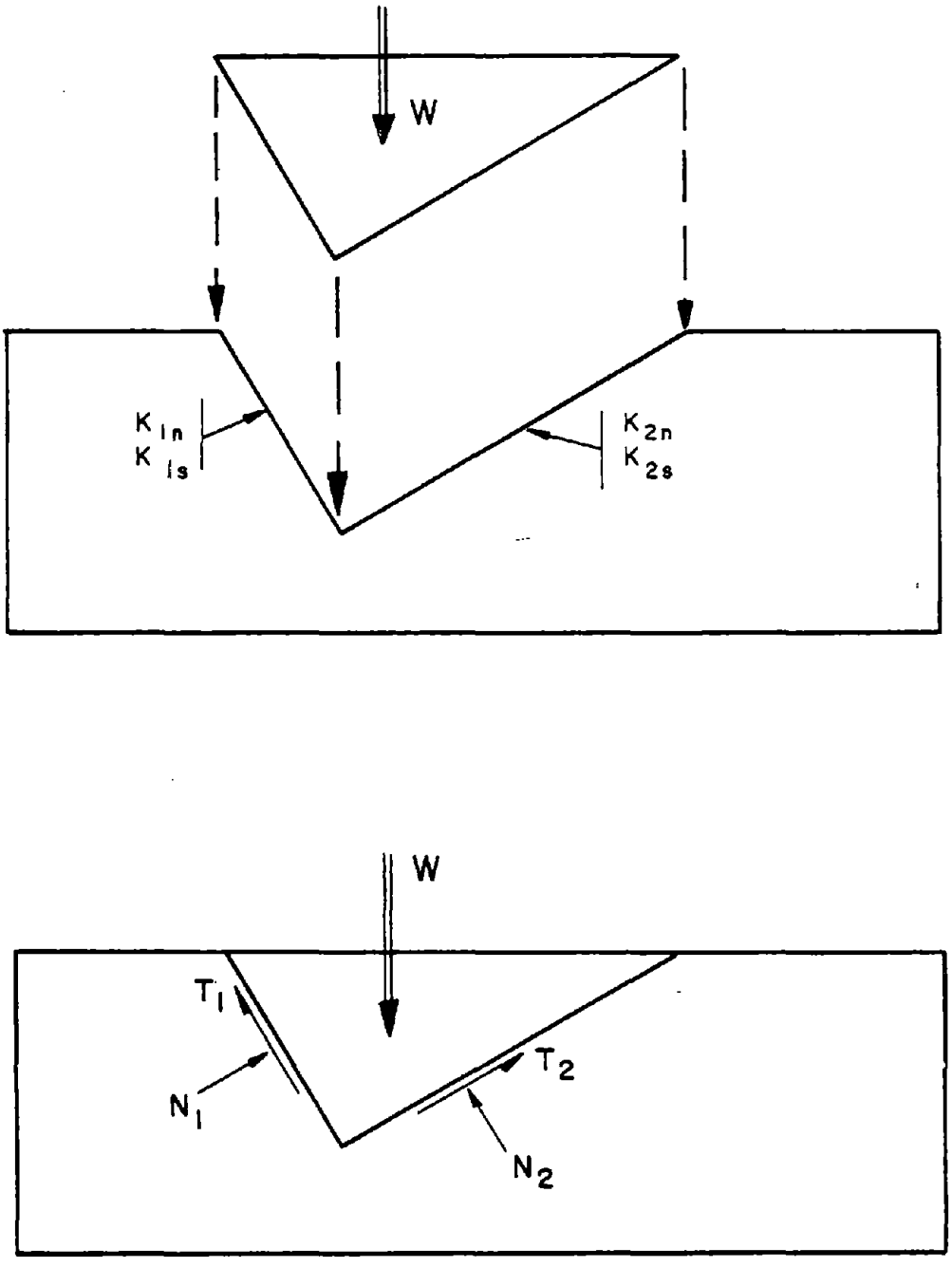

Figure 4.26 Stiffness Approach--Idealized Case

Section 4.2 where FS was calculated two different ways. In rock slope analyses FS is usually defined as the ratio of resisting to driving forces. However, the definition assumes that both forces act in the same direction. The condition is seldom fulfilled in real problems.

Figure 4.27 shows the shear forces that should be considered in a typical stability analysis. As derived in Figure 4.2, the shear force along the line of intersection is W sin θ*. T_1 and T_2 are shear forces perpendicular to the line of intersection. In the special case where K = 1 (the situation considered in conventional analyses) T_1 and T_2 are both zero; therefore, the entire shear resistance along the joint planes counteracts W sin θ. Whenever K does not equal unity the shear resistance must counteract T_1 and T_2 in addition to W sin θ. In fact, the effect is magnified because the presence of T_1 and T_2 actually decreases the shear resistance. As indicated in Section 4.1, T_1 and T_2 increase at the expense of N_1 and N_2. As N_1 and N_2 decrease the frictional resistance declines. The crucial questions are, how do T_1 and T_2 affect the stability of the wedge, and how can they be incorporated into stability calculations?

St. John addressed this problem in analyzing symmetric wedges with purely frictional resistance. As indicated in Section 4.2, St John defined the factor of safety as:

$$FS = \frac{2N \tan \Phi}{\sqrt{(2T)^2 + (W \sin \theta)^2}} \qquad (4.56)$$

Thus, the driving force was considered the vectorial sum of the shear forces** in the joint planes. The resultant shear forces in the two planes are mirror images of one another because the wedge is symmetric. At limiting equilbrium the direction of impending motion is down the line

* This simplified model presumes that gravity is the only force acting on the wedge.

**St. John computed the T forces through a stiffness analysis; however, the derivation of T is not a salient feature of the current discussion.

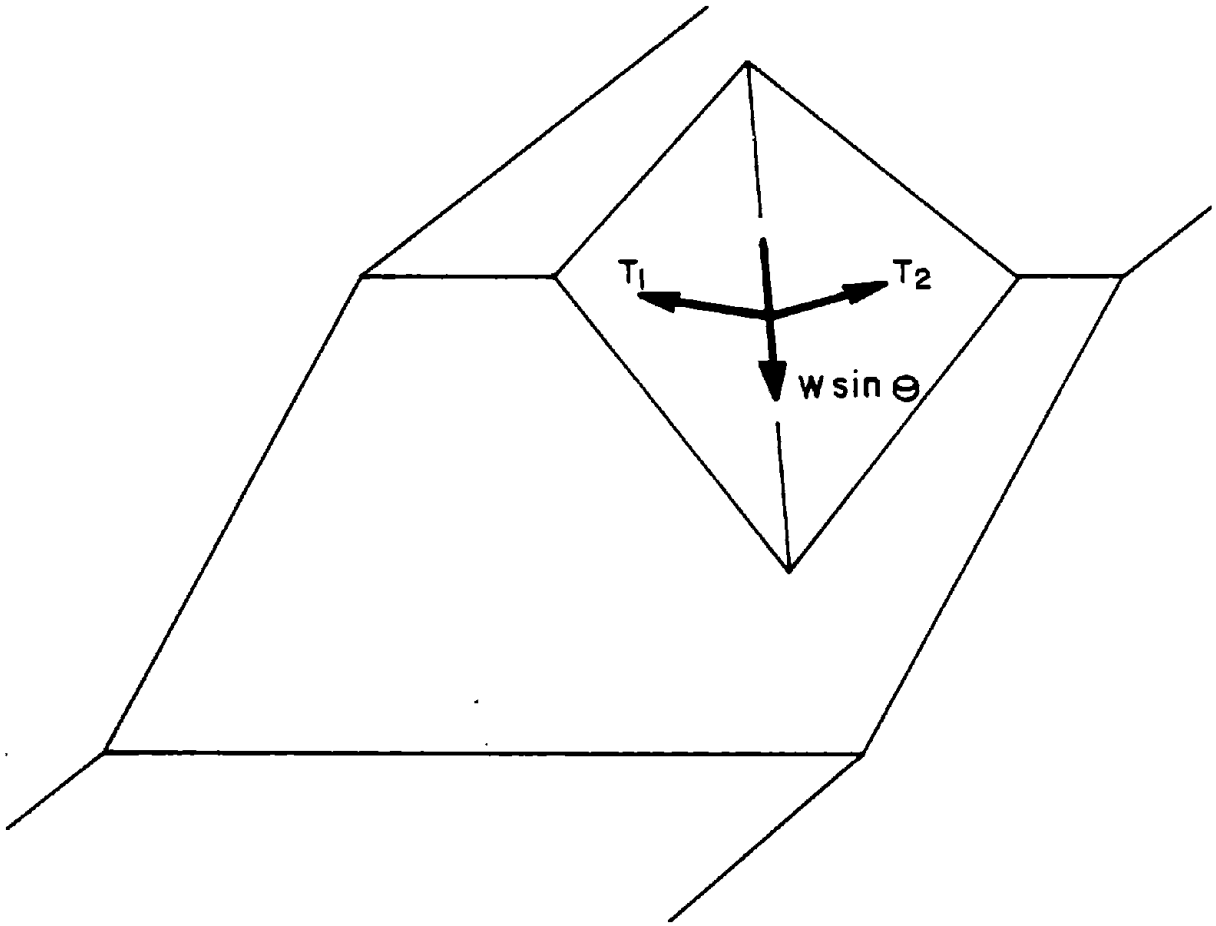

Figure 4.27 Shear Forces on Joint Planes

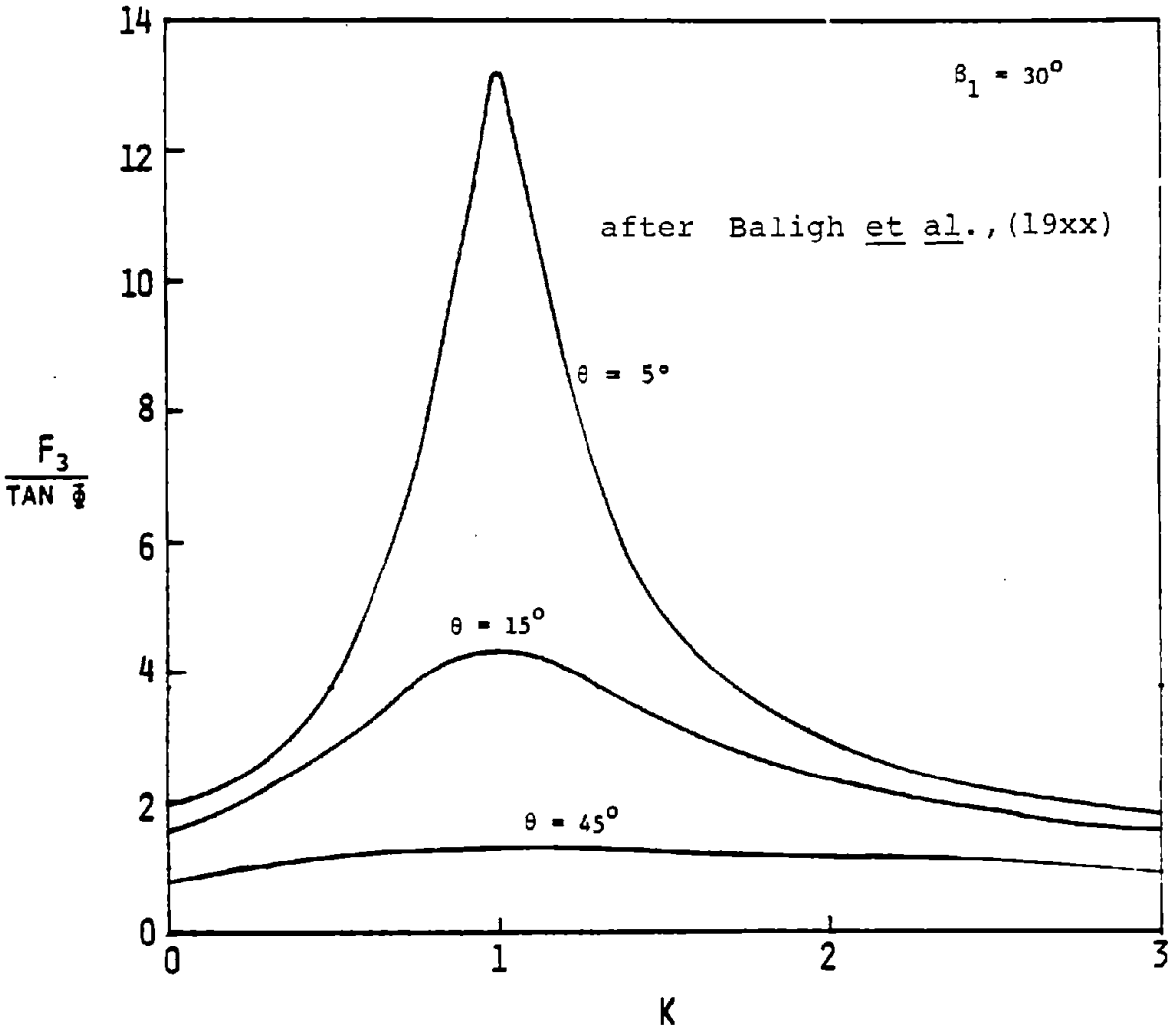

Figure 4.28 $F_3/\tan \Phi$ vs. K; $\beta_1 = 30^\circ$

of intersection and into the notch i.e., the wedge has a tendency to "settle" in the notch as well as move down the line of intersection.

The direction of motion is an important consideration in examining stability problems. What are the practical implications of a wedge settling in its notch? Surely there is a limit to the amount of movement that can occur in this direction. A minor amount of settlement may not be significant from an engineering standpoint. The important question is What happens after failure? Settlement may be tolerable but sliding down the line of intersection is clearly unacceptable. Strictly speaking, limiting equilibrium cannot provide any insight into post-failure behavior because it is concerned solely with the condition of the system just at failure.

Baligh et al. (19xx) have done some interesting work in the area investigating the influence of K, the stress ratio, on the stability of symmetric wedges. They used the stress approach developed by Steiner (as presented in Section 4.2) to determine the forces on the joint planes; hence, both T and N are functions of K. Like St. John, Baligh et al. treated the driving force as the vectorial sum of the two shear components on each plane. They define the factor of safety as F_3:

$$FS = F_3 = \frac{2N \tan \Phi}{\sqrt{(2T)^2 + (W \sin \theta)^2}} \tag{4.56}$$

The equation can be rewritten as:

$$\frac{F_3}{\tan \Phi} = \frac{2N}{\sqrt{(2T)^2 + (W \sin \theta)^2}}$$

As shown in Figures 4.28 and 4.29, the quantity $F_3/\tan \Phi$ can be plotted as a function of K. The three curves in each figure correspond to wedges whose lines of intersection plunge at 5°, 15° and 45°. Figure 4.28 and Figure 4.29 were developed for β's of 30° and 45° respectively.

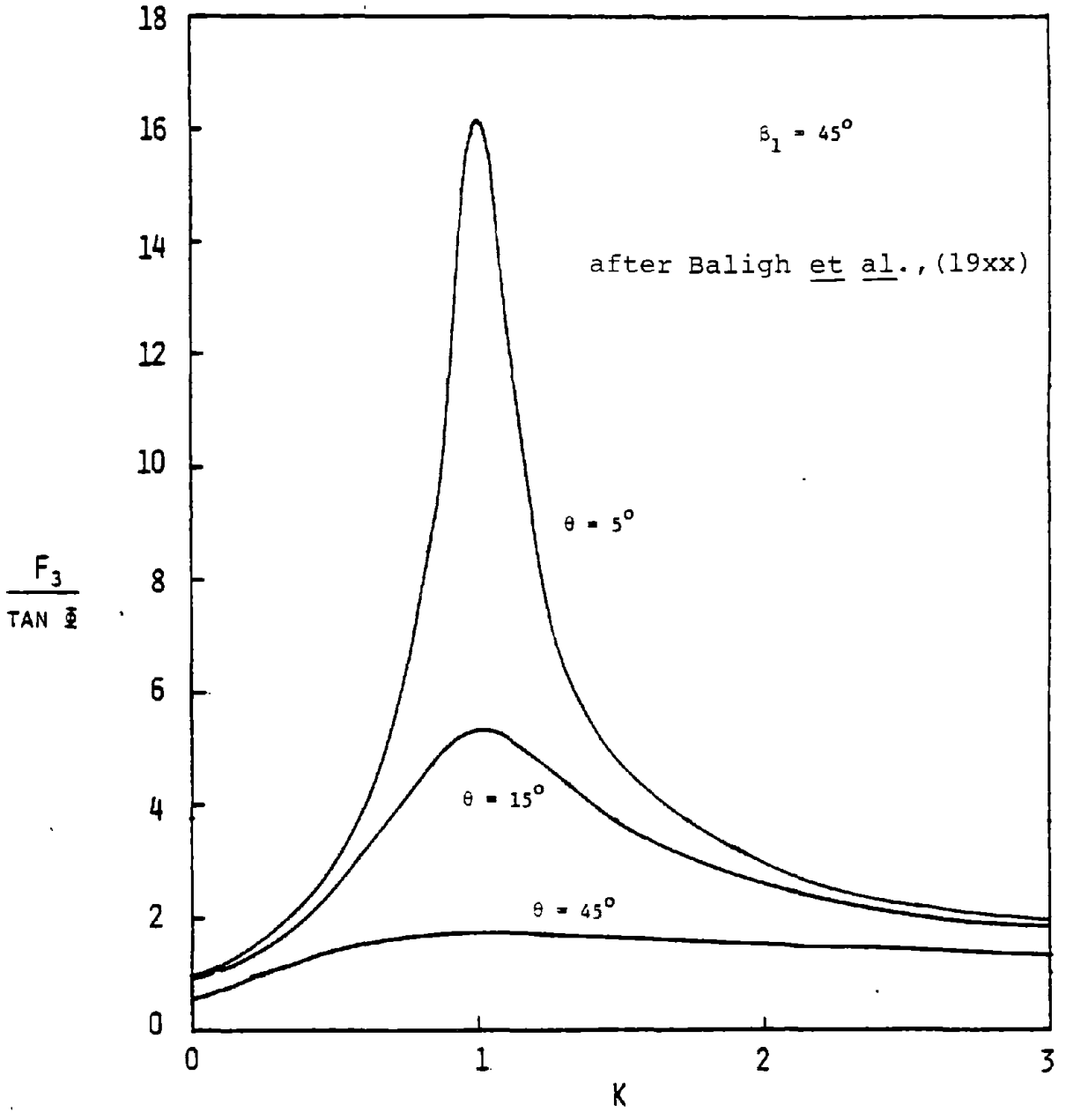

Figure 4.29 $F_3/\tan \Phi$ vs. K; $\beta_1 = 45^\circ$

All of the curves have a maximum at K = 1.0. When K = 1.0, T is zero and the impending motion is down the line of intersection. Also,

$$\frac{F_3}{\tan \Phi} = \frac{1}{\tan \Phi \cos \beta} \tag{4.57}$$

The plots are helpful in visualizing how rock wedges fail. Figure 4.30 is a schematic representation of an F curve similar to the ones in Figures 4.28 and 4.29. (The term tan Φ will be considered a constant. It can be factored into the ordinate scale.) At some arbitrary time (say t_p in Figure 4.25) the stresses on the joint planes correspond to point A. If some additional loads are placed on the wedge the stresses on the joint planes will change - the incremental stresses will depend on the stiffnesses as discussed in Section 4.4. Let the new stress state correspond to point B. At B the wedge is at limiting equilibrium; any additional loads will initiate movement. The direction of movement will be along the line of intersection and into the notch. However, as soon as the wedge begins to settle into its notch the lateral stresses will increase. This "wedging" action increases K which in turn increases N and decreases T. According to this conceptual model the wedge can sustain additional loadings and pass from point B to C and D.* With each incremental load the wedge settles a little more and K increases. Finally, the wedge reaches point E where T is zero. At E i.e., K = 1.0 the direction of movement is exclusively along the line of intersection. Theoretically, there now is nothing to prevent the wedge from sliding along the line of intersection out of its notch.

A similar effect occurs when K > 1.0 i.e., to the right of the maximum. This situation would correspond to passive conditions and the initial movement would be <u>out</u> of the notch and along the line of intersection. K would eventually reach 1.0 as the load increased.

*In the model tan Φ is assumed to be constant even after initial failure (point B).

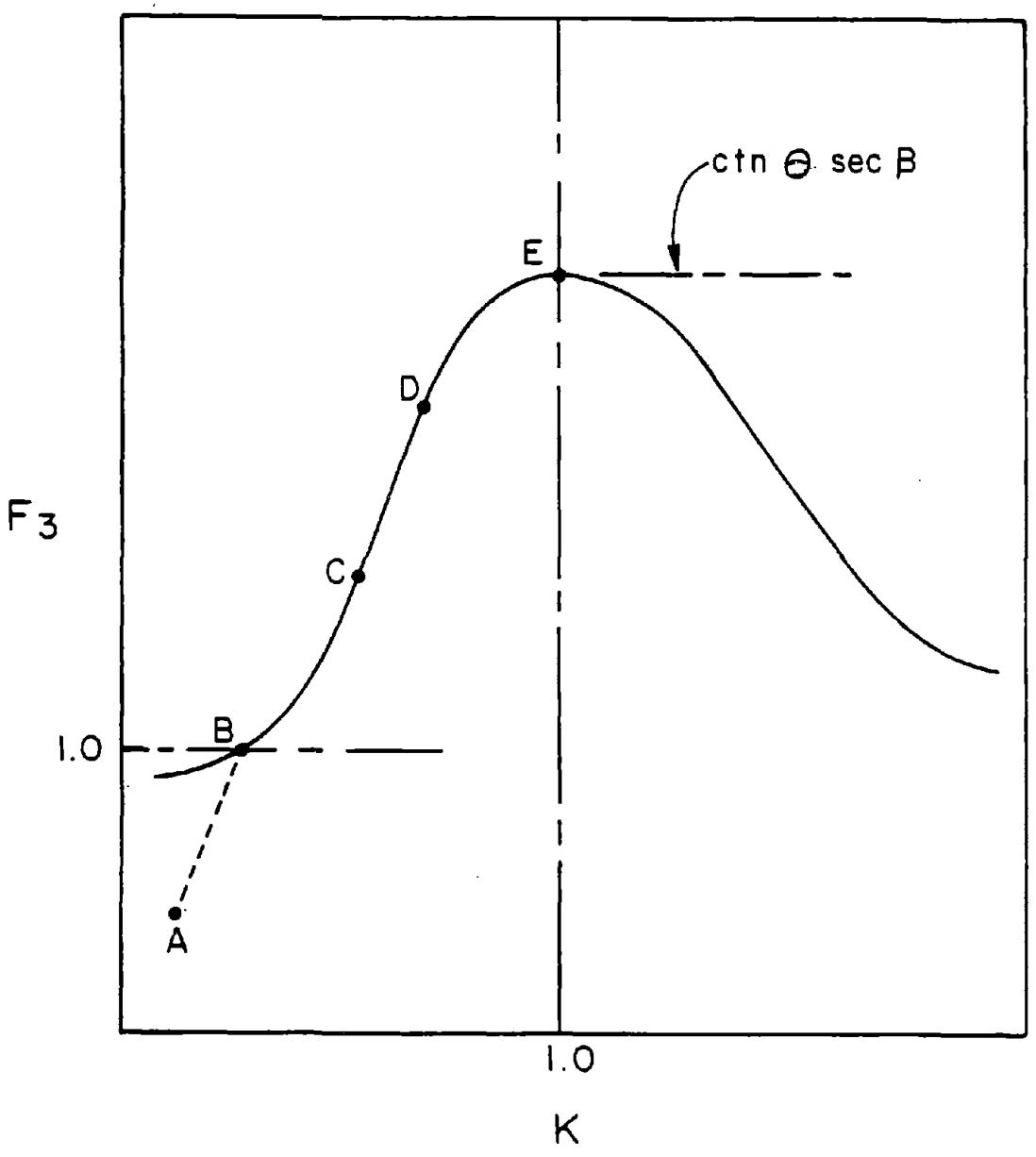

Figure 4.30 Schematic Failure Sequence

Thus, it is possible to define two factors of safety; FS_I, the initial factor of safety, corresponds to point B; FS_U, the ultimate factor of safety, corresponds to point E. FS_U is the value used in traditional stability calculations. The engineer must use his judgement in deciding whether to use FS_I of FS_U as a design criterion in a particular situation. If movements must be kept to an absolute minimum FS_I would be the more appropriate choice. If one merely wanted to design against catastrophic movements, FS_U would be the better choice.

The distinction between the two factors of safety is clear from Figure 4.30. However, that figure is a highly idealized model that ignores some important effects. In particular, it assumes that the shear strength of the joint planes consists solely of frictional resistance that can be expressed with a constant Φ. In reality Φ may be composed of interlocking asperities as well as mineral to mineral friction. The asperities may shear off as movement occurs. In effect, Φ should decrease as the wedge is loaded beyond initial failure. Also, the model neglects cohesion along the joints. This cohesion may consist of bridges of intact rock which will shear when movement commences. One simplistic method for treating these effects is to neglect the cohesion and asperities in computing FS_U. (This is the approach that is used in the method and computer program that will be described in Section 4.6).

All the wedges considered in the discussion of factor(s) of safety have been symmetric with respect to their geometric, stiffness, and frictional characteristics. Under these conditions i.e.

$$\beta_1 = \beta_2 \tag{4.58}$$

$$\Phi_1 = \Phi_2 \tag{4.59}$$

$$k_{1s} = k_{2s} \tag{4.60}$$

$$k_{1n} = k_{2n} \tag{4.61}$$

the impending motion is in the vertical plane that contains the line of intersection. The resultant of all the driving forces and the resultant of the shear resistances are in that same plane; in fact, the two resultants are colinear. Thus, the FS used by St. John and Baligh et al. is a direct comparison of colinear forces. Given the assumption of rigid body movement FS is rigorously defined from the standpoint of mechanics or statics.

FS is much more difficult to define if the wedge is asymmetric i.e., any of the conditions prescribed by Equation 4.58 to 4.61 are violated. Most asymmetric conditions will introduce a displacement component out of the vertical plane that contains the line of intersection. (The situation is shown in Figure 4.12 α is generally non zero for asymmetric conditions.) Also, the resultant of all the driving forces will no longer be colinear with the resultant of all the resisting forces.

The forces (and resultants) are shown in Figure 4.31 which is a plane view of the notch. Each joint plane has a shear component in the direction parallel to the line of intersection. The two components add up to W sin θ. The components in planes 1 and 2 are $n \cdot W \sin \theta$ and $(1 - n) \cdot \sin \theta$ respectively. Each plane also has a shear force perpendicular to the line of interaction (T_1 and T_2). The resultants of ($T_1 + n\ W \sin \theta = \bar{S}_1$) and ($T_2 + (1-n)\ W \sin \theta = \bar{S}_2$) are shown in Fig. 4.31. The shear resistance in each plane is in the direction of the respective resultant. Thus, $\bar{R}_1$ is in the direction of $\bar{S}_1$ and $\bar{R}_2$ is in the direction of $\bar{S}_2$. Both $\bar{R}_1$ and $\bar{R}_2$ represent the maximum possible shear resistance that can be mobilized; therefore, their magnitudes (but not directions) may differ from $\bar{S}_1$ and $\bar{S}_2$. Figure 4.31 indicates that the sum of the resistances $\bar{R} = (\bar{R}_1 + \bar{R}_2)$ is <u>not</u> in the same direction as the sum of the driving forces $D = (\bar{S}_1 + \bar{D}_2)$. $(\bar{R}_1 + \bar{R}_2)$ cannot be compared directly with $(\bar{S}_1 + \bar{S}_2)$ because of the disparity in directions. Thus, FS must be defined in terms of some arbitrary criterion; there is no unequivocal definition.

The computer program that will be described in Section 4.6 uses the following definition:

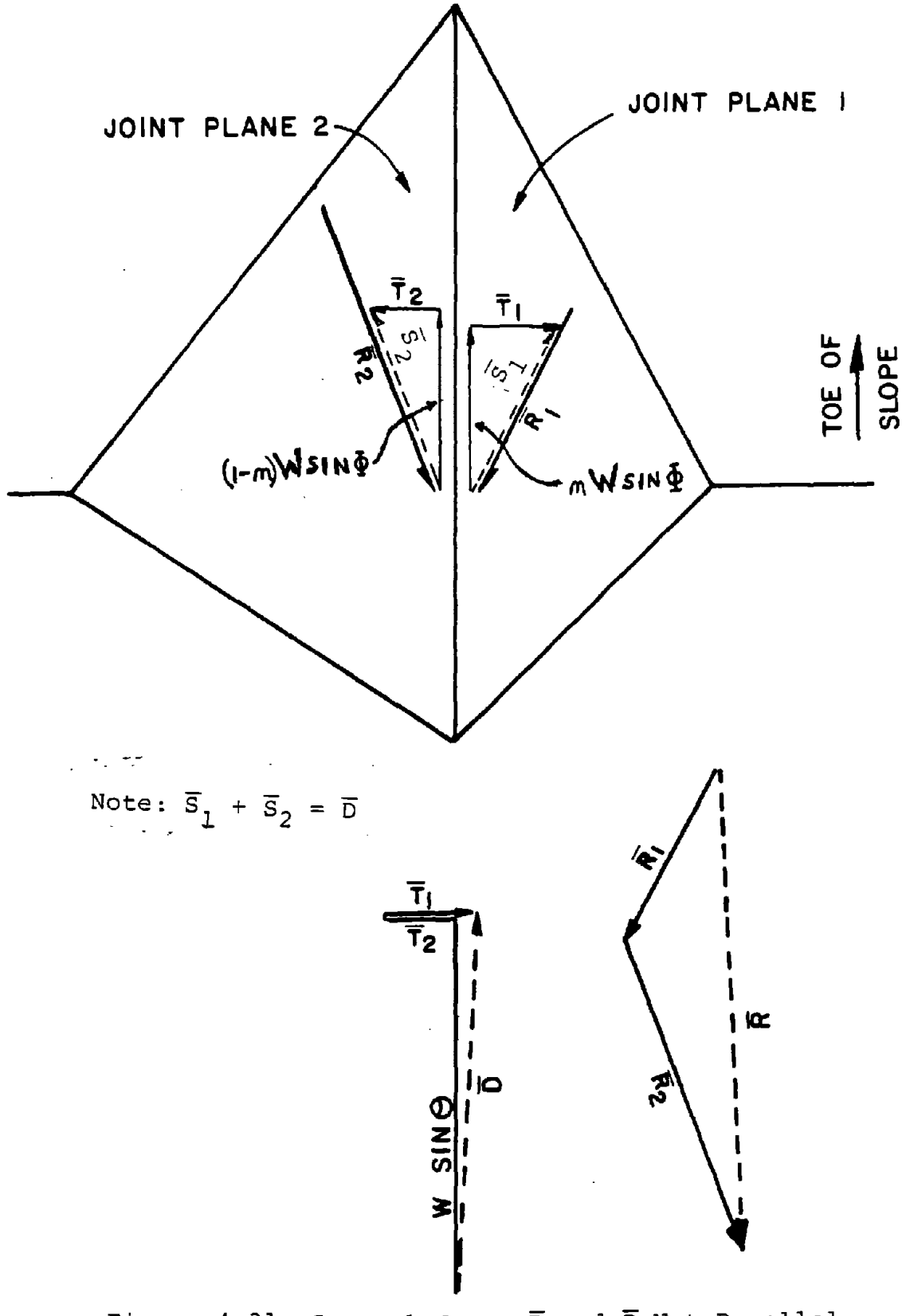

Figure 4.31 General Case--$\bar{D}$ and $\bar{R}$ Not Parallel

$$FS = \frac{\bar{R} \cdot \bar{\Delta}}{\bar{D} \cdot \bar{\Delta}} \tag{4.62}$$

$\bar{R}$ is the resultant vector of all resisting forces

$\bar{D}$ is the resultant vector of all driving forces

$\bar{\Delta}$ is the direction of impending motion

FS is considered the ratio of the components of $\bar{R}$ and $\bar{D}$ in the direction of $\bar{\Delta}$.

The definition of $\bar{\Delta}$ is somewhat ambiguous because the "direction of impending motion" is considered the direction of displacement due to an imposed load. Thus, $\bar{\Delta}$ will not correspond to failure conditions unless the load creates a condition where FS = 1.0. Different loads will produce different Δ's. The program offers the user two options:

1. $\bar{\Delta}$ is displacement that would occur under a purely vertical load, i.e., In what direction would the wedge move if its unit weight suddenly increased by a small percentage? $\bar{\Delta}$ is based on the current stiffness.

2. $\bar{\Delta}$ is the displacement that occurs under all the "current loads". Current loads include all loads except the weight of block; they are the loads that are analyzed using the stiffness approach.

In the special case where there is total symmetry Equation 4.57 will yield the same FS as Equation 4.56.

4.6 Computer Program SWARS-2PM

The stiffness and stress approaches discussed in Sections 4.2 to 4.5 and in Appendix G have been incorporated into a computer program, SWARS-2PM. SWARS-2PM is a modified version of SWARS-2P which was originally developed by Campbell (1974) using the conventional assumption

regarding the absence of T_1 and T_2 forces on the joint planes. SWARS-2PM retains all the versatility of its predecessor with respect to loading conditions and ground water options; in addition, it determines the reactions on the joint planes according to the method prescribed in Section 4.4. If the failure mode involves sliding on both planes*, the program computes the two factors of safety defined in Section 4.5: FS_I and FS_U. The stress approach is used to calculate the reactions on the joint planes due to the weight of the wedge. No further comments are necessary on this procedure which follows the analysis described in Section 4.2.

The generalized stiffness approach is used to calculate the reactions due to all other loads. In implementing the generalized stiffness approach, SWARS-2PM utilizes the relations developed in Appendix G with two modifications:

1. A_1, the area of joint plane 1, replaces the term h csc β_1 in Equation G.3.
2. A_2, the area of joint plane 2, replaces the term h csc β_2 in Equation G.6.

The program resolves the resultant of all "stiffness" loads into components along the A, B and C axes shown in Figure 4.32. The B and C components (Figure 4.33) correspond to the respective Y and X components in Equations G.10 and G.9. The A component that lies along the line of intersection is part of $\bar{D}$, the driving vector, that appears in the denominator of the FS equation:

$$FS = \frac{\bar{R} \cdot \bar{\Delta}}{\bar{D} \cdot \bar{\Delta}} \qquad (4.62)$$

$\bar{\Delta}$, the direction of impending motion, is composed of components along the A, B and C axes. Δ_B and Δ_C ARE related to δ_h and δ_v, the magnitude and direction of the displacement, in the generalized stiffness approach:

*If the failure mode involves sliding on a single plane, SWARS-2PM will perform exactly the same analysis as SWARS-2P.

$\bar{U}_i$: STRIKE

$\bar{V}_i$: DIP

$\bar{W}_i$: $\bar{U}_i \times \bar{V}_i$

$\bar{A}$: $\dfrac{\bar{W}_1 \times \bar{W}_2}{|\bar{W}_1 \times \bar{W}_2|}$

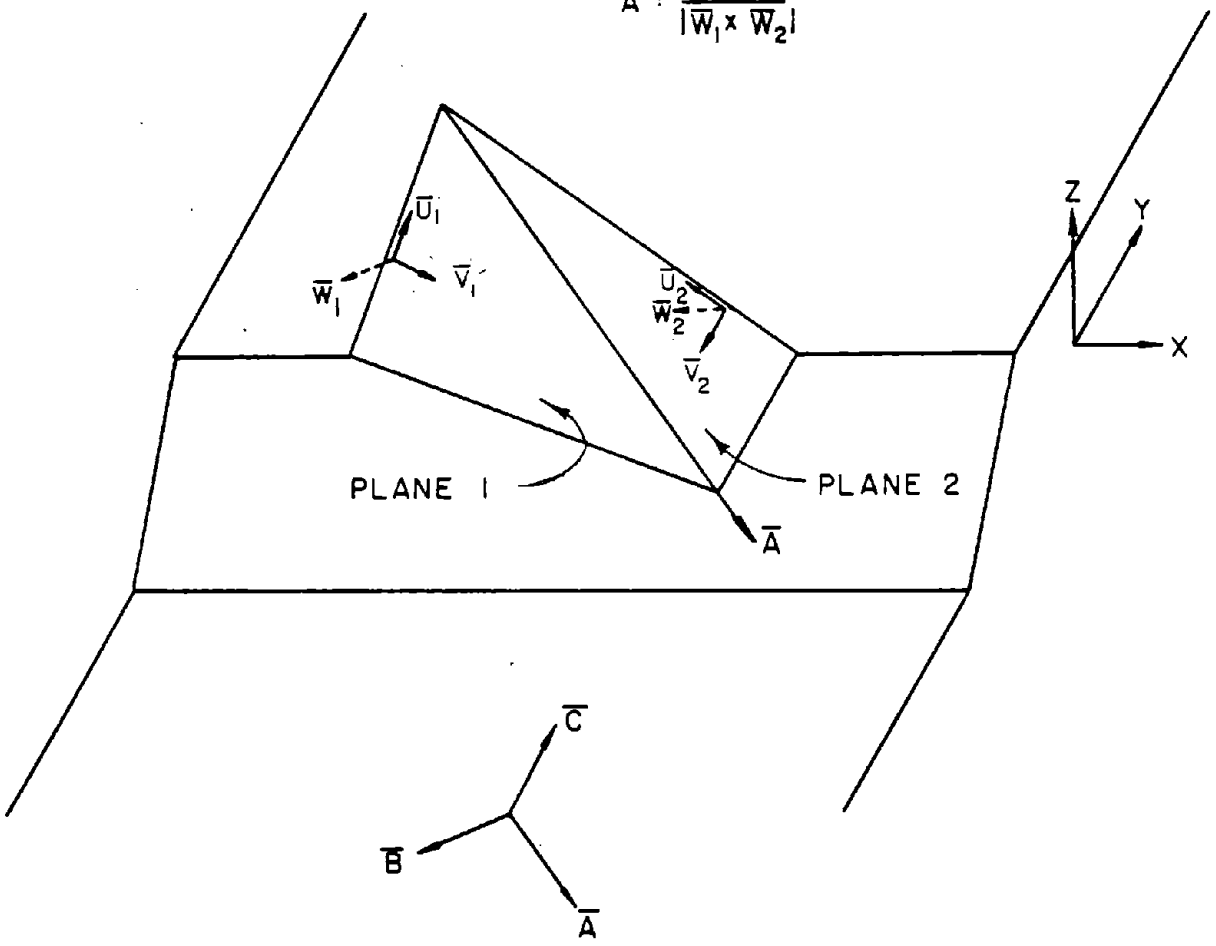

$\bar{A}, \bar{B}, \bar{C}$: UNIT VECTORS FORMING SETS OF ORTHAGONAL AXES

$\bar{A}$: LINE OF INTERSECTION

$\bar{B}$: $\bar{B} \perp \bar{A}$; $\bar{B} \perp$ Z AXIS

$\bar{B} = \dfrac{\bar{A} \times (0,0,1)}{|\bar{A} \times (0,0,1)|}$

$\bar{C} = \bar{B} \times \bar{A}$

Figure 4.32 A, B, C Coordinate System

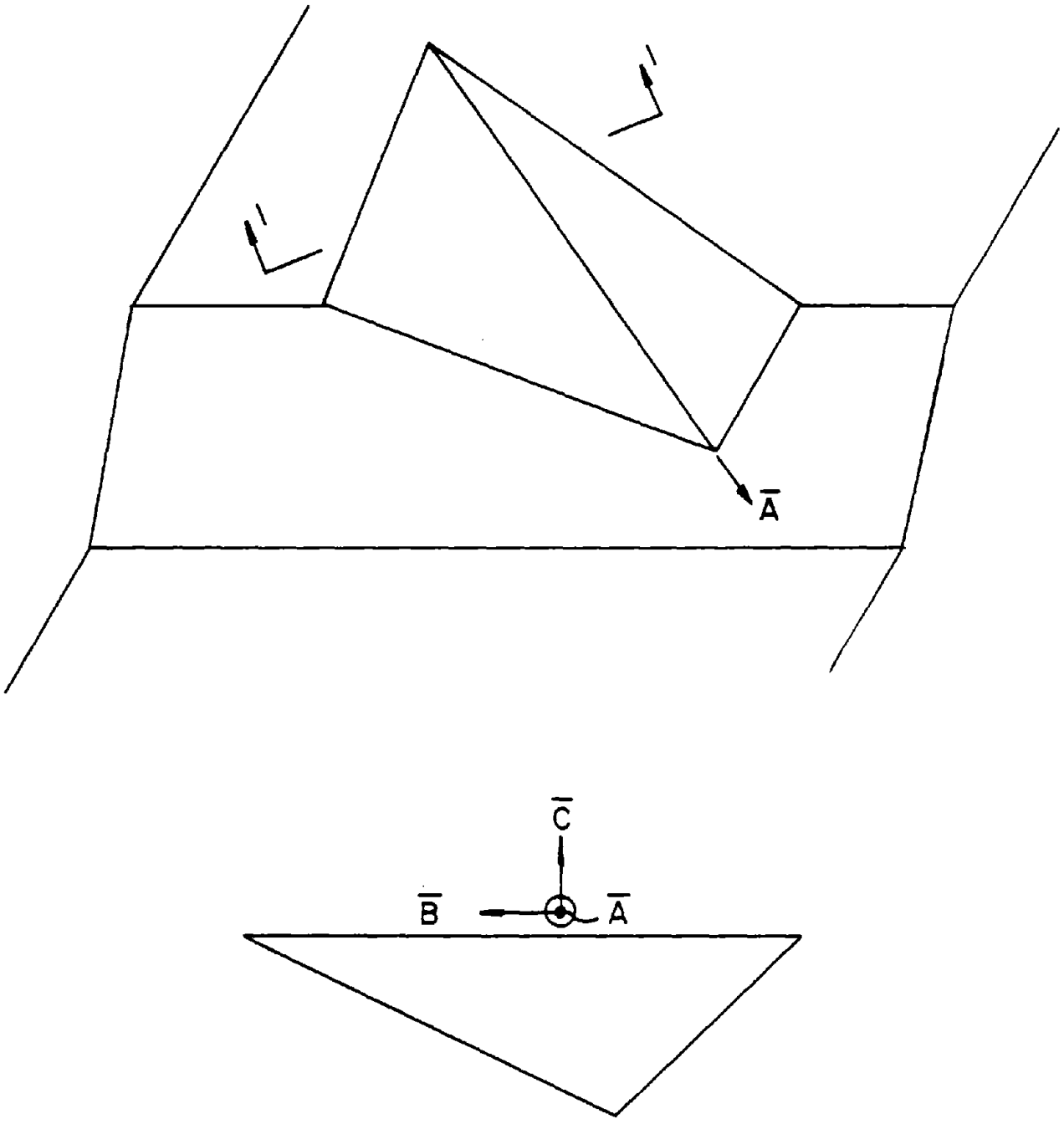

Figure 4.33 Cross Section Perpendicular to $\bar{A}$

$$\Delta_B = \delta_t \sin \alpha \tag{4.63}$$

$$\Delta_C = -\delta_t \cos \alpha \tag{4.64}$$

In computing Δ_A, the program assumes that the shear stiffness in the direction parallel to the line of intersection is identical to the shear stiffness in the direction perpendicular to the line of intersection.* Thus,

$$\Delta_A = \frac{F_A}{A_1 k_{1s} + A_2 k_{2s}} \tag{4.65}$$

where F_A is the load component in the A direction

If the user selects the option wherein Δ is considered the displacement that would occur in response to a purely vertical load, the program computes the Δ_A, Δ_B and Δ_C that would occur under an imaginary vertical load of unity. (The imaginary load is not considered in the $\bar{R}$ or $\bar{D}$ computations.)

Appendix UM5 contains a complete listing of SWARS-2PM as a users' manual. SWARS-2PM expands the powerful capabilities of SWARS-2P to include force assumptions that correspond better to reality.

4.7 Conclusions

Approximations of force application that are used in standard equilibrium analyses for rock wedges can lead to significant inaccuracies. Particularly the assumptions that the reactions on a joint plane are perpendicular to the plane can result in substantial underestimation or

*The program can easily be modified to accept two shear stiffness for each joint plane but such a refinement is probably unwarranted given the state of the art concerning the measurement of stiffness values.

overestimation of the factor of safety if the real situation deviates from the assumed one. However force assumptions have to be made, since stress distribution is by definition unknown in rigid body analysis and the force analysis is thus indeterminate. This chapter has shown that better force assumptions can be made by including the effects of joint stiffness and, of the in situ stress field. The usual normality assumption implies that the joint has no shear stiffness and that the stress field is uniform, i.e., K = 1. These restrictive situations can be made more realistic through consideration of actual stiffness and stress state ranges. This was introduced by other researchers but only for relatively simple geometries and for frictional resistance only. More importantly no relation between stress and stiffness effects had been established although they seem to have common causes.

The developments reported in this chapter greatly expand the stiffness and stress approaches to non-symetric and tetrahedron shaped wedges and realistic resistance representation. By applying the thereby generalized stability analyses to typical geometries, relations were determined between geometry and stiffness (or stress field) on one hand, and required friction angle (as an expression of safety) on the other hand. The stability of narrow wedges and of wedges with one steeply inclined joint plane is very sensitive to stiffness changes; a result of particular importance in view of the fact that stiffnesses can vary considerably. Stress field changes have the greatest effect on wedges with flat lines of intersection.

A direct consequence of the work on stiffness and stress approaches was the clarification of their relative significance. The stress approach correctly models the behavior of a wedge in the natural environment subject basically to its own weight. This is so because the history of a slope has led to a certain stress state which governs the current stability of wedges. Joint stiffnesses in contrast can only be used to determine stress changes due to additional loads, the stiffnesses cannot provide information on the present natural state of stress. The stiffness approach can therefore be used to make predictions on the effect of additional loads.

Based on this relation between stress and stiffness approaches and on the generalized formulations of the two approaches, it was possible to develop a method for stability analysis and a computer program, SWARS-2PM. This method for wedge stability analysis makes force assumptions that are much closer to reality and includes the powerful features of SWARS-2, particularly representation of joint resistance with a frictional and cohesional component, water-seismic- and external driving force effects, bolting and the possibility to investigate all wedges that can be formed from a number of joint sets and slope geometries. In addition to being a comprehensive analysis method by itself it can also be incorporated in the probabilistic wedge analysis as will be shown in Chapter 4, Part III.

CHAPTER 5

COMPLETE LIMIT EQUILIBRIUM ANALYSIS - THE METHOD OF "ARTIFICIAL SUPPORTS"

Summary and Practical Applications

The method of artificial supports (MAS) described in this Chapter reduces and eliminates problems associated with the rigid body assumption in limit equilibrium analysis. Although this goal is similar to those of Chapters 2 (SWARS) and 4 (Stress and stiffness approach) the approach here is more basic. Rather than addressing and eliminating specific problems, thorough rethinking and laying the groundwork for an encompassing improvement of limit equilibrium analysis is intended. The method of artificial supports addresses the by-definition-unknown stress and force distribution in surfaces supporting rigid bodies. A satisfactory representation of the actual reactions is achieved through introduction of artificial supports and reactions in these supports.

The concept and analytical formulation of the method are developed in this chapter as are the concept, analytical components and an algorithm for a complete wedge analysis based on MAS. Where necessary, computer programs for the analytical components have also been developed. Specifically these analytical components are the analysis of (in plane) rotational sliding failure, either in free rotation or around a fixed point, translational sliding failure and toppling (covering thus all modes of failure and indicating the encompassing nature of the approach). These analyses methods can be used individually and to some extent have been incorporated, in the previously described wedge analysis methods (Chapters 2 and 4). In addition, the component analysis can be employed in conjunction with each other if a complete wedge analysis needs to be performed. This can be done by following the detailed algorithm described in this chapter and using the component analyses where indicated. No "all encompassing" computer program has as yet been developed. The algorithm permits a slope designer to quickly examine which component analyses are needed. (The gain of doing this by computer would be small. However, once better knowledge of failure mechanisms becomes available, and together with additional user oriented input-output routines such a program may be desirable.) Equally important as the practical user oriented analysis methods and programs are the entire concept and methodology. It seems that a new and promising way has been opened to a more satisfactory consideration of rigid body reactions and thus a more satisfactory limit equilibrium analysis.

Specifically, this chapter starts with a brief review of common wedge stability approaches and then introduces the method of artificial supports. The three-support model, the simplest version of the MAS, and the corresponding computer program PF3 is developed and used to analyze the sliding modes of failure. It is at this point that

rotational and translational failure can be compared, translational failure being a special case of rotational failure. A number of cases with different force applications and support geometries are investigated. Rotational failure is usually the critical mode, if driving forces other than the weight become significant - a fact that so far has not been generally recognized. The difference between the two critical coefficients of friction (rotation and translation) increases with the distance of the applied force vector from the center of gravity and as the center of rotation moves closer to the supports.

To examine the correctness of the three-support model an n-support model and associated analysis was developed. Specifically a 10-support model is applied to the previously considered 3-support cases, i.e., to cases with the same applied forces. It can be concluded that the 3-support model provides results of satisfactory accuracy if a sufficient number (between 5 and 10) of 3-support geometries are used to determine the critical coefficient of friction and the mean taken.

The MAS and its applications are then extended to include the remaining modes of failure which are sliding rotation about a fixed axis, toppling and translational sliding along a line of intersection. For the fixed point rotation an analysis method and computer program (ROTFA) were developed, while the toppling and intersection sliding analyses are extensions of previously known methods to include the MAS concept. This is followed by the description and example application of the algorithm for the complete wedge failure analysis.

5.1 Introduction -

Wedge stability analysis, the convenient and most frequently used method for rock slope design, has been discussed extensively in Chapters 2-4. The methods described there attempt to improve the practical usefulness of wedge analyses and also to reduce the limitations associated with limit equilibrium analysis. As mentioned there, these limitations are due to the rigid body assumption which does not permit the determination of stress distributions, thus makes the problem indeterminate and requires assumptions regarding force and moment applications. The restrictive assumptions, usually excluding moments and requiring normability of reactions on the joint plane, have to some extent been eliminated in SWARS (Chapter 2) and SWARS-2PM (Chapter 3) while maintaining the practical efficiency needed by the designer. Since some limitations particularly with regard to possible failure modes remain, a basic investigation on limit equilibrium approaches for block and wedge-stability was undertaken. This led to the method of artificial supports (MAS) disucssed in this chapter. As will be seen this method as presented here attempts to fulfill two purposes:

-1 Provide a practical means to examine conditions that are not treated by SWARS and SWARS-2PM, not only the method and computer program will be provided but also criteria based on which the user can decide if he needs to go beyond SWARS and SWARS-2PM or not.

-2 Provide the analytical structure for a complete limit equilibrium analysis, an analysis that will not restrict force and moment assumptions and consider all failure modes. Only the analysis and the algorithm will be provided at the present time, incorporation in a computerized program with designer oriented features will be done later, once designer requirements and interaction with stochastically based methods are more clearly established.

To set the stage for the method of artificial supports the present procedure for wedge stability analysis shall be recalled. Calculating the factor of safety (FS) for rock wedges (like the ones in Fig. 5.1) usually comprises the following steps:

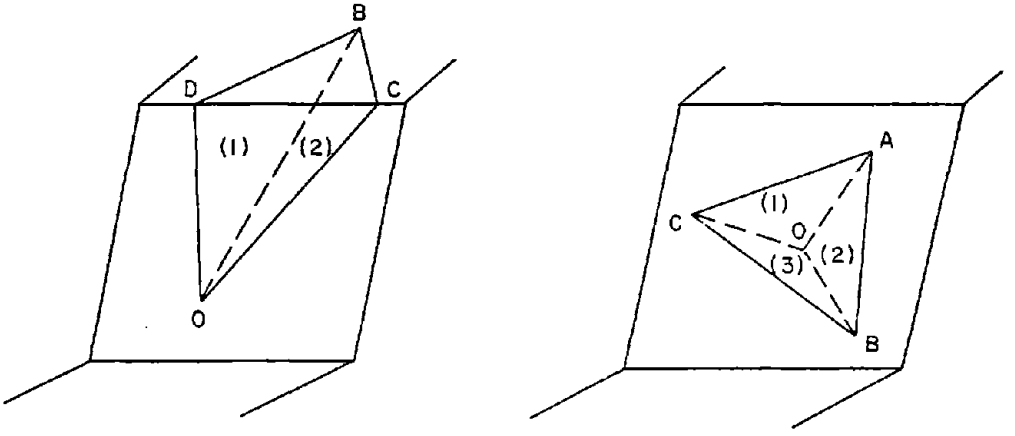

(a) 2-P wedge

(b) 3-P wedge

Figure 5.1: General wedge formations

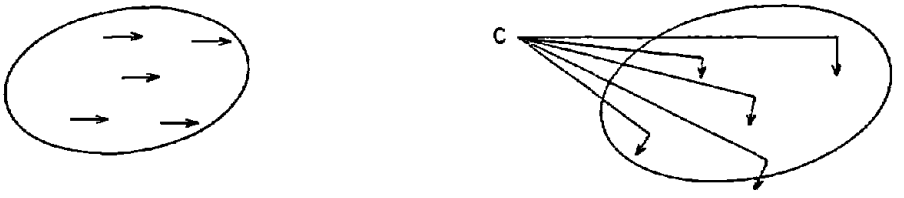

(a) Linear translation: all points on the body moving with the same velocity.

(b) Rotation about point C: every point on the body moving in a circular arc with C as center.

Figure 5.2: Translation and rotation

1. Determination of geometry, (including geometric feasibility i.e., whether a failure wedge can be formed).
2. Determination of forces due to weight, water pressure, surcharge, point loads, seismic effects, stabilizing forces (like bolts).
3. Determination of the mode of failure from the resultant force and geometry.
4. Determination of available resistance due to frictional and cohesive force components.
5. Determination of $FS = \frac{\text{(total available resistance)}}{\text{(driving force)}}$.

The usual procedure only considers translational sliding failure (but not or only to a limited extent failure) by rotational sliding and toppling:

a) Rotational sliding on one plane:
In this case the wedge slides on a joint plane with a non-linear motion. The initial motion is a rotation about an axis perpendicular to the supporting plane. Figure 5.2 illustrates the difference between a linear translaton and a rotational sliding on a plane.

b) Toppling about an edge:
This is again a rotational mode of failure but is caused by "out of joint plane" moments. As shown in Figure 5.3, if force F increases from 0, a point will be reached when the cube will fail by toppling about the edge. Although the frictional resistance may be large enough to prevent sliding, the moment of the applied force F may cause toppling instability.

As indicated before all commonly used sliding wedge analyses either limit themselves to translational failure (often simplified) and neglect or simplify rotational failure analysis. Consequences of simplified translational failure analysis have been described in Chapter 4. A specific example as to how such simplified rotational analysis may cause problems, is discussed in Appendix H. The cause

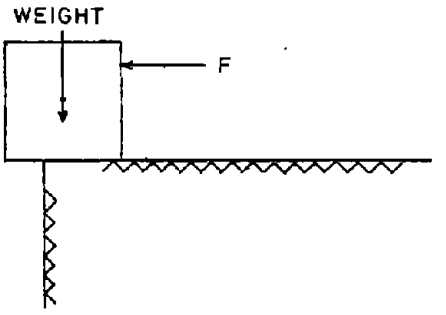

Figure 5.3: Cube toppling about the edge of a table

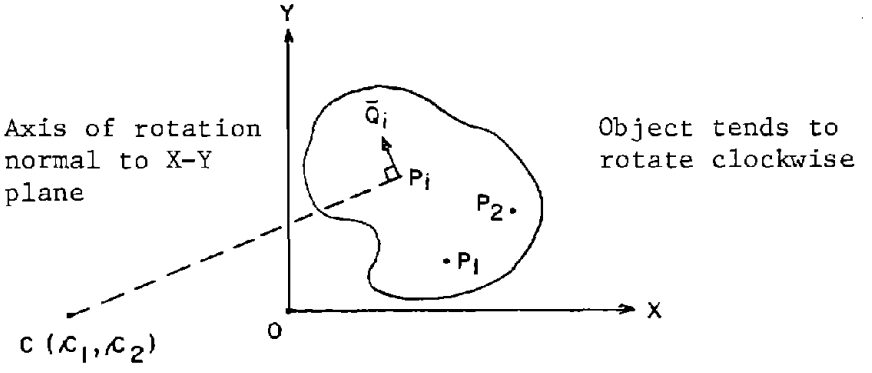

Figure 5.4: Reaction at point of contact

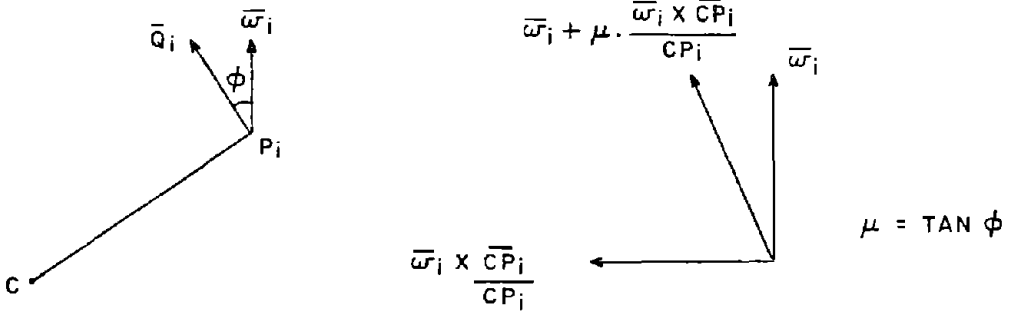

Figure 5.5: Vector representation of reaction

for these and other problems is the fact that overall moment equilibrium (in 3-dimensional space) and the distribution of reactions are often ignored or over-simplified. This can be corrected with the method of Artificial Supports (MAS).

5.2 Method of Artificial Supports

5.2.1 Introduction and Assumptions

When an object slides on a plane the initial motion is very often not a pure translation. In fact the initial motion is always a rotation about an axis perpendicular to the plane. If the axis is far away from the object, however, translation and rotation are practically identical. In order to analyze rotational failure the moments of the applied forces on the object have to be considered. A system of forces $\bar{F}_i$ acting on an object through points with position vector $\overline{OT}_i$ can be represented completely by: -1) a resultant force $\bar{R}$ which acts through O and -2) a resultant moment $\bar{M}_o$ of the moments of forces $\bar{F}_i$ about O:

$$\bar{R} = \Sigma\bar{F}_i$$

$$\bar{M}_o = \Sigma\overline{OT}_i \times \bar{F}_i$$

The method of artificial supports can be used to find a critical coefficient of friction μ at which sliding occurs. It makes the following basic assumptions:

(1) The plane is flat.

(2) The reaction between the object and the plane can be represented by a number of points of contact, the so-called "artificial supports", $P_i, i = 1,n$. The position vector of P_i is $\overline{OP}_i$ and the reaction through P_i is $\bar{Q}_i$ (Fig. 5.4).

(3) When limiting equilibrium is reached, each reaction $\bar{Q}_i$ acts at an angle equal to the friction angle ϕ with the normal on the plane.

The direction of $\bar{Q}_i$ (see Figure 5.4) is perpendicular to $\overline{CP}_i$ where C is the center of rotation which has to be a point common to both the plane and the axis of rotation about which the object begins to rotate.

5.2.2 Vector Representation

By assumption (3), $\bar{Q}_i$ is parallel to the vector (see Figure 5.5)

$$(\bar{w}_1 + \mu\, \bar{w}_1 \times \overline{CP}_i/CP_i)$$

where w_1 = normal vector,

μ = $\tan \phi$,

CP_i = magnitude of $\overline{CP}_i$

Therefore $\bar{Q}_i = A_i\ (\bar{w}_1 + \mu\, \bar{w}_1 \times \overline{CP}_i/CP_i)$ where A_i = proportionality constant. Note that $(A_i/\cos\phi) = Q_i$ and so A_i is also the normal reaction.

In limiting equilibrium,

forces: $\sum^{n} \bar{Q}_i + \bar{R} = 0$, $\bar{R}$ = resultant applied force

moments: $\sum^{n} \overline{OP}_i \times \bar{Q}_i + \bar{M}_o = 0$, $\bar{M}_o$ = resultant applied moment vector.

i.e.,
$$\sum^{n} A_i(\bar{w}_1 + \mu\, \bar{w}_1 \times \overline{CP}_i/CP_i) + \bar{R} = 0 \qquad (5.1)$$

$$\sum^{n} A_i\, \overline{OP}_i \times (\bar{w}_1 + \mu\, \bar{w}_1 \times \overline{CP}_i/CP_i) + \bar{M}_o = 0$$

Without loss of generality, let

$$\bar{w}_1 = (0,0,1)$$

$$\overline{OP}_i = (p_{i1}, p_{i2}, 0)$$

$$\overline{OC} = (c_1, c_2, 0)$$

$$\overline{CP}_i = (c_{i1}, c_{i2}, 0) = \overline{OP}_i - \overline{OC}$$

then $\bar{w}_1 \times \overline{CP}_i/CP_i = (-c_{i2}, c_{i1}, 0)/CP_i$,

$\bar{w}_1 + \mu\, \bar{w}_1 \times \overline{CP}_i/CP_i = (-\mu\, c_{i2}/CP_i, \mu\, c_{i1}/CP_i, 1)$ and

$\overline{OP}_i \times (\bar{w}_1 + \mu\, \bar{w}_1 \times \overline{CP}_i/CP_i) = (p_{i2}, -p_{i1}, \mu\, (p_{i1}\, c_{i1} + p_{i2}\, c_{i2})/CP_i)$

Equations 5.1 can then be expanded into algebraic forms:

$$
\begin{aligned}
-\mu\sum_{i}^{n} A_i c_{i2}/CP_i + r_1 &= 0 && (5.2a)\\
\mu\sum_{i}^{n} A_i c_{i1}/CP_i + r_2 &= 0 && (5.2b)\\
\sum_{i}^{n} A_i + r_3 &= 0 && (5.2c)\\
\sum_{i}^{n} A_i p_{i2} + m_1 &= 0 && (5.2d)\\
-\sum_{i}^{n} A_i p_{i1} + m_2 &= 0 && (5.2e)\\
\sum_{i}^{n} A_i \mu(p_{i1}c_{i1}+p_{i2}c_{i2})/CP_i + m_3 &= 0 && (5.2f)
\end{aligned}
\qquad (5.2)
$$

where $\bar{R} = (r_1, r_2, r_3)$, $\bar{M}_o = (m_1, m_2, m_3)$

Note that the third force equation and the first and second moment equations are linear in A_i:

$$
\begin{aligned}
A_1 + A_2 + A_3 + \ldots + A_n &= -r_3 && (5.2c)\\
A_1p_{12} + A_2p_{22} + \ldots + A_np_{n2} &= -m_1 && (5.2d)\\
A_1p_{11} + A_2p_{21} + \ldots + A_np_{n1} &= m_2 && (5.2e)
\end{aligned}
\qquad (5.3)
$$

5.2.3 Physical Interpretation of Equations (5.2)

It should be noted that A_i is the normal reaction at p_i and is assumed positive. Equations 5.2 can then be explained in physical terms. From Figure 5.6,

$$c_{i2}/CP_i = \sin\theta_i$$

$$c_{i1}/CP_i = \cos\theta_i$$

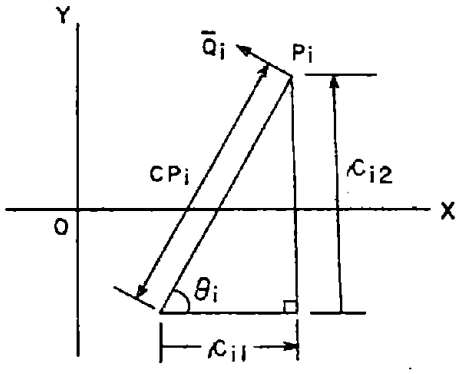

Figure 5.6: Rotational failure

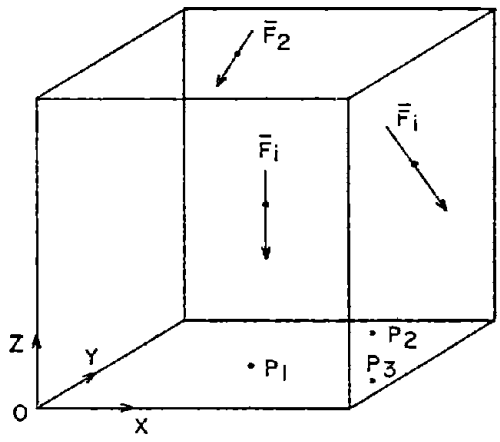

Figure 5.7: The 3-supports model

Equations 5.2a can be re-written as,

$$-\sum^{n}(\mu A_i)\ \sin\theta_i + r_1 = 0$$

(μA_i) (= normal reaction times friction coefficient) is just the frictional force in the XY-plane and multiplication by $\sin\theta_i$ yields the component in the X-direction.

Similarly for equation 5.2b:

$$\sum^{n}(\mu A_i)\cos\theta_i + r_2 = 0$$

where $(\mu A_i \cos\theta_i)$ is the frictional force in the Y-direction. Equation 5.2c is the equation of normal reactions on the XY-plane and of normal components of the forces applied to the XY-plane.

In equation 5.2d and 5.2e moments about the X and Y - axes respectively are considered. Equation 5.2f is the moment equilibrium about the Z-axis.

5.2.4 Proof that Rotational Failure is Always More Critical Than Translational Failure

The critical coefficient of friction with respect to translation is,

$$\mu_t = \frac{\text{tangential component of resultant applied force}}{\text{normal component of resultant applied force}}$$

$$= \frac{\sqrt{r_1^2 + r_2^2}}{(-r_3)}$$

Substituting the expressions for r_1, r_2 and r_3 given by equations 5.2a, 5.2b and 5.2c, one obtains:

$$\mu_t = \frac{\mu_r \sqrt{(\Sigma A_i c_{i2}/CP_i)^2 + (\Sigma A_i c_{i1}/CP_i)^2}}{\Sigma A_i}$$

where μ_r = critical coefficient of friction with respect to rotation. Using the notation of Section 5.2.3 and re-arranging:

$$\frac{\mu_t}{\mu_r} = \frac{\sqrt{(\Sigma A_i \cos\theta_i)^2 + (\Sigma A_i \sin\theta_i)^2}}{\Sigma A_i}$$

It will be proven mathematically in the following section (5.2.5) that $((\Sigma A_i \cos\theta_i)^2 + (\Sigma A_i \sin\theta_i)^2)$ is always less than $(\Sigma A_i)^2$ for $n > 1$ and if not all θ_i's are equal. In the actual case these conditions are fulfilled since n (the number of points of support) must be greater than 1 and the points of support do not lie on the same straight line (indicating that no all θ_i's are equal). Therefore $\mu_r > \mu_t$ and the rotational failure mode is more critical. The assumption of translational failure usually overestimates safety.

However, when the axis of rotation is far away from the object, such as in the case when there is only 1 force (the weight) acting on the object,

$$\theta_i \approx \theta_j \ (\approx\theta) \text{ and}$$

$$(\Sigma A_i \cos\theta_i)^2 + (\Sigma A_i \sin\theta_i)^2$$

$$\approx \cos^2\theta (\Sigma A_i)^2 + \sin^2\theta (\Sigma A_i)^2$$

$$\approx (\Sigma A_i)^2$$

which implies $\mu_t \approx \mu_r$.

5.2.5 Mathematical Proof That $\mu_t < \mu_r$

The objective is to prove that

$$\left(\sum_{i=1}^{n} A_i\cos\theta_i\right)^2 + \left(\sum_{i=1}^{n} A_i\sin\theta_i\right)^2 < \left(\sum_{i=1}^{n} A_i\right)^2$$

$$\text{Left Hand Side} = \sum_{i=1}^{n} (A_i\cos\theta_i)^2 + 2 \sum_{\substack{i=1,n-1 \\ j=2,n \\ i<j}} A_iA_j\cos\theta_i\cos\theta_j$$

$$+ \sum_{i=1}^{n} (A_k\sin\theta_i)^2 + 2 \sum_{\substack{i=1,n-1 \\ j=2,n \\ i<j}} A_i A_j\sin\theta_i\sin\theta_j$$

$$= \sum_{i=1}^{n} A_i^2 + 2 \sum_{\substack{i=1,n-1 \\ j=2,n \\ i<j}} A_iA_j\cos(\theta_i-\theta_j)$$

Since $\cos(\theta_i-\theta_j) < 1$ when $\theta_i \neq \theta_j$,

$$\text{Left Hand Side} < \sum_{i=1}^{n} A_i^2 + 2 \sum_{\substack{i=1,n-1 \\ j=2,n \\ i<j}} A_iA_j$$

$$< \left(\sum_{i=1}^{n} A_i\right)^2$$

Since the rotational failure mode is thus more critical than the translational failure mode, sliding on a plane is usually in form of rotation and not translation. It will now be shown how suitable sliding models with artificial supports can be developed and how they can be used together with equations 5.2 to determine μ_r.

5.3 Sliding Models

5.3.1 The Three-supports Model

By inspecting equations 5.2, one can see that for given applied forces and moments, there are a total of (n+3) unknowns. These unknowns include the critical coefficient of friction for rotation, the X and Y - coordinates of the center of rotation, and the n normal reactions. By considering three supporting points only, the number of unknowns will equal the number of equations (6) and the problem becomes statically determinate when limiting equilibrium is assumed.

The method is described using a cube model of size 12x12x12 with three supports (figure 5.7).

5.3.2 The Method of Solution

A_1, A_2 and A_3 are first found by equations 5.3. They have to be all non-negative. If at least one of them is negative, the supporting base formed by the three chosen supports cannot keep the cube in equilibrium since it is assumed that no tension can occur between the supporting plane and the cube. In other words the three supports must form a stable base for the cube before limiting (sliding) equilibrium is reached.

The remaining three equations in 5.2 are:

$$-\mu\sum_{i}^{3} A_i c_{i2}/CP_i + r_1 = 0 \qquad (5.2a)$$

$$\mu\sum_{i}^{3} A_i c_{i1}/CP_i + r_2 = 0 \qquad (5.2b)$$

$$\mu\sum_{i}^{3} A_i (p_{i1}c_{i1} + p_{i2}c_{i2})/CP_i + m_3 = 0 \qquad (5.2f)$$

From equations 5.2a and 5.2b and rearranging,

$$r_2\sum_{i}^{3} A_i c_{i2}/CP_i + r_1\sum_{i}^{3} A_i c_{i1}/CP_i = 0$$

and also

$$m_3\sum_{i}^{3} A_i c_{i2}/CP_i + r_1\sum_{i}^{3} A_i (p_{i1}c_{i1}+p_{i2}c_{i2})/CP_i = 0, \qquad (5.4)$$

which is derived from equations 5.2a and 5.2f.

By noting that

$$c_{i1} = p_{i1} - c_1,$$

$$c_{i2} = p_{i2} - c_2,$$

$$CP_i = (c_{i1}^2 + c_{i2}^2)^{1/2}$$

c_1 and c_2, the coordinates of the center of rotation, can be found from equations 5.4. By substituting the known values of c_1 and c_2 into equations 5.2a, 5.2b or 5.2f, μ can be found.

Since the computations are complicated and solving equations 5.4 requires numerical methods, the computer program PF3 (Plane failure - 3 supports) was developed and is used to calculate the location (c_1, c_2) of the center of rotation and the critical coefficient of friction μ. (For details and documentation of PF 3 see Appendix UM8.)

5.3.3 Case Studies

The "three-supports" model has been applied to many different cases to illustrate the practicality of the method and to show that rotation is indeed the critical mode in most instances. In this section three typical cases are discussed to show the main features of the "three-supports" model. This will be followed by Section 5.3.4 where a series of systematic case studies will be performed to investigate the effect of different variables.

Case I: Single Force

A single inclined force $\bar{F}_1$ (10,10,-20)* acts through the center (6,6,6)* of the cube. The three supports P_i are at (7,8,0), (11,7, 0) and (10,10,0) (see Figure 5.8).

The summarized results are:

Force: $\bar{F}_1$ = (10,10,-20) at (6,6,6)

The reactions Q_i at the 3 supports are thus found to be 8.91, 2.23, 13.4 respectively; the critical friction angle for rotation ϕ_r

*Consistent units should be used.

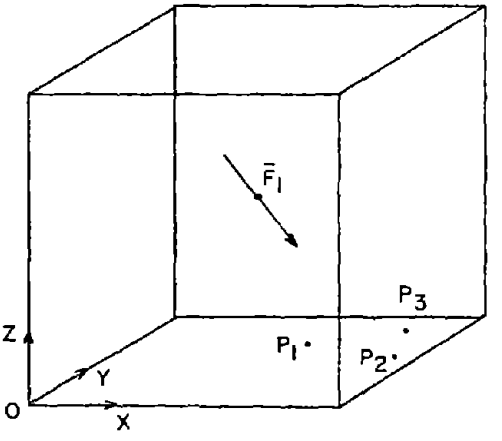

Figure 5.8: Case I = Single force

Solution set of Eq.5.3 Solution set of Eq. 5.2

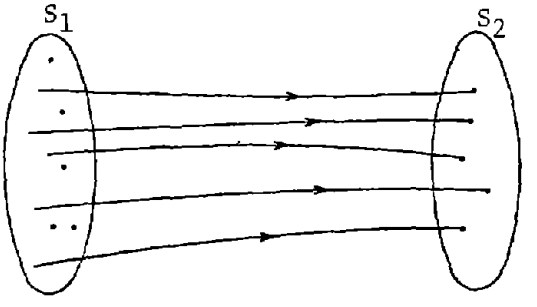

Both sets S_1 and S_2 contain an infinite number of elements

Figure 5.10: Solution sets

Figure 5.12: A 10-supports case study

is 35.26° and that for translation is 35.26°. The center of rotation is at (32400,-32300,0). As expected for a single applied force, the center of rotation is very far away from the cube and rotation equals translation. This is representative of cases where gravity and one or more additional forces act through the center of gravity, for instance the often assumed concurrence of weight and bolt forces in sliding wedge analysis (the application of bolt forces through the center of gravity is a simplifying assumption, however, (see Chapter 2)).

Case II: Weight and One Applied Force (Not Acting Through the Center of Gravity)

$\bar{F}_1$ = (0,0,-10) at (6,6,6) (weight)

$\bar{F}_2$ = (5,0,-4) at (8,11,0)

	Support 1	Support 2	Support 3
P_i	(3,7)	(12,1)	(10,10)
Q_i	8.04	1.72	5.65

$\phi_r = 24.68°$; $\phi_t = 19.65°$

Center of rotation = (6.19, 1.48)

There is a considerable difference between ϕ_r and ϕ_t.

Case III: Weight and a Force Couple

$\bar{F}_1$ = (0,0,-10) at (6,6,6) (weight)

$\bar{F}_2$ = (4,0,0) at (0,11,3)

$\bar{F}_3$ = (-4,0,0) at (0,1,3)

	Support 1	Support 2	Support 3
P_i	(3.5,8)	(8,3.5)	(10,8)
Q_i	7.53	6.99	1.21

$\phi_r = 50.52^o$; $\phi_t = 0.0^o$

Center of rotation = (5.44, 6.38)

In this case $\bar{F}_2$ and $\bar{F}_3$ form a couple and $\bar{F}_1$ can be considered to be the weight. The assumption of translational failure is completely incompatible with the real situation.

5.3.4 Systematic Case Studies

In order to study more closely how ϕ_r varies with different sets of applied forces and locations of the three supports, a series of systematic case studies were conducted. For each set of applied forces, eight different (support) point sets of reactions are used (see Figure 5.9).

The results of the case studies are summarized in the form (φ_r, Q_1, Q_2, Q_3, c_1, c_2) in tables 5.1 through 5.9 where:

ϕ_r = critical friction angle for rotation

Q_1, Q_2, Q_3 = magnitude of reactions at P_1, P_2, P_3 respectively

c_1, c_2 = X and Y-coordinates of the center of rotation.

When a tensile reaction ($A_i < 0$) occurs at P_i, the supporting base formed by P_1, P_2 and P_3 is not stable and ϕ_r, c_1 and c_2 cannot be calculated. To denote this fact the symbol "U_i" is used in summaries in Tables 5.1 - 5.9; when both A_i and A_j are negative, "U_{ij}" is used. Once this occurs in a calculation the locations of the 3 supports are modified until all "A_i's" are positive. These new support locations are listed in the tables together with the associated results.

(When the numerical accuracy test described in Appendix UM8 fails, a warning message is given together with the three errors in Equations 5.2a, 5.2b and 5.2f.)

Comments on the Results of the Systematic Case Studies

Let $d = \mu_r - \mu_t$

From the examples above and additional ones not recorded here, the following conclusions can be drawn.

1. If the set of applied forces consists of a single force (e.g. weight) or if the forces are nearly parallel to each other, d is small and practically negligible (i.e., that the error in a

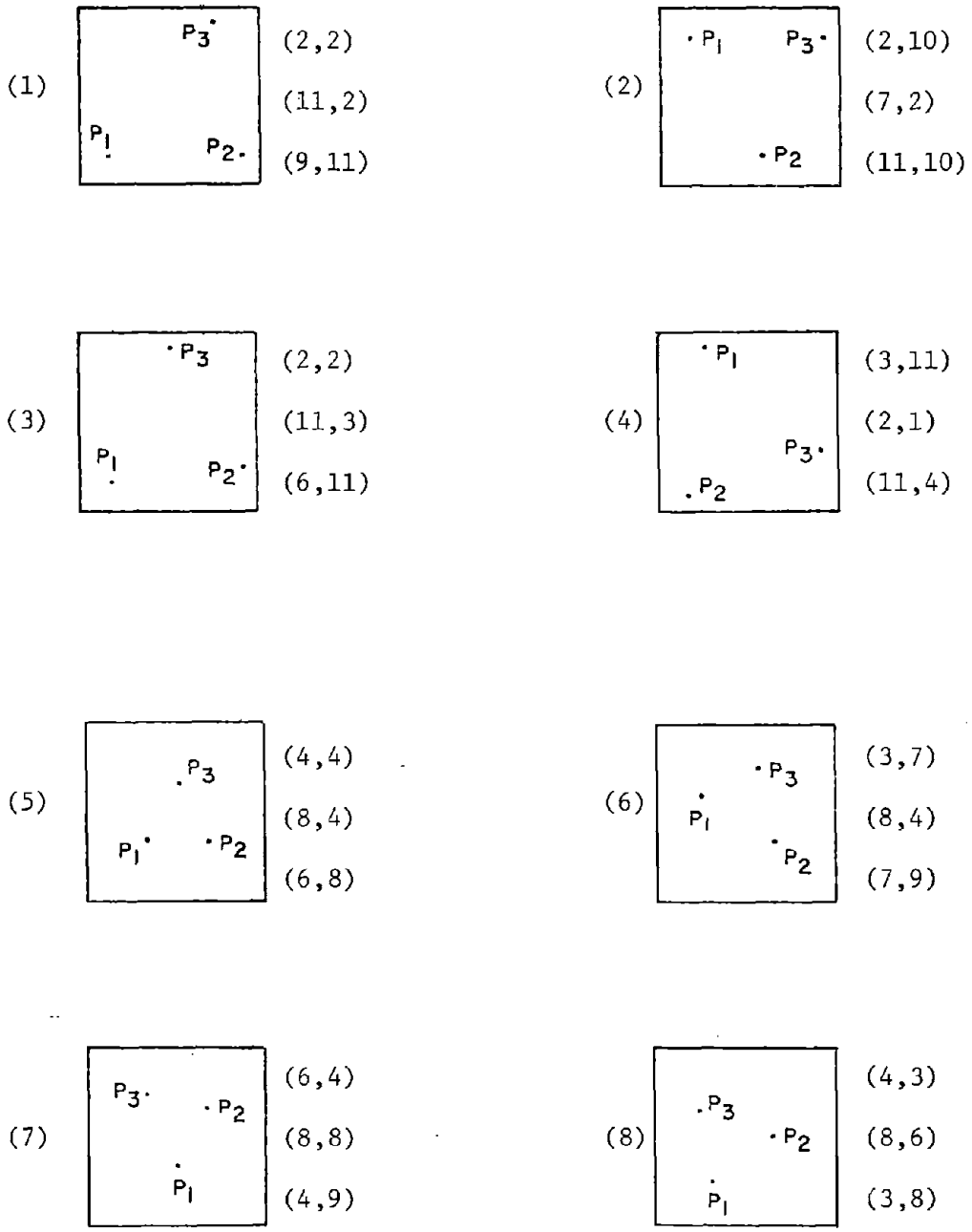

Figure 5.9: Configuration of the 8 point sets

Table 5.1

Results of systematic case studies - Case 1

(1) Forces: (5.77,-1,-10) at (6,6,6)
(.1,-.5,-3) at (6,9,6)

ϕ_t = 28.08° μ_t = .5334

Point Sets	Results	μ_r
1	(-28.18,1.62,6.58,6.55,14.90, 32.50)	-.5357
2	U1 (A_1 is negative)	
(1.5,10),(7.5,2), (11.5,10)	(-28.24,.55,7.38,6.82,13.30, 23.40)	-.5371
(The above point set is derived by modifying point set 2)		
3	(-28.14,.00,9.21,5.53,18.5,49.6)	-.5349
4	U2	
(3.5,11.5),(2.5,1.5), (11.5,4.5)	(-28.12,3.49,.78,10.50,24.90, 77.50)	-.5343
5	U1	
6	U1	
(7,6),(11,6),(9,10)	(-28.26,6.92,7.84,0.00,12.50, 21.10)	-.5376
(5,6),(10,3),(9,8)	(-28.51,.93,5.55,8.32,10.1,11.6)	-.5431
7	U3	
(9,3),(11,7),(7,8)	(-28.29,4.83,5.43,4.51,12.10, 19,80)	-.5382
8	U13	
(7,3),(11,6),(6,8)	(-28.20,2.41,8.74,3.61,14.00,28.20)	-.5363

The negative sign of μ_r indicates the rotation is anticlockwise.

Table 5.2

Results of systematic case studies - Case 2A

Forces: (0,0,-10) at (6,6,6)

(3,-1,0) at (6,9,6)

$\phi_t = 17.55°$ $\mu_t = .3163$

Point Set	Results	μ_r
1	(20.66,2.9,3.75,4.04,4.64,-2.48)	.3771
2	Eqs. 5.4 unsolved	
3	(20.72,1.89,5.36,3.44,5.53,-2.01)	.3783
4	(20.45,2.72,1.37,6.58,5.43,-2.36)	.3729
5	U1	
6	U1	
7	U3	
8	U3	

When point set 2 was used, equations 5.4 could not be solved. One can, however, notice a substantial difference between μ_r and μ_t, probably because the second applied force acts at a considerable distance from the center of the cube.

Table 5.3

Results of systematic case studies - Case 2B

Forces (0,0,-8) at (6,6,6)
(3,-1,0) at (6,9,6)

ϕ_t = 21.57°, μ_t = .3953

Point Set	Results	μ_r
1	(25.29,1.99,3.66,3.20,5.60,-2.56)	.4725
2	Eqs. 5.4 unsolved	
3	(25.55,1.24,4.98,2.65,6.69,-1.45)	.4780
4	(25.26,1.98,.94,5.92,6.50,-1.67)	.4718
5	U1	

Table 5.4

Results of systematic case studies - Case 2C

Forces: (0.0,-10) at (6,6,6)

(3,-1,0) at (6,12,6)

$\phi_t = 17.55°$, $\mu_t = .3163$

Point Set	Results	μ_r
1	(25.93,3.02,3.9,4.2,5.55,-.023)	.4862
2		
3	(26.7,1.98,5.61,3.61,7.83,1.14)	.5030
4	(26.53,2.85,1.44,6.89,8.72,2.01)	.4994
5	U1	
(6,3),(10,3),(8,7)	(40.19,3.27,1.96,7.85,7.18,4.08)	.8448
6	U1	
(4,7),(9,4),(8.9)	(17.55,2.19,6.67,1.62,-1.75 E9*,-5.24E9) ***Warning: .000,-.000,-168.91	.3163
7	U3	
(8,2),(10,6),(6,7)	(37.32,3.21,4.05,5.31,7.59,3.18)	.7624
8	U3	
(5,3),(9,6),(4,8)	(17.55,2.46,7.48,.55,-1.74E9,-5.21E9) ***Warning: .000,-.000,-169.03	.3163
(5,3),(10,6),(5,8)	(35.21,3.62,6.85,1.76,5.84,3.10)	.7057

In two of the cases above, the accuracy test on μ_r, c_1 and c_2 is not satisfied. The thru values following the warning message are the errors in equations 5.2a, 5.2b and 5.2f respectively. For this set of applied forces, μr seems to be very senstitive to the support locations.

* -1.75E9 = -1.75×10^9

Table 5.5

Results of systematic case studies - Case 2D

Forces: (0,0,-7) at (6,6,6)
(3,-1,0) at (6,12,6)
$\phi_t = 24.31°$, $\mu_t = .4518$

Point Set	Results	μ_r
1	(36.13,1.67,3.97,3.03,9.48,1.18)	.7299
2	Eqs. 5.4 unsolved	
3	Eqs. 5.4 unsolved	
4	Eqs. 5.4 unsolved	
5	U1	

Table 5.6

Results of systematic case studies - Case 3A

Forces: (0,-2.59,-9.66) at (6,6,6)

(.5,-2,-2.5) at (9,6,6)

ϕ_t = 20.79°, μ_t = .3797

Point Set	Results	μ_r
1	(21.24,5.44,5.09,2.52,-5.58,1.95)	.3887
2	(21.18,1.45,10.2,1.37,-10.3,1.85)	.3874
3	(21.37,4.99,6.24,1.82,-4.71,2.16)	.3901
4	(21.22,1.50,4.66,6.88,-9.09,1.73)	.3883
5	U3	
(5,3),(9,3),(7,7)	(21.24,5.77,4,88,2.40,.63,2.95) ***Warning: 0.000,-.000,-1.691	.3886
6	U3	
(3,6),(8,3),(7,8)	(21.97,2.95,10,.16,.385,3.58)	.4033
7	U3	
(6,2),(8,6),(4,7)	(22.11,7.43,5.68,.012,2.40,2.76)	.4063
8	U3	
(5.5,0),(8.5,7),(4.5,5)	(21.21,5.8,6.26,.98,-8.36,1.74)	.3883

Table 5.7

Results of systematic case studies - Case 3B

Forces: (0,-2.59,-9.66) at (6,6,6)

(5,-2,-2.5) at (12,6,6)

$\phi_t = 20.79°$, $\mu_t = .3797$

Point Set	Results	μ_r
1	Eqs. 5.4 unsolved	
2	(22.73,.57,10.32,2.29,2.59,2.33)	.4189
3	Eqs. 5.4 unsolved	
4	(22.45,1.24,4.05,7.87,-.527,1.85)	.4131
5	U3	
(5,2),(9,2),(7,6)	(21.35,2.13,5.26,5.66,-.873,2.83) ***Warning: .000,-.000,-4.047	.3909
6	U3	
(3,5),(8,2),(7,7)	(23.56,.52,8.45,4.29,2.8,3.33)	.4361
7	U3	
(8,0),(10,4),(6,5)	(21.26,2.59,3.53,6.92,-1.27,2.98) ***Warning: .000,-.000,-4.285	.3891
8	U3	
(6,0),(10,3),(5,5)	(21.14,.77,6.31,5.95,-1.46,3.06) ***Warning: .001, .000,-4.902	.3866

Table 5.8

Results of systematic case studies - Case 4A

Forces: (5.77,-1,-10) at (6,6,6)

(1,.5,-4) at (6,9,6)

$\phi_t = 25.87°$, $\mu_t = .4849$

Point Set	Results	μ_r
1	(-26.26,1.85,5.71,8.05,9.5,15.7)	-.4933
2	(-26.20,0.73,6.55,8.33,10.4,20.8)	-.4921
3	U1	
(2.5,2.5),(11.5,3.5), (6.5,11.5)	(-26.07,1.03,8.31,6.25,10.2,29.3)	-.4893
4	U2	
(4,11.5),(3,1.5), (12,4.5)	(-25.98,5.12,.81,9.64,11.9,50)	-.4872
5	U1	
(7,6),(11,6),(9,10)	(-26.48,6.95,6.18,2.51,9.42,13.7)	-.4982
6	U1	
(5,7),(10,4),(9,9)	(-26.68,2.03,6.57,7.06,9.17,11.5)	-.5026
7	U3	
(8,3),(10,7),(6,8)	(-26.51,2.2,10.3,3.2,9.47,14)	-.4989
8	U13	
(7,3.5),(11,6.5), (6,8.5)	(-26.19,2.36,8.58,4.66,9.92,21.1)	-.4919

Table 5.9

Results of systematic case studies - Case 4B

Forces: (5.77,-1,-20) at (6,6,6)

(1,.5,-4) at (6,9,6)

$\phi_t = 15.79°$, $\mu_t = .2829$

Point Set	Results	μ_r
1	(-15.80,6.47,6.35,12.1,21.7,196)	-.2829
2	(-15.80,4.14,11.3,9.50,20.3,177)	-.2829
3	(-15.80,3.10,10.9,10.9,21.5,194)	-.2829
4	(-15.80,8.97,1.19,14.78,30.5,316)	-.2829
5	U1	
(5,5),(9,5),(7,9)	(-15.80,3.87,12.5,8.59,10.5,45.3)	-.2831
6	U1	
(4,7),(9,4),(8,9)	(-15.80,4.72,11.2,9.02,12.3,69.3)	-.2830
7	U3	
(7,3),(7,7),(5,8)	(15.79,5.28,14.2,5.51,-104,-1500) ***Warning: -.000,-.000,.397	.2829
8	U1	
(6,4),(10,7),(5,9)	(-15.80,8.39,11.8,4.80,14.0,91.3)	-.2829

physical test for the actual friction angle between the cube and the plane may be greater). This can be explained by the fact that nearly parallel forces can be approximated by one single force in which case all the reaction vectors $\bar{Q}_i$ are parallel to the applied force and translation results. In translational failure $\mu_r = \mu_t$ and the center of rotation is infinitely far away from the cube.

2. If there is more than one applied force, the farther away from the center of the cube the applied forces, the greater the difference d. This trend can be explained by the fact that greater moments about the center of the cube make it easier for the object to rotate.

3. "d" increases as the center of rotation C moves closer to the 3 artificial supports P_i. If C lies within the base formed by the three support points, d reaches maximum values, and the closer the three supports, the greater will d be. This can be explained by the fact that, if the three joints are closer, the moment arm of each reaction becomes smaller and to resist rotation, μ_r has to be greater.

5.3.5 The n-Supports Model

5.3.5.1 Problem Statement and Principle of Solution

The 3-support model described above is often a simplification of the real situation. In the actual case the number of contacts between the object and the plane can be greater than three and the problem becomes statically indeterminate. A question arises as to whether the results obtained with the 3-support model can satisfactorily describe the actual conditions. The main point is whether the various critical coefficients of friction found with the 3-supports analysis can satisfactorily approximate the actual critical coefficients of friction. To investigate this problem an n-supports model is needed.

So far the six equations 5.2 are the only known equations relating the different quantities. In addition, since no tensile forces are considered,

$$A_i \geq 0, \qquad i = 1,n \tag{5.5}$$

If the points of contact P_i are chosen beforehand, there still remain (n+3) unknowns (i.e., A_i, μ_r and c_1, c_2). A solution has to be in the form (A_1, A_2, ... A_n, μ_r, c_1, c_2) which can be thought of as a vector with (n+3) components. Generally there are an infinite number of solution vectors which constitute a solution space with (n+3-6=n-3) degrees of freedom. If n=3 there are no degrees of freedom and so there is only one solution vector which means that the problem is determinate. If n > 3, the number of solution vectors becomes infinite.

Therefore it is impossible to consider every solution vector in the solution space. However, this problem is not uncontrollable because if one can find a finite number of "representative" solution vectors, one obtains a good impression of the entire solution space. In principle every representative solution vector has to be calculated, which is difficult because of the nature of equations 5.2a, 5.2b and 5.2f. In contrast, equation 5.3 (equations 5.2c, 5.2d and 5.2e are referred to as equation 5.3) are much easier to manipulate because they are linear in A_i.

For every solution vector (A_1, A_2, ... A_n, μ_r, c_1, c_2) of equation 5.2, there is a sub-vector (A_1, A_2, ... A_n), the solution vector of equation 5.3 because equation 5.2 include equation 5.3 (see Figure 5.10).

By finding all the representative solution vectors of 5.3, which will be discussed later, the representative solution vectors of the entire space can also be found by solving the 3 non-linear equations 5.2a, 5.2b, 5.2f with each representative solution vector of 5.3 as input. The first step is to define what vectors can be regarded as representative of the solution set of equation 5.3 under constraints equation 5.5.

It should be noted that the solution space of eq.5.3 under constraints eq.5.5 is a convex body in n-dimensional space (n-3) degrees of freedom. This convex body is bounded by a number of corner points, whose position vectors are the "boundary solution vectors" $\bar{D}_m$ = (0, 0, ... A_i, 0, ... A_j, 0, ... A_k, 0, ... 0) in which at least (n-3) A_i's are zeroes. Physically, each $\bar{D}_m$ represents a 3-support case. After all the $\bar{D}_m$'s are found (see 5.4.5.2), all the solution vectors of equation 5.3 can be expressed as a convex linear combination of $\bar{D}_m$, m = 1, nb where nb = number of boundary solution vectors:

For every solution vector $\bar{A}_m$ of equation 5.3,

$$\bar{A}_m = \alpha_1 \bar{D}_1 + \alpha_2 \bar{D}_2 + \ldots + \alpha_{nb} \bar{D}_{nb}$$

where $\alpha_1 + \alpha_2 + \ldots + \alpha_{nb} = 1$ and $\alpha_i \geq 0$.

A set of "representative" solution vectors of equation 5.3 is defined to be a set which contains all the $\bar{D}_m$'s and a number of other vectors which are convex linear combinations of the $\bar{D}_m$'s. There can be many reasonable ways of forming these combinations and in the following case study, a "random" method is used.

Each solution vector of the representative set will then be input into the 3 non-linear equations 5.2a, 5.2b and 5.2f, which can be solved because the number of unknowns (μ_r, c_1, c_2) is now 3. (They are solved by numerical methods using the subroutine ZSYSTM of IMSL, as was the case in PF3, see Appendix UM8 for details.)

5.3.5.2 Finding the Boundary Vectors

To find a boundary vector, (n-3) of the A_i's in equation 5.3 are set equal to zero. Then equation 5.3 are solved for the remaining 3 A_i's. If these 3 A_i's satisfy constraints, equation 5.5 also, a boundary vector is found.

To exhaust all the boundary vectors, $({}_nC_{n-3})$ or less trials are required. $({}_nC_i)$ is the number of ways of choosing i objects

from among n different objects,

$$ {}_{n}C_{i} = \frac{n!}{(n-i)!\ i!}\ , \qquad n \geq i $$

Examples are:

n	${}_{n}C_{n-3}$
3	1
10	120
20	1,140
50	19,600
100	161,700

The realization of the n-supports model is feasible but cumbersome. Particularly for the purposes of examining the validity of the simpler 3-supports model the efforts required would not be worthwhile. As a reduced version of the n-supports model the 10-supports model was therefore developed.

5.3.6 The 10-Supports Model

5.3.6.1 Description of the 10-Supports Model

As a step towards a more realistic description of the failure mechanism (compared to the 3-supports model), a 10-supports model (n=10) is analyzed. The method of analysis follows that of the more general n-supports model and can be outlined as follows.

1. Choose the ten support points.
2. Find all the boundary solution vectors $\bar{D}_i$, i=1, nb.
3. The values of the normal reactions A_i from each boundary vector are substituted into equations 5.2a, 5.2b and 5.2f, reducing the number of unknowns to 3 (μ_r, c_1, c_2). These 3 equations can then be solved by the subroutine SOLVE. (See "remarks" at the end of this outline.) With this step the critical coefficient of friction and the center of rotation can be found for each boundary

vector (such a boundary vector represents a three-supports case). This is equivalent to analysing a number (nb) of 3-supports cases where all the 3-supports are taken from the set of ten supports.

4. Solve equations 5.2a, 5.2b and 5.2f using the values from nb combinations of the boundary vectors. Each convex linear combination is usually dominated by one or two boundary vectors e.g. $\bar{D}_3$ and $\bar{D}_4$.

Let $\bar{D}_3$ = (0,3,4,3,0,0,0,0,0,0)

$\bar{D}_4$ = (0,0,2,6,2,0,0,0,0,0)

The combination vector $\bar{C}$ may be

$\bar{C}$ = (.01,1.9,3,3.6,.7,.03,.61,.10,.04)

which is approximately (.6 * $\bar{D}_3$ + .3 * $\bar{D}_4$)

$\bar{C}$ represents a case in which most of the reactions are at points 2, 3, 4, 5 and 6, which approximates a 5-support case. The procedure for forming such combinations is:

1. $\bar{C}_i = 0$
2. Generate 50 random numbers rv_i, i=1, 50 and $0 < rv_i < 1$
3. wt = 1.0
4. j = 0
5. j = j + 1
6. $\bar{C}_i = \bar{C}_i + wt * rv_j * \bar{D}_{i+j-1}$
7. $wt = wt * (1 - rv_j)$
8. If ($wt \leq .0001$), go to #9

10. Go to #5 if $j < 50$
9. $\bar{C}_i = \bar{C}_i + wt * \bar{D}_i$

$\bar{C}_i$ is now formed and can then be input into the 3 non-linear equations 5.2a, 5.2b and 5.2f, so that μ_r, c_1 and c_2 can be obtained by SOLVE. $\bar{D}_{i+j-1}$ is taken to be $[(i+j-2)_{\text{mod nb}} +1]$ when (i+j-1) > nb. For example, if nb = 38 and (i+j-1) = 40, then $\bar{D}_{i+j-1}$ is taken to be $\bar{D}_2$.

5. Solve equations 5.2a, 5.2b and 5.2f for 100 random combinations of the form $\bar{C} = (rv_1 * \bar{D}_1 + rv_2 * \bar{D}_2 + \ldots + rv_{nb} * \bar{D}_{nb}) / \sum^{nb} rv_i$.

This step is performed, although Step 4 has already lead to a solution for μ_r, c_1 and c_2. Its purpose is to simulate the randomness of the situation. On the other hand, the reason for performing Step 4 as outlined above is that, although the actual normal reactions are usually random, only a few (e.g. 5) of the supports are dominant, having relatively large reactions.

Remarks

A computer program PF10 is used to carry out the above calculations (see Figure 5.11). Step 3 is conducted by the subroutine SOLVE, which uses ZSYSTM of the IMSL to solve the 3 equations with a maximum error of .005 in each equation. Only the algorithm(but neither a listing nor a user's manual)is provided for this program because its purpose is only to serve as a tool in examining the validity of the 3-supports model. The fully documented 3-supports model satisfies the requirements for practical use (as will be shown below) and therefore no documentation for the 10-supports model is included.

5.3.6.2 Case Study Using the 10-Supports Model

This case will serve as a basis for comparison between the 3-supports and 10-supports models. The cube model and the set of applied forces of the 3-supports model-case (2A) (see Section 5.3.4) are used.

The forces are: $\bar{F}_1 = (0,0,-10)$ at $(6,6,6)$

$\bar{F}_2 = (3,-1,0)$ at $(6,9,6)$

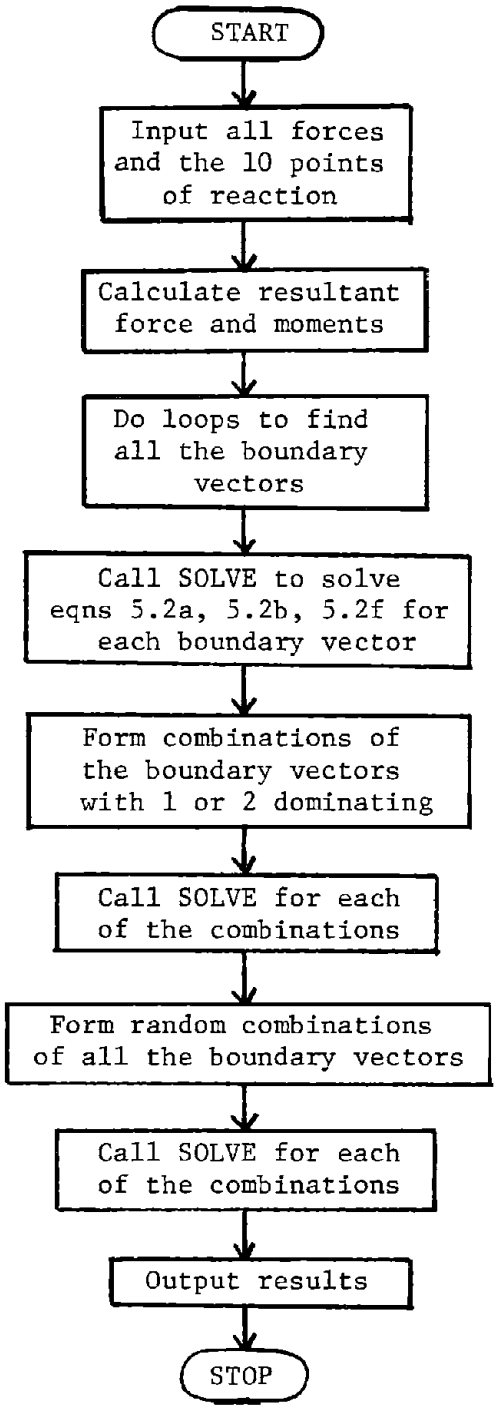

Figure 5.11 Algorithm of PF10

Therefore, $\mu_t = .3113$, $\phi_t = 17.55°$

Step 1: (see Section 5.3.6.1): The ten supports chosen are:

$P_1 = (0,0)$, $P_2 = (12,0)$, $P_3 = (12,12)$, $P_4 = (0,12)$,

$P_5 = (2,2)$, $P_6 = (11,2)$, $P_7 = (9,11)$, $P_8 = (6,4)$,

$P_9 = (10,4)$, $P_{10} = (8,8)$.

Step 2: 38 boundary vectors are found, some examples are:

$\bar{D}_1 = (3.5,2.0,4.5,0,0,0,0,0,0,0)$

$\bar{D}_2 = (0,5.5,1.0,3.5,0,0,0,0,0,0)$

. . . . . .

$\bar{D}_{38} = (0,0,0,0,0,0,0,3.75,2.75,3.5)$

Step 3: These boundary vectors are input into the subroutine SOLVE and 26 cases are solved successfully. In the remaining 12 cases equations 5.2a, 5.2b and 5.2f cannot be solved. Successful examples are:

(3.5,2.0,4.5,0,0,0,0,0,0,0,.3549,1.94,-6.79), which corresponds to the sub-vector $\bar{D}_1$ and $\mu_r = .3549$, $c_1 = 1.94$, $c_2 = -6.79$.

(0,5.5,1.0,3.5,0,0,0,0,0,0,.3429,4.65,-9.67) which corresponds to $\bar{D}_2$ and $\mu_r = .3429$, $c_1 = 4.65$, $c_2 = -9.67$.

For the 26 cases, values of μ_r range from .3429 to .4185 with a mean of .3712 and a standard deviation of .018143.

Step 4: 38 (= nb) combinations are formed which are then input to SOLVE. An example of a combination is

$\bar{C}_2$ = (.16,4.89,1.42,2.99,.41,.13,.00,.00,.00,.00), which is dominated by $\bar{D}_2$.

The corresponding entire solution vector is

(.16,4.89,1.42,2.99,.41,.13,.00,.00,.00,.00,.3446,4.35,-9.33)

for which μ_r = .3446, c_1 = 4.35, c_2 = -9.33.

Only 35 of the 38 cases are solved and the values of μ_r range from .3446 to .4349, with a mean of .3773 and a standard deviation of .021604.

Step 5: 100 random combinations are generated. Two examples of entire solution vectors, which do not vary much among themselves, are:

(.66,.72,.87,.59,.58,1.11,.69,1.32,1.88,1.58,.3750,5.23,-2.38)

(.48,1.00,.92,.66,.79,1.20,.88,1.46,1.33,1.28,.3731,5.19,-2.63)

All the 100 cases are solved and the values of μ_r range from .3671 to .3778 with a mean .3733 and standard deviation .002617.

5.3.6.3 Observations and Comments

Average values for the critical coefficient of friction using different assumptions obtained with the 10-supports model are:

translation	3-supports	few supports	10-supports
μ_t = .3163	μ_r = .3712	μ_r = .3773	μ_r = .3733

The mean coefficient of friction using a "few supports" model is derived from Step 4 in the previous section.

The 10-support model should be the most realistic. However, as can be observed above and from another case study not recorded here, the mean value for μ_r using the 3-support model does not deviate much from that of the 10-support model. Therefore it is sufficiently accurate provided that a sufficient number of support sets are analyzed and the mean for μ_r taken.

5.4 Extension of the Method of Artificial Supports to Other Modes of Failure

5.4.1 Introduction

One of the basic principles underlying the Method of Artificial Supports is that the macroscopic concept of friction (friction = normal reaction x coefficient of friction) can be applied to hypothetical points of contact (the artificial supports). In light of this principle, other modes of sliding failure (and other non-sliding modes as will be shown in Section 5.5) can be modelled. The following sections discuss the extension of the method to include rock wedge rotation about the point 0 (Fig. 5.13) and sliding on two planes.

5.4.2 Wedge Rotation About 0

A wedge resting on two intersecting joint planes (see Figure 5.13) can fail in one of several modes. One mode is rotation about the lower tip 0 on one of the joint planes. In Figure 5.13 rotation on plane (1) is shown. The Method of Artificial Supports will now be applied to this failure mode and the following assumptions are made:

1. The basic assumptions of Section 5.2.1 apply, but now the axis of rotation is fixed at 0.

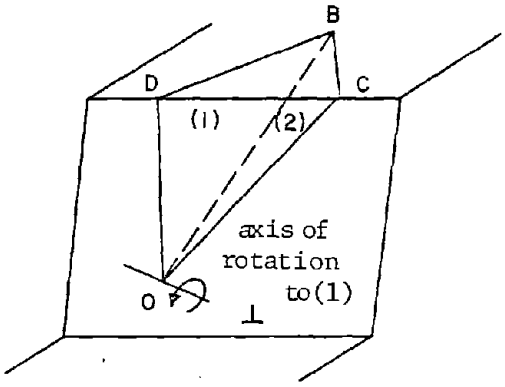

Figure 5.13: Rotation about 0

2. All the reactions at 0 are tangential in the plane on which the wedge rotates ("in-plane" reactions). This is justified since the motion is planar, and thus reactions normal to the plane should not have a significant influence. The soundness of this justification will be examined later.

3. It is also assumed that the wedge is "simply supported" (just touching, no tensile forces) at point 0.

The 3-supports model described earlier will be used to analyze this mode of failure -- in-plane rotation about 0.

5.4.3 Equations of Limiting Equilibrium

The six equations of limiting equilibrium are similar to equation 5.2, but now $(c_1, c_2) = (0,0)$. The tangential reactions r_x and r_y (see Figure 5.14) at 0 are introduced in equations 5.2a and 5.2b, which become equations 5.6a and 5.6b shown below:

The six equations are:

$$
\begin{aligned}
-\mu \sum^{3} A_i \, p_{i2}/0P_i + r_1 + r_x &= 0 \qquad (5.6a)\\
\mu \sum^{3} A_i \, p_{i1}/0P_i + r_2 + r_y &= 0 \qquad (5.6b)\\
\sum^{3} A_i + r_3 &= 0 \qquad (5.6c)\\
\sum^{3} A_i \, p_{i2} + m_1 &= 0 \qquad (5.6d)\\
-\sum^{3} A_i \, p_{i1} + m_2 &= 0 \qquad (5.6e)\\
\mu \sum^{3} A_i \, 0P_i + m_3 &= 0 \qquad (5.6f)
\end{aligned}
\qquad (5.6)
$$

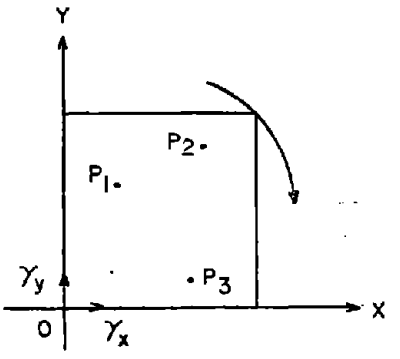

r_x acts in the positive x-direction
r_y acts in the positive y-direction

Figure 5.14: Rotation about 0

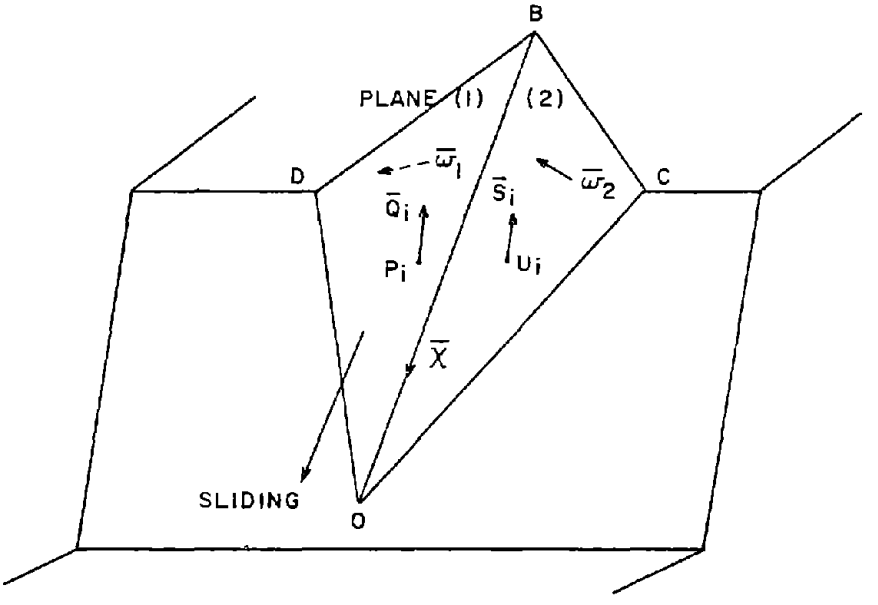

Figure 5.15: Sliding on two planes

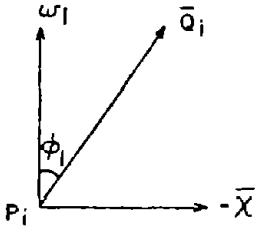

$\bar{Q}_i = A_i(-\bar{\omega}_1 - \mu_1 \bar{X})$

where A_i = normal reaction

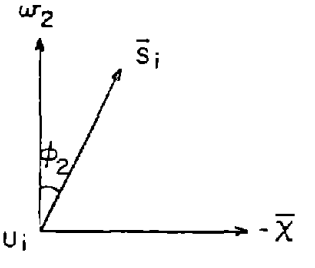

$\bar{S}_i = B_i(\bar{\omega}_2 - \mu_2 \bar{X})$

where B_i = normal reaction

Figure 5.16: Reaction Vectors

5.4.4 Method of Solution

A_1, A_2 and A_3 are first found by solving equations 5.6c, 5.6d and 5.6e. If they are all non-negative, they are substituted into equation 5.6f to find μ. Then r_x and r_y can be solved by equations 5.6a and 5.6b respectively. r_x and r_y should be non-negative because the block is assumed to be simply supported at 0; negative r_x or r_y would mean that there is tension between the block and the point of contact at 0.

The above calculations are performed by the computer program ROTFA (Rotation - Fixed Axis). The algorithm and user's manual for ROTFA are given in Appendix UM9. Two example applications are described in the following section.

5.4.5 Example Applications

The same forces and support points as in Cases 3A and 3B (Section 5.3.4) are used. For comparison, the results for the 'fixed axis of rotation at 0' case are listed together with that of the free-rotation case and the translational case (see Section 5.3.4). μ_h denotes the critical coefficient of friction for rotation about 0; μ_r denotes that for the free rotational case and μ_t that in the translational case.

(5A) corresponds to 3A in Section 5.3.4

Forces: (0,-2.59,-9.66) at (6,6,6)
(.5,-2,-2.5) at (9,6,6)
$\mu_t = .3797$

Point Set[1]	(μ_h, r_x, r_y)	(μ_r, c_1, c_2)
1	(.3627,1.77,1.06)	(.3887,-5.58,1.95)
2	(.3575,1.22,.88)	(.3874,-10.3,1.85)
3	(.3627,1.79,1.07)	(.3901,-4.71,2.16)
4	(.3626,1.49,.86)	(.3883,-9.09,1.73)
5	U3[2]	U3
(5,3),(9,3),(7,7)	(.3782,1.69,.62)	(.3886,.63,2.95)*
6	U3	U3
(3,1),(8,3),(7,8)	(.3684,1.64,.90)	(.4033,.385,3.58)
7	U3	U3
(6,2),(8,6),(4,7)	(.3796,1.53,.51)	(.4063,2.40,2.76)
8	U3	U3
(5.5,0),(8.5,7),(4.5,5)	(.3704,1.30,.70)	(.3883,-8.36,1.74)

(5B) corresponds to case 3B in Section 5.3.4

Forces: (0,-2.59,-9.66) at (6,6,6)
(.5,-2,-2.5) at (12,6,6)
μ_t = .3797

Point Set	(μ_h, r_x, r_y)	(μ_r, c_1, c_2)
1	(.3950,1.79,.65)	unsolved
2	(.4010,1.32,.25)	(.4189,2.59,2.33)
3	(.3964,1.84,.64)	unsolved
4	(.3992,1.60,.40)	(.4131,-.521,1.85)
5	U3	U3
(5,2),(9,2),(7,6)	(.4071,1.63,.26)	(.4523,3.81,3.14)
6	U3	U3
(3,5),(8,2),(7,7)	(.4028,1.54,.34)	(.4361,2.8,3.33)
7	U3	U3
8	U3	U3
(6,0),(10,3)(5,5)	(.4050,1.77,.42)	(.4219,3.06,3.97)*

[1]The configuration of the point sets are shown in Figure 5.9
[2]U3 means A_3 is negative, i.e., the support base is unstable.
*Means the results (μ_r, c_1, c_2) may not be reliable due to numerical accuracy problems.

5.4.6 Comparison of the Three Modes of Failure

It is interesting to see that generally in Case 5A $\mu_r > \mu_t > \mu_h$ while in 5B $\mu_r > \mu_h > \mu_t$ for each point set. However, these results do not imply that the object (e.g. rock wedge) always fails in the free rotation mode (μ_r) because in the actual case kinematic restrictions may affect mode of failure.

In case of a wedge resting on two joint planes, one obvious kinematic limitation is that the wedge cannot rotate on one plane and move towards any part of the second plane. Another limitation may be that the wedge is not free to move past point 0 because of an obstacle at 0. If this is so, the wedge may fail by rotation about 0 even though $\mu_r > \mu_t > \mu_h$. The relative values of these critical friction coefficients together with the kinematic limitations determine the actual mode of failure.

5.4.7 Justification for Assumption '2' (only in-plane reactions at 0)

In Section 5.4.2, it was assumed that any normal reaction r_z at 0 can be neglected in calculating μ_h. To examine whether this is a reasonable assumption, Case 5A is re-worked, adding a normal reaction of $r_z = 1$ (Case 6A1 below) and $r_z = 2$ (Case 6A2 below). The critical coefficient μ_h with a non-zero r_z is denoted μ_{hz}.

(6A1) Forces: (0,-2.59,-9.66) at (6,6,6)
(.5,-2,-2.5) at (9,6,6)
r_z = (0,0,1) at (0,0,0)
μ_t = .3797

Point Set	(μ_{hz}, r_x, r_y)	(μ_h, r_x, r_y) in 5A
1	(.3623,1.50,1.32)	(.3627,1.77,1.06)
2	(.3657,1.12,1.04)	(.3575,1.22,.88)
3	(.3617,1.52,1.34)	(.3627,1.79,1.07)
4	(.3620,1.32,1.20)	(.3626,1.49,.86)
5 (5,3),(9,3),(7,7)	(.3765,1.47,.97)	(.3782,1.69,.62)
6 (3,6),(8,3),(7,8)	(.3731,1.41,1.03)	(.3684,1.64,.90)

(6A1) (continued)

Point Set	(μ_{hz}, r_x, r_y)	(μ_h, r_x, r_y) in 5A
7 (6,2),(8,6),(4,7)	U3	(.3776,1.53,.51)
8 (5.5,0)(8.5,7),(4.5,5)	U3	(.3704,1.30,.70)

(6A2) Forces: (0,-2.59,-9.66) at (6,6,6)
(.5,-2,-2.5) at (9,6,6)
r_z = (0,0,2) at (0,0,0)

Point Set	(μ_{hz}, r_x, r_y)	(μ_h, r_x, r_y) in 5A
1	(.3619,1.24,1.58)	(.3627,1.77,1.06)
2	(.3742,1.01,1.20)	(.3575,1.22,.88)
3	(.3606,1.25,1.61)	(.3627,1.79,1.07)
4	(.3615,1.11,1.53)	(.3626,1.49,.86)
(5,3),(9,3),(7,7)	(.3749,1.26,1.72)	(.3782,1.69,.62)
(3,6),(8,3),(7,8)	U1	(.3648,1.64,.90)

Comments

It can be observed that μ_{hz} can be smaller or greater than μ_h (usually smaller). However, the two values do not deviate significantly from each other, justifying the assumption '$r_z \approx 0$'.

This phenomenon can be explained by the fact that when r_z increases, the normal reactions at the nearby supports decrease while those that are further away increase, but by a smaller amount only. As a result, $\sum^{n} A_i OP_i$ remains essentially unchanged because the increases and decreases in the A_i's compensate each other in the sum $\sum^{n} A_i OP_i$.

5.4.8 Wedge Sliding on Two Planes

The most common mode of failure for a wedge resting on two intersecting joint planes is sliding on both of the base planes along the line of intersection. The principles of the Method of Artificial Supports can also be applied to this mode of failure. It will now be

shown how a factor of safety can be derived for this mode of failure using the Method of Artificial Supports.

Vector notations

To derive the factor of safety for sliding on two planes, the following vector notations have to be introduced (see Figure 5.15). $\bar{w}_1$ and $\bar{w}_2$ are the normals to the planes 1 and 2 respectively. $\bar{x}$ is the unit vector along BO, the line of intersection. P_i is a point of reaction on plane 1. $\bar{Q}_1$ is the associated reaction vector. Under limit conditions the projection of $\bar{Q}_i$ on plane 1 is assumed to be parallel to OB* and $\bar{Q}_i$ is at an angle ϕ_1 relative to $(-\bar{w}_1)$. Similarly, $\bar{S}_i$ of plane 2 encloses angle ϕ_2 with $(\bar{w}_2)$ (see Figure 5.16).

If joint plane 1 is not completely persistent, a cohesive resistance H_1 exists. The corresponding cohesive force vector on plane 1 is $(-H_1\,\bar{x})$ since the cohesive force directly opposes the sliding motion which is in the direction of $\bar{x}$. Similarly, the cohesive resistance vector on plane 2 is $(-H_2\,\bar{x})$.

Equation of limiting equilibrium

Assuming n points of reaction (supports) on plane 1 and m points on plane 2, the equation of limiting equilibrium of forces is

$$\sum^{n} A_i(-\bar{w}_1-\mu_1\bar{x}) - H_1\bar{x} + \sum^{m} B_i(\bar{w}_2-\mu_2\bar{x}) - H_2\bar{x} + \bar{R} = 0$$

i.e., $$(-w_1-\mu_1\bar{x})\sum^{n} A_i + (\bar{w}_2-\mu_2\bar{x})\sum^{m} B_i = -\bar{R} + H_1\bar{x} + H_2\bar{x}$$

μ_1 = coefficient of friction of wedge on plane 1

μ_2 = coefficient of friction of wedge on plane 2

R = resultant driving force.

*The assumption -- projection of $\bar{Q}_i$ being parallel to OB -- makes the simplifying assumption criticized in Chapter 4. This has been done only for reasons of clarity; the Method of Artificial Supports permits one to use other directions of the reaction $\bar{Q}_i$.

Since the vector $(-\bar{R} + H_1\bar{x} + H_2\bar{x})$ is a linear combination of $(-\bar{w}_1-\mu_1\bar{x})$ and $(\bar{w}_2-\mu_2\bar{x})$, these three vectors are coplanar.

$$\therefore (-\bar{R}+H_1\bar{x}+H_2\bar{x}) \cdot (-\bar{w}_1-\mu_1\bar{x})X(\bar{w}_2-\mu_2\bar{x}) = 0$$

The expression is equal to

$$\mu_2(\bar{R}-H_1\bar{x}-H_2\bar{x}) \cdot \bar{x}X\bar{w}_1+\mu_1(\bar{R}-H_1\bar{x}-H_2\bar{x}) \cdot \bar{x}X\bar{w}_2-(\bar{R}-H_1\bar{x}-H_2\bar{x}) \cdot \bar{w}_2X\bar{w}_1 = 0$$

by expanding the expression and noting that $\bar{x}$ X $\bar{x}$ = 0.

It further follows that

$$\mu_2\bar{R} \cdot \bar{x}X\bar{w}_1+\mu_1\bar{R} \cdot \bar{x}X\bar{w}_2+(H_1+H_2)\bar{x} \cdot \bar{w}_2X\bar{w}_1 = \bar{R} \cdot \bar{w}_2X\bar{w}_1$$

The above equation can be rewritten as

$$\mu_2\bar{R} \cdot \frac{\bar{x}X\bar{w}_1}{|\bar{w}_2X\bar{w}_1|} + \mu_1\bar{R} \cdot \frac{\bar{x}X\bar{w}_2}{|\bar{w}_2X\bar{w}_1|} + (H_1+H_2)(\bar{x} \cdot \frac{\bar{w}_2X\bar{w}_1}{|\bar{w}_2X\bar{w}_1|})$$

$$= \bar{R} \cdot \frac{\bar{w}_2X\bar{w}_1}{|\bar{w}_2X\bar{w}_1|} \qquad (5.7)$$

The term on the right-hand side is equal to $(\bar{R} \cdot \bar{x})$ which is the component of the resultant force along BO, the direction of sliding. This is the driving force which causes the wedge to slide along BO. The first two terms on the left hand side are proportional to μ_2 and μ_1 respectively and are the frictional resistances from planes 2 and 1 respectively. The remaining term is equal to (H_1+H_2), which is the total cohesive resistance derived from the two planes.

Derivation of factor of safety

Equation 5.7 relates the values of μ_1, μ_2, H_1 and H_2 at which limiting equilibrium occurs. Equation 5.7 can be rewritten as

$$\mu_2\bar{R} \cdot \frac{\bar{x}X\bar{w}_1}{|\bar{w}_2X\bar{w}_1|} + \mu_1\bar{R} \cdot \frac{\bar{x}X\bar{w}_2}{|\bar{w}_2X\bar{w}_1|} + (H_1+H_2) = \bar{R} \cdot \bar{x}$$

For the case in which the wedge is stable,

L.H.S. > R.H.S.

i.e., resisting forces available > driving force.

A factor of safety FS can be defined as

$$FS = [\mu_2\bar{R} \cdot \frac{\bar{x}X\bar{w}_1}{|\bar{w}_2X\bar{w}_1|} + \mu_1\bar{R} \cdot \frac{\bar{x}X\bar{w}_2}{|\bar{w}_2X\bar{w}_1|} + (H_1+H_2)]/(\bar{R} \cdot \bar{x})$$

This expression for FS coincides with that of the analysis by Hendron, Cording and Aiyer (1971).

Comments on Equation 5.7

Equation 5.7 can be rewritten as

$$\mu_2\bar{R} \cdot \bar{G}_1 + \mu_1\bar{R} \cdot \bar{G}_2 + H = \bar{R} \cdot \bar{x} \qquad (5.8)$$

where $\bar{G}_1$, $\bar{G}_2$ are vectors depending on the geometry and $H = H_1+H_2$.

For given geometry, applied forces and H, the failure condition equation 5.8 is linear in μ_1 and μ_2.

When there is only frictional resistance (H = 0), the well known fact is confirmed that only direction (and not the magnitude) of $\bar{R}$ affects the stability of the wedge.

5.5 "Complete" Rock Slope Stability Analysis

5.5.1 Introduction

As has been shown so far, it is possible, with the Method of Artificial Supports as a working tool, to analyze all the sliding

modes of failure of a rock wedge (translational sliding on 1 or 2 planes, free rotational sliding, and rotational sliding around a fixed axis, in particular the axis through the 'tip' 0). This Section describes as an example of a complete stability analysis, the procedure by which the overall stability of a 2-P wedge (wedge formed by 2 intersecting joint planes, see Figure 5.1a) can be determined. (No encompassing computer program has been written to execute this algorithm,but with the analyses and computer programs described in the previous Sections it is possible to carry out the whole algorithm step by step.) The stability analysis of a 3-P wedge (see Figure 5.1b) can be performed in a similar way except that additional kinematic restrictions have to be considered.

5.5.2 Stability Analysis of a 2-P Wedge, Definitions and Assumptions

The purpose of this analysis is to determine the stability of a rock wedge formed in a slope by two discontinuity planes. The general shape is shown in Figure 5.17. There can be any number of applied forces at different points. These forces include the weight, possible water pressures, surcharges and other artificial loads.

Vector Notations Used

Each applied force is represented by a force vector $\bar{F}_i$ and the position vector $\overline{PF}_i$ of its point of application relative to 0. The coordinate axes are chosen such that the x-axis is horizontal and parallel to the projection of the edge DC on a horizontal plane. The z-axis is vertically upward and the y-axis points horizontally into the slope.

The vectors associated with the geometry are depicted in Figure 5.18.

$\bar{w}_1$ and $\bar{w}_2$ are unit normal vectors to planes 1 and 2 respectively. $\bar{w}_1$ points into the mass while $\bar{w}_2$ points out of it. The vector $\bar{x}_{12}$ is parallel to $\overline{BO}$ and is given by $\bar{x}_{12} = \bar{w}_2 \times \bar{w}_1$.

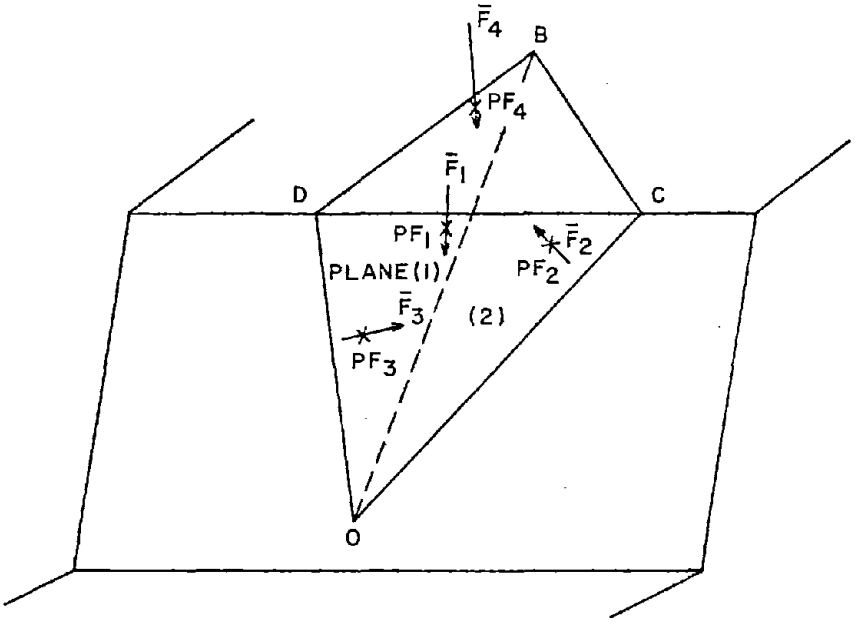

Figure 5.17: 2-P wedge

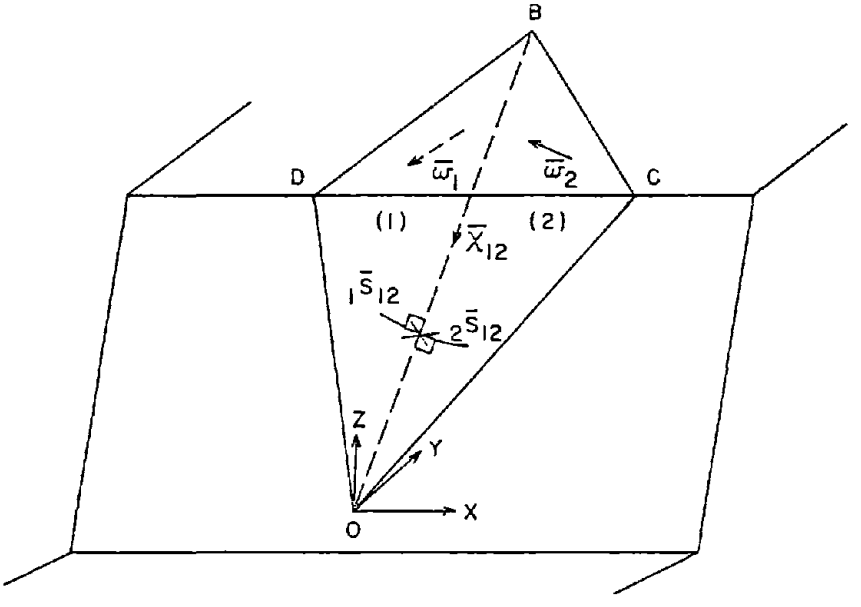

Figure 5.18: Vector Notations

In the following analysis, $\bar{R}$ (acting at 0) represents the resultant of the applied forces while $\bar{M}_o$ is the resultant moment vector of the applied forces about 0.

$$\bar{R} = \sum \bar{F}_i$$

$$\bar{M}_o = \sum \overline{PF}_i \times \bar{F}_i$$

Thus the entire force system is reduced to a force $\bar{R}$ at 0 and a moment $\bar{M}_o$.

Assumptions

To be consistent, the joints are assumed to be fully persistent and the reactions between the wedge and the joint planes are never tensile. (In representing sliding resistance a friction and cohesion term could be used; however, cohesion implies tensile resistance, which has been excluded in the method of artificial supports. Consequently, full persistence is assumed. However, if the user desires, cohesion can be introduced in form of additional forces at the supports.)

It is also assumed that all the reactions can be represented in point form, just like the applied forces.

5.5.2 Modes of Failure

There are three major modes of failure:

Mode TO = Toppling
Mode S1(S2) = Sliding on plane 1 or plane 2
Mode S12 = Sliding on both planes

Mode S1(S2) is further subdivided into:

Near translational	T1(T2)
Free rotational	RF1(RF2)
Restrained Rotational	RR1(RR2)

The identification of these modes and the determination of the respective safety factors will now be discussed. (Note that the analysis method and expressions have been incorporated in SWARS for the modes that SWARS considers, i.e., TO, T1(T2), S12.)

1. Mode TO. Toppling About an Edge. This mode of failure takes place when the reactions on the plane containing the edge cannot balance the moments of the applied forces about the edge.

Taking edge OD as an example, whether the wedge will rotate out of the slope about the edge OD depends on the applied forces and their corresponding points of application. However, one needs only to consider $\bar{R}$ and $\bar{M}_o$ since they are equivalent to the set of applied forces. Since $\bar{R}$ intersects the axis OD, it cannot cause a toppling moment about OD. Then the condition for toppling depends only on $\bar{M}_o$ and is:

$$\bar{M}_o \cdot \overline{OD} < 0 \tag{5.9}$$

Similarly, the condition for toppling about OC is

$$\bar{M}_o \cdot \overline{OC} < 0 \tag{5.10}$$

The condition for toppling about DB and CB depends on M_o and on $\bar{R}$ because $\bar{R}$ causes a moment about the edges. The respective conditions are:

$$(\bar{R} \times \overline{OD} + \bar{M}_o) \cdot \overline{DB} < 0 \tag{5.11}$$

$$(\bar{R} \times \overline{OC} + \bar{M}_o) \cdot \overline{CB} > 0 \tag{5.12}$$

2. Mode S1(S2). Sliding on One Plane Only

For a particular problem, this mode of failure may occur on either one of the two joint planes. Sliding can occur on plane 1 if:

$$\bar{M}_o \cdot \bar{x}_{12} \geq 0 \tag{5.13}$$

Sliding can occur on plane 2 if:

$$\bar{M}_o \cdot \bar{x}_{12} \leq 0 \tag{5.14}$$

It should be noted that when $\bar{M}_o \cdot \bar{x}_{12} \simeq 0$ (within measurement errors), both S1 and S2 have to be considered, i.e., further investigations have to be conducted for both planes.

After determining on which plane sliding can occur, the three submodes have to be examined:

Submode T1(T2). Near-Translational Failure

T1(T2) takes place if only the weight or if the applied forces can be represented by one resultant at a certain point (e.g.,the forces are concurrent or parallel). Mathematically, this is expressed as,

$$|\bar{R} \cdot \bar{M}_o| \approx 0 \tag{5.15}$$

If equation 5.15 holds, one has to examine whether the wedge would slide towards the line of intersection OB. Taking plane 1 as an example, if

$$\bar{R} \cdot {}_1\bar{S}_{12} > 0 \tag{5.16}$$

the wedge moves toward the line of intersection and a single plane failure on plane 1 is not possible. If $\bar{R} \cdot {}_1\bar{S}_{12} \leq 0$ single plane sliding occurs and the critical coefficient of friction can be found from the ratio of tangential to normal components of the applied forces. (The analagous procedure is applied to plane 2.)

Submode RF1 or RF2. Free Rotational Sliding

Theoretically mode T1(T2) is a special case of this mode. The rotational mode (RF) is only considered, if equation 5.15 does not hold, since calculations involved in mode T1(T2) are much simpler. The critical coefficient of friction for mode RF is indeterminate because it depends on the positions of the points of contact. But the range of possible values for the coefficient and the center of rotation can be assessed by the Method of Artificial Supports. After a number of sets of possible values are found, a kinematic test is carried out on the possible centers of rotation. For example, for anti-clockwise rotation on plane 1, it is necessary that

$$\overline{OC}_r \cdot \overline{BO} \geq 0 \qquad (5.17)$$

for the rotation (with axis of rotation at C_r) to be kinematically possible. After kinematically impossible cases are rejected, a critical coefficient of friction can be determined for the remaining cases. For example, the greatest of all critical coefficients or the mean can be taken to be the critical coefficient.

If all the cases are found to be kinematically impossible (i.e., some part of the wedge tends to rotate towards the line of intersection) rotation about O (in some rare cases, about B) has to be considered, that is Mode RR.

Submode RR1(RR2). Rotation about O (or B)

This case occurs when the wedge tends to rotate towards O. The approach described in Sections 5.4.2 to 5.4.4 is used to find possible values of critical friction coefficients. If the wedge tends to rotate uphill (a rare case) and it also rotates towards B, then rotation about B is considered.

As before, the critical coefficient may be taken to be the greatest for all kinematically possible cases (or the mean). If again all the cases are found to be kinematically impossible (i.e., tensile

reactions or direction of rotation being into the other plane), then single-plane failure is impossible.

Mode S12. Sliding on Both Planes

In this mode the wedge slides along the line of intersection BO, making contact with both planes. This mode has always to be considered unless there are some kinematic obstacles (e.g.,the wedge touches 'horizontal ground' at O). The fact that failure on one single plane is possible does not rule out the possibility of failure on both planes.

The determination of the factor of safety for this mode was described in Section 5.4.8.

5.5.6 Algorithm for the 2-Plane Wedge Analysis

This algorithm summarizes the analysis procedure described before (Figure 5.19).

The modes of failure considered are recalled: toppling (the case of completely lifting off from base planes is automatically included in toppling) (TO); sliding on plane 1 (S1) or on plane 2 (S2); sliding on both planes (S12). S1(2) is further divided into near-tranlational sliding T1(2); free rotational sliding (RF1,RF2), when the plane rotation is not restrained kinematically; and restrained rotational sliding (RR1,RR2), about the fixed axis at O or B.

After the geometry and applied forces on a wedge are determined, the procedure shown in Figure 5.19 starts by examining failure by toppling about an edge. If the wedge is found to be stable with respect to toppling, then the possibility of sliding failure is investigated on plane 1 (S1). If this is not possible (i.e., $\bar{M}_o \cdot \bar{x}_{12} < 0$), then S2 may be a potential mode. If S1 is a possible mode, T1, RF1 and RR1 are examined to see which one is in fact the potential mode. (It is possible that none can occur.) After that, plane 2 is considered in an analagous manner. Finally, whenever a mode is found to

Figure 5.19: Summarizing Algorithm

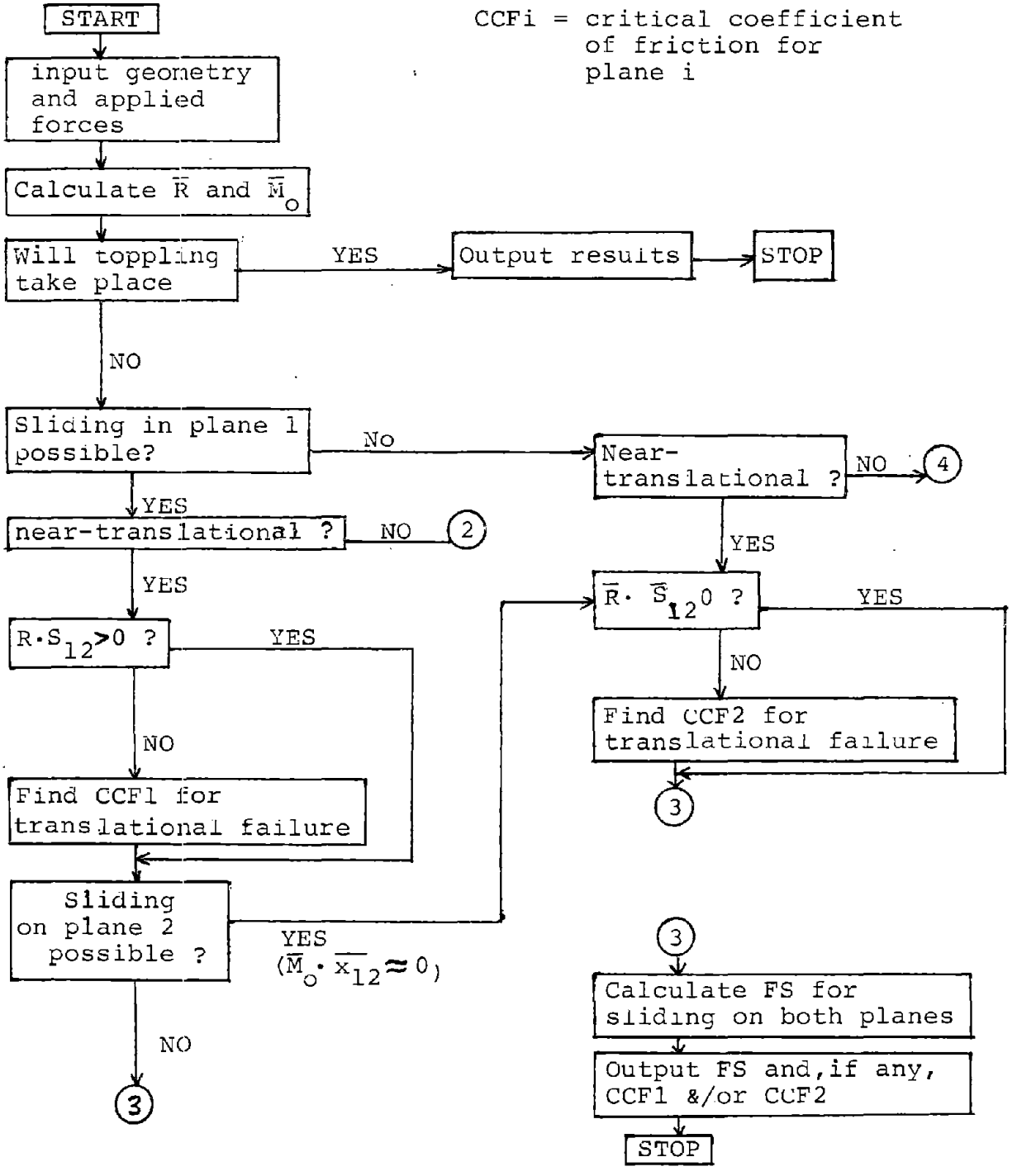

Figure 5.19: Summarizing Algorithm
(continued)

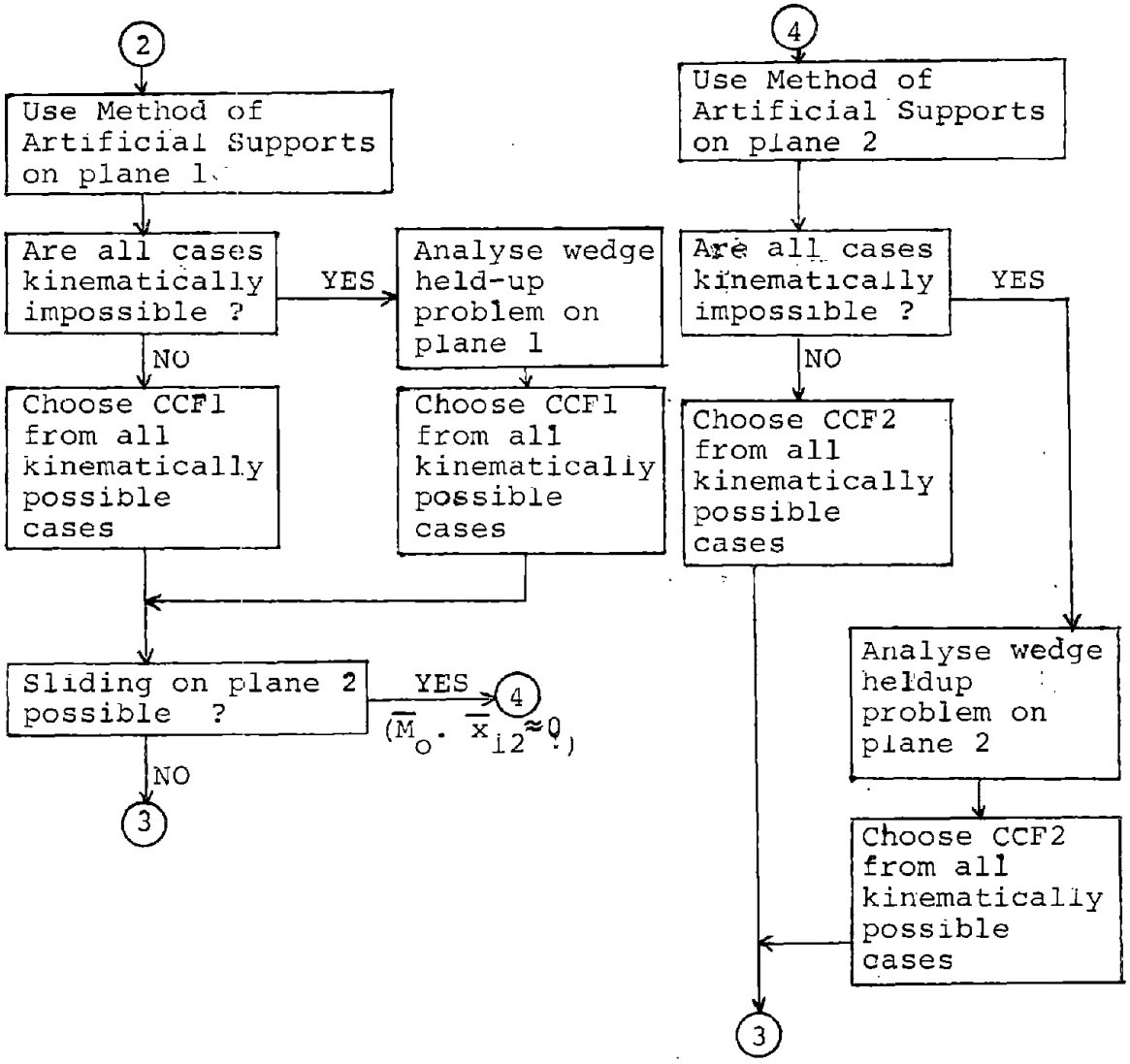

be possible, the factor of safety or critical coefficient of friction is determined. The procedure terminates with the determination of the factor of safety for two-plane failure (S12).

5.6 Conclusions

The method of artificial supports makes it possible to eliminate or reduce most of the restrictions that are usually a part of wedge stability analysis. The major problem associated with rigid body assumptions, the unknown stress and force distributions acting in the supporting planes, is greatly reduced by specifically considering a variety of reactions in the joint planes. The appropriate consideration of these reactions leads to an analysis method that correctly models all modes of failure. In particular it was shown that the usual assumption of translational failure can be incorrect and cause unsafe predictions, if forces other than the weight are significant. Most satisfactory and convenient is the fact that the methodology employed in the artificial support model can be applied to all failure modes of a wedge. This was demonstrated with a procedure for a "complete" stability analysis of a 2-joint wedge.